Spatio-temporal distribution of temperature, salinity and suspended sediment on the deltaic front of the Magdalena River: Influence on nutrient concentration and primary productivity

Student:

Ana Carolina Torregroza Espinosa

Ph.D. (c) Inter-Institutional Doctorate program in Marine Sciences

Universidad del Norte

Advisor:

Dr. Juan Camilo Restrepo López

Associate Professor. Department of Physics and Geology - Universidad del Norte

Co-advisor:

Dr. Jaime Humberto Escobar Jaramillo

Associate Professor. Department of Civil and Environmental Engineering- Universidad del Norte

Barranquilla, June 2020

Acknowledgements

To my PhD advisors, Drs. Juan Camilo Restrepo and Jaime Humberto Escobar, thank you for your encouragement, advice, support, patience, and never-ending enthusiasm. Thanks for all the opportunities you have given me and for allowing me to pursue my interests through this research. Huge thanks to Dr. Alexander Correa Metrio for his wonderful support in data analysis and to Dr. Mark Brenner for his valuable contributions to my research.

Thanks to the Water Analysis Laboratory of the Universidad del Norte for always making me feel very welcome. Thanks to Dr. Carlos Jaramillo at the Smithsonian Tropical Research Institute and its Center for Tropical Paleoecology and Archeology (CTPA), Dr. Maria Velez at the University of Regina, and again to Dr. Mark Brenner at the University of Florida for allowing me to do a research internship.

I am grateful to Sindy, Oscar and Silvio for their wonderful friendship and support over the years, whether it was in the lab, in the field, or at the office.

I am indebted to my family members, who have been a constant source of love and understanding, regardless of how much I neglected them. A special thanks to my personal guide, for encouraging me to pursue my dreams. Daniel and Eliana, thank you for sticking by me through the highs and lows of my PhD. Also, thanks to Frank, Daniel and Eliana for the cathartic gatherings on so many "bordillo" afternoons.

This project would not have been possible without the help of the Administrative Department of Science, Technology and Innovation COLCIENCIAS through the Nacional Doctorates Program 727 (National Doctorates), and the Foundation for the Promotion of Research and Technology (Ban Republic). Thanks to Drs. Natalia Hoyos, Jorge Pierini, Jean Michael Martínez, and Alice Newton for trusting my research, and Dr. Eric Wolanski for providing the LOICZ model used in this research.

Presentation

This document is presented in fulfillment of the requirements for the degree of Doctor of Marine Science within the Universidad del Norte. It contains relevant information to understand the physical and biogeochemical functioning at the Magdalena River mouth. This document presents important information relevant to the study of turbid and tropical estuaries.

The document is divided into five chapters. The first chapter **(Chapter 1)** provides an overview and defines the research objectives. The second chapter **(Chapter 2)** looks into the fluvial and oceanographic influences on suspended sediment dispersal in the Magdalena River Estuary. The third chapter describes **(Chapter 3)** nutrient Input and net ecosystem productivity in the mouth of the Magdalena River. The fourth chapter **(Chapter 4)** looks at the relationship between temperature, salinity and chlorophyll-a in the mouth of the Magdalena River. Finally, the fifth chapter **(Chapter 5)** presents the most relevant conclusions and future research topics, based on the results of this research**.**

Publications during candidature

Peer-reviewed papers

Torregroza-Espinosa Ana Carolina., Correa-Metrio Alex Restrepo Juan Camilo., Escobar Jaime., Hoyos Natalia., Pierini Jorge., Martínez Jean-Michel. 2020. Fluvial and oceanographic influences on suspended sediment dispersal in the Magdalena River Estuary. Journal of Marine Systems, 204: 103282. https://doi.org/10.1016/j.jmarsys.2019.103282.

Submitted papers

Torregroza-Espinosa Ana Carolina., Restrepo Juan Camilo., Escobar Jaime., Brenner Mark., Newton Alice., Nutrient Input and Net Ecosystem Productivity in the Mouth of the Magdalena River, Colombia. Submitted to Estuarine, Coastal and Shelf Science. Minor Revision (April 2020).

Conferences

Torregroza-Espinosa Ana Carolina., Restrepo Juan Camilo., Escobar Jaime., Hoyos Natalia., Pierini Jorge. 2018. Estimation of Surface Suspended Sediment Concentration in the Magdalena River Mouth Using MODIS Images. Particles in America (PIA), Vitoria, Brazil.

Publications included in this thesis as chapters

Torregroza-Espinosa Ana Carolina., Correa-Metrio Alex Restrepo Juan Camilo., Escobar Jaime., Hoyos Natalia., Pierini Jorge., Martínez Jean-Michel. 2020. Fluvial and oceanographic influences on suspended sediment dispersal in the Magdalena River Estuary. Journal of Marine Systems, 204: 103282. https://doi.org/10.1016/j.jmarsys.2019.103282 – incorporated into Chapter 2.

Torregroza-Espinosa Ana Carolina., Restrepo Juan Camilo., Escobar Jaime., Brenner Mark., Newton Alice., Nutrient Input and Net Ecosystem Productivity in the Mouth of the Magdalena River, Colombia. Submitted to Estuarine, Coastal and Shelf Science (Minor Revision, April 2020) – incorporated into Chapter 3.

Content

CHAPTER 1 ..... **10**

1. Introduction **10**

References 13

CHAPTER 2 ..... **18**

2. Fluvial and Oceanographic Influences on Suspended Sediment Dispersal in the Magdalena River Estuary **18**

Abstract 18

Introduction 19

Study Zone 20

Methods 23

Image Calibration 24

River plume estimation 25

Effects of fluvial and oceanographic variables 27

Results 27

Calibration Model 27

Estimated Surface Suspended Sediment Concentration 30

Shape and area of solid and diffuse plumes 37

Direction and length of the solid plume 42

Influence of Fluvial and Oceanographic Factors 44

Discussion 46

Calibration Model 46

Turbidity Plume Features 48

References 50

CHAPTER 3 ..... **60**

3. Nutrient Input and Net Ecosystem Productivity in the Mouth of the Magdalena River, Colombia **60**

Abstract 60

Introduction 61

Study Zone 62

Methods 65
Data Collection and Laboratory Analysis 65
Additional Model Requirements 65
Stratified Muddy LOICZ model 66
Results 67
Nutrient Concentrations 67
Salinity and SPM Gradients 68
Stratified Muddy LOICZ Model 74
Water-Salt Balance 74
Dissolved Inorganic Phosphorus (DIP) Transport 76
Net DIN Transport 79
Discussion 82
Biogeochemical Dynamics in the Magdalena River Estuary 82
Stratified Muddy LOICZ Model 86
References 87
CHAPTER 4 96
4. Spatio-temporal variability of temperature, salinity and chlorophyll a in the Magdalena River mouth 96
Abstract 96
Introduction 97
Study Zone 98
Methods 101
Data acquisition 101
Processing and Data Analysis 103
Results 104
SSS: Calibration Model 104
Spatio-temporal distribution of SSS, SST and Chl-a 105
Monthly inter-annual patterns of SSS, SST and Chl-a 109
Monthly patterns of SST, SSS and Chl-a 112
Trophic State Index (TSI) in the Magdalena River mouth 114

Influence of Fluvial and Oceanographic Factors 115
Discussion 117
SSS and SST Patterns in the Magdalena River mouth 117
Primary Productivity in the Magdalena River mouth 118
References 121
CHAPTER 5 130
5. Conclusions and Future Research 130

List of Tables

CHAPTER 1

Table 1. In situ measurements of surface suspended sediment concentration 28
Table 2. Models obtained for the estimation of the surface suspended sediment concentration 29
Table 3. Surface suspended sediment concentrations (SSSC) calculated in the Magdalena River mouth with the selected model 31
Table 4. Characteristics of plumes delimited in the Magdalena River mouth 41
Table 5. Summary statistics of fixed effects of the models obtained 46

CHAPTER 2

Table 1. Additional information required for the Muddy-LOICZ model 66
Table 2. Averages and standard deviations of dissolved inorganic nutrient concentrations 67
Table 3. Hydrologic variables for the Magdalena River Estuary 74
Table 4. Seasonal variation of dissolved inorganic phosphorus 77
Table 5. Seasonal difference in the partition (distribution) coefficient 77
Table 6. Seasonal difference in dissolved inorganic phosphorus 77
Table 7. Seasonal variation of dissolved inorganic nitrogen 79
Table 8. Seasonal variation of dissolved inorganic nitrogen 80

CHAPTER 3

Table 1. Trophic State Index (TSI) 103

List of Figures

CHAPTER 1

Figure 1. Magdalena River mouth. 23
Figure 2. Definition of the diffuse plume, solid plume and mixing area 26
Figure 3. Scatter plot of the MODIS-derived surface suspended sediment concentrations (SSSC) vs. in- situ measurements 30
Figure 4. SSSC in the Magdalena River mouth 36
Figure 5. SSSC and delimitation plume for 2006 (typical year) 38
Figure 6. SSSC and delimitation plume for 2010 (anomalous year) 39
Figure 7. Diffuse and solid plume, and mixing area. A) Diffuse and solid plume in the Magdalena River mouth 40
Figure 8. Elongation ratio in the Magdalena river mouth 41
Figure 9. Solid plume in the Magdalena River 43
Figure 10. Streamflows and sediment transport in the Magdalena River 44
Figure 11. Principal Component Analysis (PCA) 45

CHAPTER 2

Figure 1. Study area. A) Location of the Magdalena River mouth 64
Figure 2. Salinity and SPM concentrations 69
Figure 3. Vertical profiles of salinity and SPM 70
Figure 4. Concentrations of particles of different grain size 72
Figure 5. Concentrations of particles of different grain size 73
Figure 6. Water-Salt Balance 75
Figure 7. DIP Budget 78
Figure 8. DIN Budget 81

CHAPTER 3

Figure 1. Magdalena River mouth 101
Figure 2. Scatter plot of the MODIS-derived SSS vs. in situ measurements 104
Figure 3. Quarterly Average of SSS in the Magdalena River mouth 106
Figure 4. Quarterly Average of SST in the Magdalena River mouth 107
Figure 5. Quarterly Average of Chl-a in the Magdalena River mouth 108

Figure 6. SSS in the Magdalena River mouth 110
Figure 7. SST in the Magdalena River mouth 111
Figure 8. Chl-a in the Magdalena River mouth for the period 112
Figure 9. Monthly average of SSS, SST and Chl-a 114
Figure 10. TSI in the Magdalena River mouth 115
Figure 11. Principal component analysis (PCA) 116

CHAPTER 1

1. Introduction

The characteristics of estuaries depend mainly on the magnitude and variability of river discharge and tidal forcing (Kjerfve, 1994). Estuaries present strong temporal and spatial gradients with respect to their physical, chemical and biological properties, as a result of changes in fluvial contributions (Nogueira et al., 1997). Therefore, biogeochemical processes are extremely complex (Fourqurean et al., 1993; Fernández-Nóvoa et al., 2015). Temperature and salinity are the most relevant features of coastal marine ecosystem dynamics (Urquhart et al., 2013), as variations in these parameters can influence the movement of water masses, water column stratification caused by density differences, transport of sediments, and mixing conditions (Bianchi, 2007; Geyer, 2010; Obeso-Nieblas et al., 2012; Osadchiev et al., 2017). Also, temperature and salinity may play roles in nutrient distributions and concentrations (Windom et al., 2006), and biogeochemical processes and ecological productivity, through alterations in biochemical reactions that regulate the enzymatic processes of respiration and photosynthesis (Xia and Jiang, 2015; Quamrul et al., 2016). The physical dynamics of estuaries/deltas of the micro-tidal domain, which are highly stratified and turbid, have been little studied. Therefore, we lack detailed knowledge regarding relationships among spatio-temporal variations in salinity and temperature, the extent and structure of convergence fronts and the mixed layer, nutrient distribution and primary productivity in this type of estuary.

Global studies have highlighted the importance of nutrients to ecosystem health in coastal environments (Kamphuis, 2000; Durrieu de Madron et al., 2003; Bianchi, 2007; Gao et al., 2008; Mbaye et al., 2016: Kiwango et al., 2018). Nutrients exert strong control over primary production and trophic status (Smith et al., 2005; Quamrul et al., 2016). Alterations to the Redfield ratio can cause environmental problems such as eutrophication, leading to deterioration in water quality (Tett et al., 2003; Mbaye et al., 2016; Kiwango et al., 2018). Inland waters normally have higher concentrations of nutrients than marine waters (Xia and Jiang, 2015). Concentrations of nutrients in estuarine areas depend on river transport and remineralization of organic matter (Gao et al., 2008; Mbaye et al., 2016). Sediments function as a nutrient reservoir, and remineralization of organic matter releases nutrients into the water column, either in dissolved form by diffusion, or as suspended particulate material (Srithongouthai et al.,

2003). The amount and properties of suspended particulate material can directly influence the concentration and distribution of nutrients (Gao et al., 2008; Mbaye et al., 2016). Thus, the biogeochemical processes that sedimented organic matter undergoes can alter the overlying water quality, mainly when hydrodynamic factors increase chemical exchanges between the sediment and water (Baumgarten et al., 2001). Despite advances in the understanding of nutrient loading and fluxes in estuarine ecosystems (Gordon et al., 1996; Smith et al., 2005; Gao et al., 2008; Swaney et al., 2011), most studies have not considered the contribution of suspended sediment to the nutrient load in estuaries (Xu et al., 2013). It is thus necessary to further investigate this topic, especially in estuaries/deltas that transport high sediment loads.

There is a complex and ever-changing relationship between nutrient loading and its effects on the ecosystem, which depends on nutrient sources and the physical dynamics of the estuary (Gilbert et al., 2005). Estuaries are particularly vulnerable to eutrophication, which originates from increased loading of nutrients or organic matter (Quamrul et al., 2016). This translates into high and fluctuating densities of phytoplankton and frequent changes in community composition. Increased primary productivity leads to rapid consumption of oxygen, which may be depleted, causing hypoxia or anoxia, thereby leading to the emergence of "dead zones" (Mbaye et al., 2016; Kiwango et al., 2018). Eutrophication in coastal areas is considered undesirable, because there are multiple negative consequences, including toxic algae (cyanobacteria) blooms, depletion of dissolved oxygen, high mortality of aquatic organisms, and alterations in the food web (Cloern, 2001). Nutrient uptake in the ecosystem is carried out by primary producers (phytoplankton), which, in turn, serve as food for secondary producers (zooplankton and fish) (Pinckney et al., 2001). Phytoplankton, which comprises the base of the trophic pyramid, is an important indicator of biogeochemical changes (Cloern, 2001). Recent studies have reported the occurrence of cultural eutrophication in estuaries (Joye et al., 2006; Zhao et al., 2012; Zhang et al., 2016; Karydis and Kitsiou, 2019), i.e. cases in which human-mediated nutrient inputs have exceeded the natural capacity of these ecosystems to absorb nutrient loads, thereby pushing the ecosystem to a new trophic state (Mitchell and Uncles, 2013; Dolbeth et al., 2016).

Density stratification, nutrient concentrations, amounts of suspended particulate matter, rates of primary productivity, and trophic status are all related in estuarine waters (Espinosa-Garzón et al., 2001; Gao et al., 2008; Quamrul et al., 2016). Nutrient

concentrations and primary productivity are higher in estuaries than in adjacent open ocean regions, where nutrients and algal abundance decreases as salinity increases. Such relations are nearly always seen, especially in situations where estuaries rapidly renew their waters (Windom et al., 2016). In general, there is a negative correlation between nutrient concentration and salinity in the mixing zone (Cravo et al., 2003). Additionally, the biochemical reactions involved in primary production (photosynthesis) are affected by temperature (Gilbert et al., 2005). Considering the importance of hydrologic, nutrient and sediment inputs to the physical and biogeochemical dynamics of estuaries (Kasai et al., 2010; Meng et al., 2015), it is necessary to generate information that enables analysis of the relationships among physical, chemical and biological processes in highly stratified and turbid estuaries/deltas.

Nutrient loading estimates in turbid estuaries must include the role of suspended sediment, which should be incorporated into estuarine biogeochemical models (Xu et al., 2013). One of the most widely used biogeochemical models to determine nutrient load is the LOICZ model (Land-Ocean Interactions in the Coastal Zone) (Gordon et al., 1996; Smith et al., 2005; Swaney et al., 2011). The LOICZ model uses mass and material balance equations (water, salts and nutrients), for one or two layers, considering whether the ecosystem is mixed or stratified (Gordon et al., 1996; Smith et al., 2005). This model is used to quantify and understand the contribution of the continental margin on the transfer of nutrients from the river to the estuarine zone, and from the estuarine zone to the ocean. It has been applied to the study of >200 estuaries worldwide (Durrieu de Madron et al., 2003; Swaney et al., 2011; Xu et al., 2013).

Multiple approaches have been used to quantify physico-chemical parameters in waters, highlighting *in situ* measurements and laboratory analysis. But these methods are limited with respect to capturing spatial and temporal variations over large areas and long time periods, as it is extremely challenging to conduct such rigorous sampling and accumulate sufficient data (Moreno-Madriñan et al., 2015: González-Márquez et al., 2018). In recent years, new techniques for monitoring water bodies have emerged, one of which is remote sensing (Hu et al., 2004). Remote sensing has been used to acquire physical, chemical and biological data in water bodies at high spatial and temporal resolution, using satellite images obtained from remote sensors (Hu et al., 2004). The inherent optical properties, obtained from color images of the ecosystem, can provide information on temperature, salinity, dissolved organic carbon, suspended solids,

chlorophyll *a*, and other variables (Ruiz-Ochoa et al., 2012; Urquhart et al., 2012; Daqamseh et al., 2019; Torregroza-Espinosa et al., 2020). All these variables can be analyzed on a year-to-year basis, enabling identification of spatial and temporal variations.

Studies that combine use of satellite-derived information, biogeochemical models and field data guarantee more robust results, especially given the variability in estuarine processes and the sensitivity of these environments to seasonal conditions. This study was carried out in the highly stratified and turbid environment of the deltaic front of the Magdalena River, and was prompted by the need to better understand the physical and biogeochemical dynamics of turbid, tropical estuaries. The study focused on investigation of seasonal changes in the spatial distribution of surface temperature, surface salinity and suspended sediment, and determination of their influence on nutrient concentrations, and primary productivity (chlorophyll-a) in the deltaic front of the Magdalena River. Specifically, I set out to: (*i*) establish the spatio-temporal patterns of suspended sediment, surface temperature, surface salinity and surface Chl-a, and their relationship to the extent and structure of convergence fronts; (*ii*) identify the role of suspended sediment on the nutrient load and define the mechanisms that control this interaction; (*iii*) evaluate patterns in the distribution and concentration of chlorophyll-a, produced by the combined effects of the structure of the convergence fronts and oceanographic variables (e.g. streamflow, winds and currents).

References

Baumgarten, M., Niencheski, L., Veeck, L. 2001. Nutrientes na coluna da água e na água intersticial de sedimentos de uma enseada rasa estuarina com aportes de origem antrópica. Atlantica, 23, 101-116.

Bianchi, T. 2007. Biogeochemistry of estuaries. New York: Oxford University Press, 689 p.

Cloern, J. 2001. Our evolving conceptual model of the coastal eutrophication problem. Marine Ecology Progress Series, 210, 223-253. http://dx.doi.org/10.3354/meps210223.

Daqamseh, S. T., Al-Fugara, A., Pradhan, B., Al-Oraiqat, A., Habib, M. 2019. MODIS Derived Sea Surface Salinity, Temperature, and Chlorophyll-a Data for Potential Fish Zone Mapping: West Red Sea Coastal Areas, Saudi Arabia. Sensors (Basel, Switzerland), 19(9), 2069. https://doi.org/10.3390/s19092069.

Dolbeth, M., Vendel, A., Pessanha, A., Patrício, J. 2016. Functional diversity of fish communities in two tropical estuaries subjected to anthropogenic disturbance. Marine Pollution Bulletin, 112, 244-254. https://doi.org/10.1016/j.marpolbul.2016.08.011.

Durrieu de Madron, X., Denis, L., Diaz, F., García, N., Guieu, C., Grenz, C., Loÿe-Pilot, M., Ludwig, W., Moutin, T., Raimbault, P., Ridame, C. 2003. Nutrients and carbon budgets for the Gulf of Lion during the Moogli cruises. Oceanologica Acta, 26, 421-433. doi:10.1016/S0399-1784(03)00024-0.

Espinosa-Garzón, L., Gaxiola-Castro, G., Robles-Pacheco, J., Nájera-Martínez, S. 2001. Temperatura, salinidad, nutrientes y clorofila a en aguas costeras de la ensenada del sur de california. Ciencias marinas, 27(3), 397-422. http://dx.doi.org/10.7773/cm.v27i3.490.

Fernández-Nóvoa, D., Mendes, R., de Castro, M., Dias, J., Sánchez-Arcilla, A., & Gómez-Gesteira, M. 2015. Analysis of the influence of river discharge and wind on the Ebro turbid plume using MODIS-Aqua and MODIS-Terra data. Journal of Marine Systems, 142, 40-46. https://doi.org/10.1016/j.jmarsys.2014.09.009.

Fourqurean, J., Jones, R., Zieman, J. 1993. Processes influencing water column nutrient characteristics and phosphorus limitation of phytoplankton biomass in Florida Bay, FL, USA: interferences from spatial distributions. Estuarine, Coastal and Shelf Science, 36, 295-314.

Gao, L., Li, D. J., & Ding, P. X. 2008. Variations of nutrients in response to the highly dynamic suspended particulate matter in the Changjiang (Yangtze River) plume. Continental shelf research, 28 (17), 2393-2403. https://doi.org/10.1016/j.ecss.2011.07.015.

Geyer, W. 2010. Estuarine salinity structure and circulation. In: A. Valle-Levinson (Ed.), Contemporary issues in estuarine physics, transport and water quality. New York: Cambridge University Press, 12-26 p.

Gilbert, P. M., Seitzinger, S., Heil, C. A., Burkholder, J. M., Parrow, M. W., Codispoti, L. A., Kelly, V. 2005. The role of eutrophication in the global proliferation of harmful algal blooms: new perspectives and new approaches. Oceanography, 18, 198-209. https://doi.org/10.5670/oceanog.2005.54.

González-Márquez, L.C., Torres-Bejarano, F.M., Rodríguez-Cuevas, C., Torregroza-Espinosa, A.C., Sandoval-Romero, J.A., 2018. Estimation of water quality parameters using Landsat 8 images: application to Playa Colorada Bay, Sinaloa, Mexico. Applied Geomatics 10 (2), 147–158. https://doi.org/10.1007/s12518-018-0211-9.

Gordon Jr, D., Boudreau, P., Mann, K., Ong, J., Silvert, W., Smith, S., Wattayakorn, G., Wulff, F., Yanagi, T. 1996. LOICZ biogeochemical modelling guidelines. LOICZ Reports and Studies No. 5, 96 p.

Hu, C., Chen, Z., Clayton, T., Swarzenski, P., Brock, J., Muller-Karger, F. 2004. Assessment of estuarine water-quality indicators using MODIS medium-resolution bands: initial results from Tampa Bay, Florida. Remote Sens. Environ, 93, 423-441. DOI: 10.1016/j.rse.2004.08.007.

Kamphuis, J. 2000. Introduction to Coastal Engineering and Management. Advanced Series on Ocean Engineering. Queens: University of Queens: World Scientific, 564 p.

Karydis, M., Kitsiou, D. 2019. Marine Eutrophication: A Global Perspective. 1st Edition, CRC Press. 194 p.

Kasai, A., Kurikawa, Y., Ueno, M., Robert, D., Yamashita, Y. 2010. Salt-wedge intrusion of seawater and its implication for phytoplankton dynamics in the Yura Estuary, Japan. Estuarine, Coastal and Shelf Science, 86, 408-414. doi:10.1016/j.ecss.2009.06.001.

Kjerfve, B. 1994. Coastal lagoons process. Elsevier Oceanography Series 60. Elsevier Science, 576 p.

Kiwango, H., Njau, K.N., Wolanski, E. 2018. The application of nutrient budget models to determine the ecosystem health of the Wami Estuary, Tanzania. Ecohydrology & Hydrobiology, 18(2): 107-119. https://doi.org/10.1016/j.ecohyd.2017.10.002.

Mbaye, M., Gaye, A., Spitsy, A., Dahnke, K., Afouda, A., Gaye, B. 2016. Seasonal and spatial variation in suspended matter, organic carbon, nitrogen, and nutrient concentrations of the Senegal River West Africa. Limnologica, 57, 1-13. http://dx.doi.org/10.1016/j.limno.2015.12.003.

Meng, J., Yu, Z., Yao, Q., Bianchi, S., Paytan, A., Zhao, B., Pan, H., Yao, P. 2015. Distribution, mixing behavior, and transformation of dissolved inorganic phosphorus and suspended particulate phosphorus along salinity gradient in the Changjiang Estuary. Marine Chemistry, 168, 124-134. https://doi.org/10.1016/j.marchem.2014.09.016.

Mitchell, S. B., Uncles, R. J. 2013. Estuarine sediments in macrotidal estuaries: future research requirements and management challenges. Ocean & Coastal Management, 79, 97-100. https://doi.org/10.1016/j.ocecoaman.2012.05.007.

Moreno-Madriñan, M., Rickman, D., Ogashawara, I., Irwin, D., Ye, J., Al-Hamdan, M. 2015. Using remote sensing to monitor the influence of river discharge on watershed outlets and adjacent coral reefs: Magdalena River and Rosario Islands, Colombia. International Journal of Applied Earth Observation and Geoinformation, 38, 204-215. https://doi.org/10.1016/j.jag.2015.01.008.

Nogueira, E., Pérez, F., Ríos, A. 1997. Seasonal patterns and long-term trends in an estuarine upwelling ecosystem (Ría de Vigo, NW Spain). Estuar. Coast. Shelf Sci, 44, 285–300.

Obeso-Nieblas, M., Gaviño-Rodríguez, J., Obeso-Huerta, H. 2012. Variabilidad espacial y estacional de temperatura, salinidad y densidad en Bahía Concepción, Golfo de California, México. Revista de Biología Marina y Oceanografía, 47(3), 489-502. DOI 10.4067/S0718-19572012000300011.

Osadchiev, A.A., Izhitskiy, A.S., Zavialov, P.O., Kremenetskiy, V.V., Polukhin, A.A., Pelevin, V.V., Toktamysova, Z.M., 2017. Structure of the buoyant plume formed by Ob and Yenisei river discharge in the southern part of the Kara Sea during summer and autumn. J. Geophys. Res. 122 (7), 5916–5935. https://doi.org/10.1002/2016JC012603.

Pinckney, J. L., Richardson, T. L., Millie, D. F., Paerl, H. W. 2001. Application of photopigment biomarkers for quantifying microalgal community composition and in situ growth rates. Org. Geochem, 32, 585–595.

Quamrul, A., Benson, B., Visser, J., Gang, D. 2016. Response of estuarine phytoplankton to nutrient and spatio temporal pattern of physico-chemical water quality parameters in little Vermilion Bay, Louisiana. Ecological informatics, 32, 79-90. https://doi.org/10.1016/j.ecoinf.2016.01.003.

Smith, S., Swaney, D., Buddemeier, R., Scarsbrook, M., Eatherhead, M., Humborg, C., Eriksson, H., Hannerz, F. 2005. River nutrient loads and catchment size. Biogeochemistry, 75, 83-107. https://doi.org/10.1007/s10533-004-6320-z.

Srithongouthai, S., Sonoyama, Y., Tada, K., Montani, S. 2003. The influence of environmental variability on silicate exchange rates between sediments and water in a shallow-water coastal ecosystem, the Seto Inland Sea, Japan. Mar. Poll. Bull, 47, 10-17.

Swaney, D., Smith, S., Wulff, F. 2011. The LOICZ biogeochemical modeling protocol and its application to estuarine ecosystems. Treatise on Estuarine and Coastal Science, 9, 136-159. https://doi:10.1016/B978-0-12-374711-2.00907-4.

Tett, P., Gilpin, L., Svendsen, H., Erlandsson, C., Larsson, U., Kratzer, S., Fouilland, E., Scory, S. 2003. Eutrophication and some European waters of restricted exchange. Continental Shelf Research, 23, 1635-1671. dx.doi.org/10.1016/j.csr.2003.06.013.

Torregroza-Espinosa, A.C., Restrepo, J.C., Correa-Metrio, A., Hoyos, N., Escobar, J., Pierini, J., Martínez, J.M. 2020. Fluvial and oceanographic influences on suspended sediment dispersal in the Magdalena River Estuary, Journal of Marine Systems, 204, 103282. https://doi.org/10.1016/j.jmarsys.2019.103282.

Windom, H., Moore, W., Niencheski, L., Jahnke, R. 2006. Submarine groundwater discharge: a large, previously unrecognized source of dissolved iron to the South Atlantic Ocean. Mar. Chem, 102, 252-266. DOI: 10.1016/j.marchem.2006.06.016.

Xia, M., Jiang, L. 2015. Influence of wind and river discharge on the hypoxia in a shallow bay. Ocean Dynamics, 65, 665-678. https://doi.org/10.1007/s10236-015-0826-x.

Xu, H., Wolanski, E., Chen, Z. 2013. Suspended particulate matter affects the nutrient budget of turbid estuaries: Modification of LOICZ model and application to the Yangtze Estuary. Estuarine, Coastal and Shelf Science, 127, 59-62. http://dx.doi.org/10.1016/j.ecss.2013.04.020.

CHAPTER 2

2. Fluvial and Oceanographic Influences on Suspended Sediment Dispersal in the Magdalena River Estuary

Abstract

The Magdalena River is the main contributor of fresh water and sediment to the Caribbean Sea. Hydrological inputs from the Magdalena River are 10287 and 4068 $m^3 s^{-1}$ at high and low flows, respectively. Sediment delivery from the Magdalena River is among the largest in the world, with 142 x 10^6 t yr^{-1} of transported suspended matter. We used MODIS images to develop a regional model and assess the spatial and temporal variability of suspended sediment concentration at the mouth of the Magdalena River, map the extent of the turbidity plume using its morphometric properties, and identify the main fluvial and oceanographic factors associated with plume variability. We analyzed monthly average suspended sediment concentration data for the period 2003-2017. MODIS images were calibrated with *in situ* measurements of suspended sediment concentrations in surface waters of the study area. A finite mixing model was used to identify turbidity thresholds and define areas within the plume. Calculated suspended sediment concentrations indicate high turbidity in the Magdalena River mouth (178.6 ± 78.7 mg L^{-1}), values that are of the same order of magnitude as those measured in the Yangtze, Huang He and Amazon River mouths. Calculated plume areas (diffuse, solid and mixing) and their shapes suggest that the Magdalena River plume has a limited area, related to conditions such as wind speed and direction, streamflow, and sediment transport. Calculated areas and shapes demonstrate the ability to generate a near-field area, which indicates the presence of a clear convergence front. The data also emphasize the importance of sediment transport from the Magdalena River to the Caribbean Sea. Such fluvial transport is important in the biogeochemistry of estuarine systems, especially in turbid estuaries, where there is marked variability in the distribution of sediment in surface waters.

Introduction

Plume formation at a river mouth is influenced by multiple processes, including mixing, horizontal advection, streamflow patterns, ocean currents, wind fields, tidal regimes and water residence time (Horner-Devine et al., 2015; Osadchiev, 2017). River plumes affect the physical, chemical and ecological dynamics of coastal zones through inputs of fresh water, dissolved nutrients, pollutants and suspended sediments (Fernández-Nóvoa et al., 2015). Thus, changes in characteristics of river plumes reflect temporal and spatial variations in the physical and chemical conditions of coastal zones (Meng et al., 2015; Kim et al., 2017b), which in turn affect processes linked to global biogeochemical cycles (Fernández-Nóvoa et al., 2017). Analysis of sediment concentrations at the mouths of rivers is critical to evaluate the impact of riverine sediment transport on marine and coastal environments, and to determine the capacity of these environments to respond to environmental perturbations caused by climate change and/or anthropogenic activities (Gao et al., 2011; Syvitski and Kettner, 2011).

High-discharge rivers with large sediment loads can have complex impacts on biogeochemical processes in receiving estuaries because of temporal variability in the hydrological regime, changes in sediment properties, and heterogeneous dispersal of suspended sediment (Xu et al., 2013). Under such conditions, the turbidity plume plays a large role in regional morphodynamics, nutrient and pollutant dispersal, and light penetration, which in turn affect the health and productivity of the estuarine ecosystem (Li et al., 2012). To better understand the influence of suspended sediment concentrations on the coastal environment, such material can be monitored by field sampling and laboratory analysis, or through *in situ* measurement. These approaches, however, are expensive, time-consuming, and in some cases a challenge because of the remote locations of river mouths. This limits the ability to monitor suspended sediment variations at high spatial and temporal resolution (He et al., 2008). What is more, horizontal advection, which determines the shape and extent of turbidity plumes, cannot be easily measured *in situ* (Jago et al., 2006). Remote sensing techniques have been used increasingly to study water quality in coastal ecosystems (Chen et al., 2015; Kim et al., 2017a; González-Márquez et al., 2018). One such application includes estimation of suspended sediment concentration in surface waters of estuarine ecosystems (Chen et al., 2015; Fernández-Nóvoa et al., 2017; Espinoza-Villar et al., 2018). Empirical models based on remotely sensed data, in combination with *in situ*

measurements of suspended sediment concentration, have improved knowledge about the dynamics, composition, occurrence and shape of turbidity plumes around the world (Devlin et al., 2012; Fernández-Nóvoa et al., 2017).

Recent studies in the Colombian Caribbean used remote sensing techniques to determine the impact of the sediment plume at the Magdalena River mouth and at its main distributary, El Canal del Dique, on coral reefs around the Rosario Islands, in the Caribbean Sea. Moreno-Madriñan et al. (2015) analyzed the turbidity plume using MODIS (Moderate Resolution Imaging Spectroradiometer) reflectance values. Restrepo et al. (2016b) calibrated MODIS images using field measurements from around the Rosario Islands, in Cartagena Bay, and in the Canal del Dique. Water turbidity at those locations is, however, lower than at the Magdalena River mouth (Restrepo et al., 2017b). The accuracy of satellite measurements decreases when applied in areas beyond zones used for calibration, because of changes in the components of coastal and inland waters (Chang et al., 2014). There is, however, no detailed information about the spatio-temporal variation of the sediment plume properties. It is thus critical to understand the inter-annual and intra-annual variability of suspended sediment concentrations, including the geometry of the turbidity plume, the horizontal gradient of suspended sediment concentrations, and the fluvial and oceanographic factors that influence suspended sediment dispersion. A more comprehensive study of the characteristics of the Magdalena River plume was therefore needed to explore patterns of suspended sediment concentration in surface waters of a tropical system with high water and sediment discharge. In this study, we used MODIS imagery to quantify the properties of the Magdalena River plume through space and time. Our main objectives were to: *(i)* determine the spatial and temporal variability of suspended sediment concentration in surface waters at the mouth of the Magdalena River, *(ii)* map the extent of the turbidity plume of the Magdalena River, as well as its morphometric properties, and *(iii)* identify the main fluvial and oceanographic factors that control the river plume variability.

Study Zone

The Magdalena River is Colombia´s main fluvial system. Its drainage basin has an area of 275438 km^2, and the main channel has a length of 1540 km. The Magdalena River is considered a tropical system of high water and sediment discharge (Restrepo et al., 2016a). Hydro-climatological patterns in the study area are affected by the seasonal position of the Intertropical Convergence Zone (ITCZ) (Poveda, 2004), During the dry

season, from January to April, average wind velocity is 6.0 m s^{-1} near the coast of Colombia (Montoya-Sánchez et al., 2018), average river discharge is 4361 m^3 s^{-1}, and average suspended sediment load is 218 x 10^3 t d^{-1} (Restrepo et al., 2016a). Northeast trade winds, with a dominant southward direction, have a strong influence during February and March and are responsible for the low rainfall during those months (Andrade, 2001). This season also exhibits high-energy wave conditions (Hs > 2.5 m) caused by strong north-east trade winds and cold fronts (Ortiz et al., 2013). During the wet season (September through November), winds are relatively weak, with average velocities of 2.0 m s^{-1} (Montoya-Sánchez et al., 2018), average river discharge is 8063 m^3 s^{-1}, and a sediment load of 531 x 10^3 t d^{-1} (Restrepo et al., 2016a). During that time, the mouth experiences low to moderate wave energy conditions (Hs < 1.5 m), with swells coming predominantly from the west and northwest (Ortiz et al., 2013). The circulation of the Colombian Caribbean basin is dominated by the Caribbean current, which flows in a west-northwestward direction through the northern Caribbean area, the Guajira emergence center, which flows westward and northward into the Caribbean Sea, and the Panama-Colombia cyclonic gyre, which flows southwest into the Caribbean Sea (Andrade, 2001). Wind stress from the northern trade winds is the primary forcing mechanism on surface currents in the Caribbean (Andrade, 2001). Close to the Magdalena River mouth, ocean currents have an average velocity of 0.3 m s^{-1} during the dry season, and 0.1 m s^{-1} during the wet season, with a southward direction in both seasons (Chassignet et al., 2006).

Deforestation, erosion, and mining in the Magdalena Basin in recent decades have led to changes in streamflow and sediment transport (Restrepo and Syvitski, 2006; Restrepo et al., 2014). There is also evidence of recent changes in hydrological patterns of the Magdalena River (Restrepo et al., 2014), specifically, a pronounced increase in streamflow since the year 2000 and a significant increase in the occurrence of extreme events such as floods and droughts. Suspended sediment load in the Magdalena River also increased, probably because of deforestation in the basin. Annual sediment load grew by an estimated 16 x 10^6 t yr^{-1} between 2000 and 2010 (Restrepo et al., 2016a). These changes have consequences for sediment dispersion, transfer of nutrients to the ocean, and the function of coastal ecosystems. The impacts of these hydrologic changes on suspended sediment concentrations in the Magdalena Basin have not been properly investigated.

The river mouth, Bocas de Ceniza, is located in the Colombian Caribbean (Figure 1). Its morphology was dramatically modified by construction of two breakwaters (7.4 and 1.4 km long), built in 1936 to prevent sedimentation and promote commercial navigation at the Port of Barranquilla. The mouth has a width of 430 m and a minimum depth of 9.1 m. A secondary mouth is located 130 km south, in Cartagena Bay, and is connected to the river through an artificial channel built during colonial times, the Canal del Dique (Restrepo et al., 2016a). The river also has a complex network of minor connections with the Ciénaga Grande de Santa Marta, the largest coastal lagoon in Colombia and a RAMSAR site (Vilardy et al., 2011). Bocas de Ceniza is a stratified, microtidal, turbid system (Restrepo et al., 2018). Surface water temperature varies between 26 °C and 31°C. Surface salinity varies considerably, from 0 within the fluvial region, to intermediate values in the mouth, to 33 in the adjacent coastal zone (Restrepo et al., 2018). Because of salinity differences, density gradients at the river mouth define the formation of a buoyant, well-defined river plume (i.e., hypopycnal) (Restrepo et al., 2018). In hypopycnal flows, when fluvial sediment inputs are much larger than marine-sediment inputs, large sediment concentrations are commonly observed near the top of the water column (Geyer et al., 2004). Such profiles have been observed in the delta front of the Magdalena River, particularly during the low-streamflow season, and because of the large amount of sediment transported by the Magdalena River (Restrepo and Kjerfve, 2000; Higgins et al., 2016). During the high-streamflow season (November 2012), the upper water layer in the river and the water at the delta front had suspended sediment concentrations of 2700 and 1500 mg L^{-1}, respectively (Restrepo et al., 2018). During the low-streamflow season (April 2013), the riverine section exhibited a suspended sediment concentration of 3100 mg L^{-1}, and the delta front had a value of 1100 mg L^{-1} (Restrepo et al., 2018).

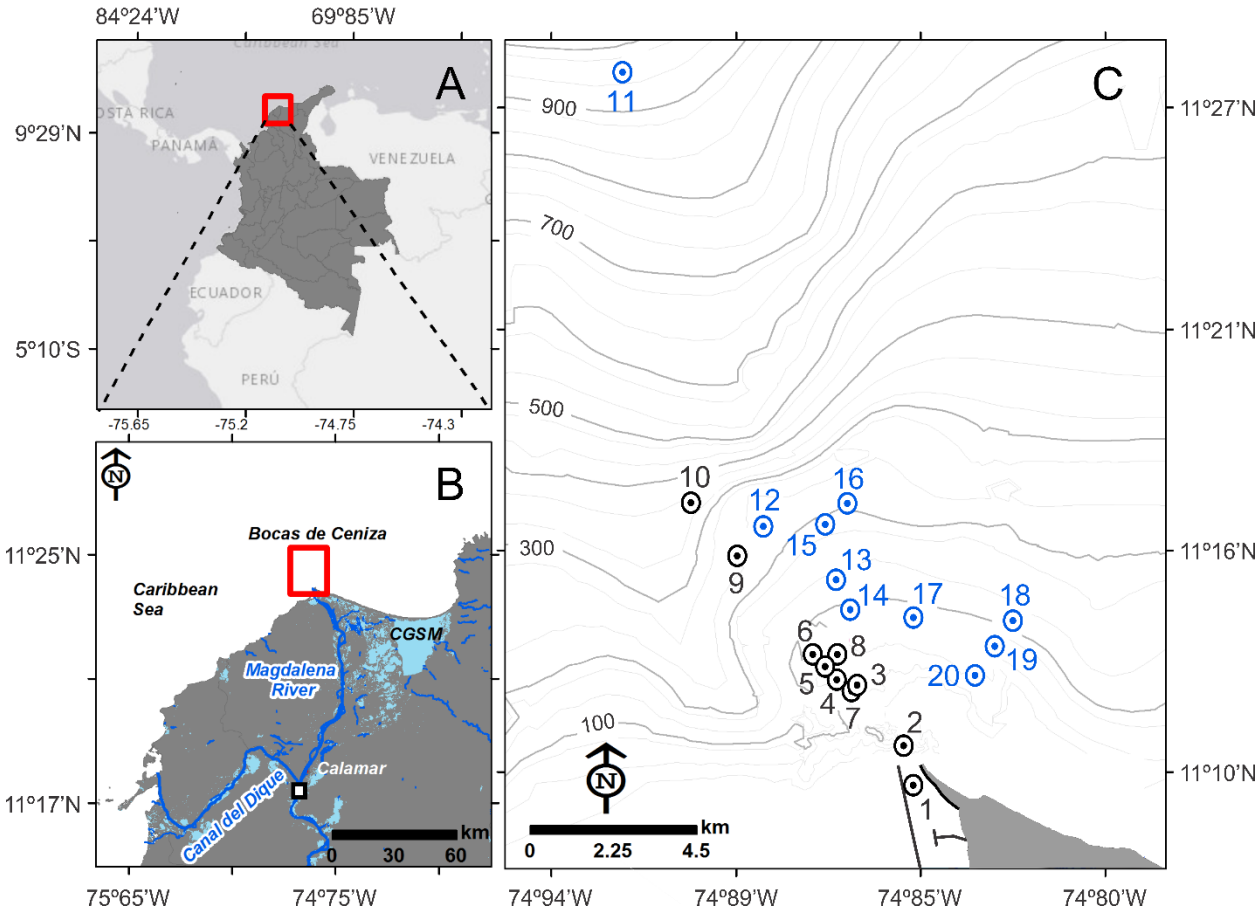

Figure 1. Magdalena River mouth. General location and sampling stations. Black points indicate the sampling stations in November 2017, and blue points indicate the sampling stations in August 2018. Depth contours in meters (m).

Methods

MODIS-Aqua images for the period 2003-2017 (720 images) were downloaded in HDF format from NASA (Ocean Color website, http://oceancolor.gsfc.nasa.gov). We used MODIS product MYD09Q1 (8-day composite) with atmospheric correction and a spatial resolution of 250 m. These images contain reflectance information from bands 1 and 2. Band 1 extends from 620 to 670 nm (red) and band 2 from 841 to 876 nm (near infrared). Images were cropped to the extent of the study area and monthly averages for bands 1 and 2 reflectance values were calculated.

Monthly wind (magnitude and direction) data were downloaded from WaveWatch III (http://polar.ncep.noaa.gov) and monthly surface current data were downloaded from the Hybrid Coordinate Ocean Model (https://hycom.org), for the same period (2003-2017), at coordinates close to the river mouth (11.30° N, -74.78° W). Monthly streamflow and suspended sediment load data for the same period (2003-2017) were retrieved from the Calamar Hydrological Station, which is the closest station, approximately 100 km upstream from the river mouth (IDEAM-Colombia, http://www.ideam.gov.co). Data on sediment grain size distribution in the study zone were acquired from a research project developed by the Universidad del Norte (Uninorte, 2019). Field measurements of suspended sediment concentration in surface waters were made at 10 sampling stations in November 2017 (sampling stations 1-10), and 10 sampling stations on August 2018 (sampling stations 11-20) (Figure 1), with a calibrated Optical Backscattering Sensor (OBS 3A, Scientific Campbell), using a sampling rate of 1 Hz. Image acquisition and processing were performed in R (R Core Team, 2018), using the package MODISTools (Tuck et al., 2014).

Image Calibration

We used MODIS images (MYD09GQ-Daily product) for calibration that were obtained on the same days as our field data were collected (November 21/2017 and August 8/2018). We fitted a statistical model to estimate suspended sediment concentration (dependent variable) from reflectance values of bands 1 and 2 (independent variables). Data normality was evaluated prior to model development using the Shapiro-Wilk Test (Yap and Sim, 2011). Because suspended sediment concentration data did not show a normal distribution, values were log-transformed. We constructed several models to explain sediment concentration as a function of single bands, and their polynomial combination (Chen et al., 2015).

We selected the best model based on multiple statistics (mean quadratic error, coefficient of determination, *p*-value and Akaike Information Criterion AIC) (Wu et al., 2014). The root mean square error (RMSE) measures the error between the observed and estimated value (Wu et al., 2014). The coefficient of determination and *p-value* indicate the significance of the model, and the nature of the relationship between variables (Wu et al., 2014). The AIC is an estimator of the relative quality of the statistical models. Given a collection of models for the data, AIC estimates the quality of each

model relative to each of the other models. Thus, AIC serves as a tool for model selection (Wu et al., 2014).

Validation of the selected model was evaluated through simple linear regression analysis, using the concentrations obtained from the MODIS spectral information and field measurement results. Suspended sediment concentrations in surface waters in the Magdalena River mouth were calculated for the period 2003-2017, using the selected model. We identified trends in the surface suspended sediment concentrations calculated using the Mann-Kendall Test (MKT) (Yue et al., 2002). The MKT is a rank-based, non-parametric statistical test that can be used to detect and evaluate the significance of monotonic trends in time series (Yue et al., 2002).

River Plume Estimation

The geographic limits of the turbidity plume had to be defined to distinguish waters affected by the river plume from those that were not, i.e., the adjacent seawater (Fernández-Nóvoa et al., 2017). For this purpose, we used a finite mixing model to split monthly suspended sediment concentrations into two components (McLachlan and Peel, 2000). This procedure was based on the idea that, at any given time, the concentration of suspended sediment in surface waters of a given area is composed of two Gaussian distributions: 1) background suspended sediment concentrations in ocean waters, and 2) suspended sediment concentration in the plume. Each of these sources contributes to the total distribution of suspended sediment by a proportion denoted by λ_1 and λ_2 (with $\lambda_1 + \lambda_2 = 1$). The algorithm we used for splitting the data into these two components (Benaglia et al., 2009) characterizes each distribution in terms of their mean (μ_1 and μ_2), their standard deviation (σ_1 and σ_2), and the proportion it contributes to the general distribution (λ_1 and λ_2) (Figure 2A). Thus, it was possible to obtain statistical values for suspended sediment concentration in both seawater and the river plume, facilitating spatial delimitation of the turbidity plume. We used the upper confidence interval of the sea surface suspended sediment concentrations as a boundary to delimit the "diffuse plume" (Figure 2B). In addition, we used the mean suspended sediment concentration of the same distribution to delimit the "solid plume" (Figure 2B). The diffuse plume includes the solid plume. We defined a "mixing area" as the difference between the area of the diffuse plume and the area of the turbid plume, i.e. a transition area between the core of the plume (i.e. solid plume) and the seawater (Figure 2B). Consequently, the surface water in the study area can be divided into three categories:

(1) seawater regime (i.e. outside the diffuse plume), (2) river plume regime (i.e. solid plume), and (3) unstable regime of the plume front (i.e. mixing area).

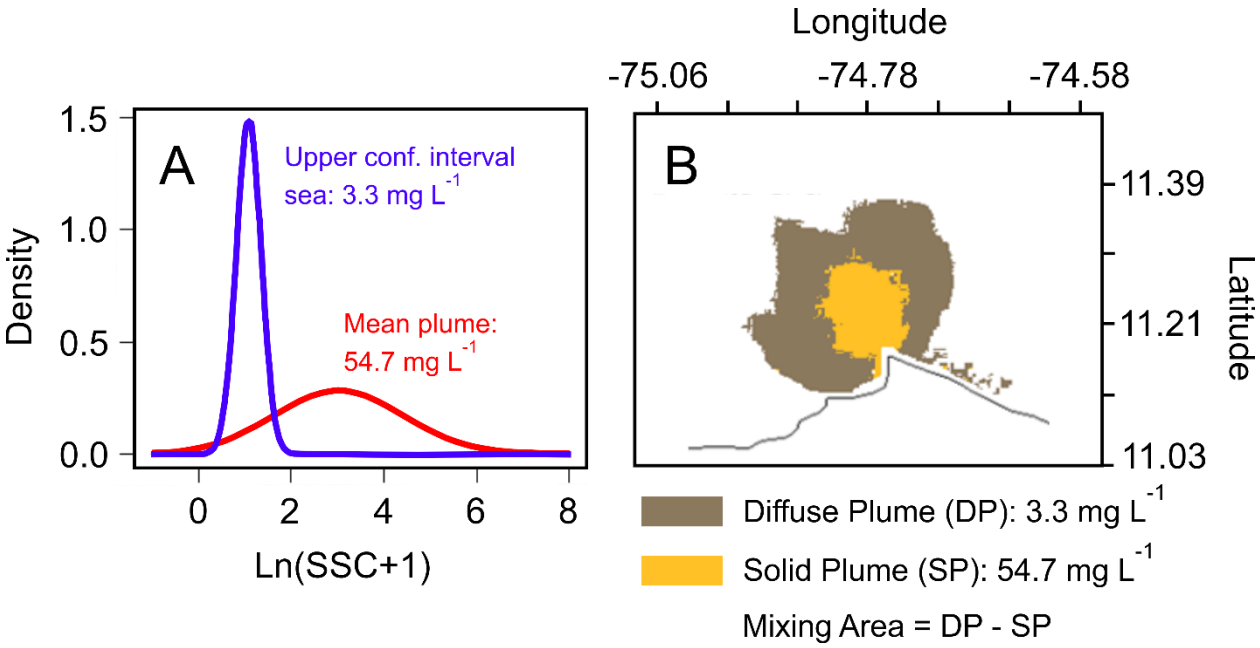

Figure 2. Definition of the diffuse plume, solid plume and mixing area for October 2004. A) Finite mixture model. The blue line indicates the density function of surface suspended sediment concentrations in ocean waters, and the red line indicates the density function of surface suspended sediment concentrations of the plume. B) Spatial representation of the diffuse plume, solid plume and mixing area. Dark brown area indicates the diffuse plume, which includes the solid plume, and orange area indicates the solid plume only. The mixing area was calculated as the difference between the areas (km^2) of the diffuse and solid plumes.

Once the solid plume was spatially delimited, vectors were drawn from the river mouth to 25,000 points located randomly inside the plume, to estimate the plume's average length (the distance from Bocas de Ceniza to the most distant boundary of the solid plume) and direction (angle in geographic coordinates). This procedure was repeated for each month of each year to characterize the intra-annual variability of the plume. Additionally, we calculated the elongation ratio (shape coefficient) as the quotient between the solid plume area and plume length. According to the elongation ratio, the

plume shape can be classified as circular (0.9~1.0), oval (0.8~0.9), less elongated (0.7~0.8), elongated (0.5~0.7), and more elongated (less than 0.5) (Gajbhiye, 2015).

Effects of Fluvial and Oceanographic Variables

A Principal Component Analysis (PCA), based on the entire dataset (plume attributes and independent explanatory variables), was used to explore the relationship among variables and select explanatory variables for plume attributes, avoiding collinearity among variables (Jolliffe, 2002). The influence of fluvial and oceanographic variables (streamflow, suspended load, winds and surface currents) on the characteristics of the turbidity plume was analyzed using additive linear models (Wood, 2006). Monthly solid plume (area, length and direction), and diffuse plume (area) characteristics were used as dependent variables, whereas monthly wind (direction and magnitude), streamflow, and suspended load were used as independent variables. Surface currents were excluded from the analyses because of their collinearity with wind. Different linear additive models were explored, all of them including fixed and random components, the former composed of the aforementioned independent variables, and the latter composed of hierarchical (monthly), seasonal, autoregressive (time, order 1) or random walk (rw) error structures (Wood, 2006). In each case, we selected the best model using multiple statistics (mean quadratic error, determination coefficient, *p-value* and Deviance Criterion Information DIC) (Wu et al., 2014). The DIC is a hierarchical modeling generalization of the Akaike Information Criterion (AIC). It is particularly useful in Bayesian model selection (Celeux et al., 2006).

Results

Calibration Model

Field measurements of suspended sediment concentrations varied from 2535 mg L^{-1} in the Magdalena River mouth (station 1) to 0 mg L^{-1} in the most distant site, located ~20 km from the river mouth (station 11) (Table 1, Figure 1). The first sampling coincided with the wet season (November 2017), whereas the second sampling took place in the transition period (August 2018). Highest concentrations were recorded in August 2018 (Table 1). In general, sampling stations close to the river mouth exhibited values >1000 mg L^{-1}.

Table 1. *In situ* measurements of surface suspended sediment concentration (SSSC), during sampling I (November 2017) and sampling II (August 2018).

	Sampling I (November 2017)			Sampling II (August 2018)	
Sampling Station	**Distance from the river mouth (km)**	**SSSC (mg L^{-1})**	**Sampling Station**	**Distance from the river mouth (km)**	**SSSC (mg L^{-1})**
1	$^{+}$0.8	2535	11	19.6	0.0
2	0.3	1963	12	7.3	851
3	2.2	1878	13	5.1	1605
4	2.7	641	14	4.2	1270
5	3.1	610	15	6.6	1061
6	3.6	316	16	6.9	1023
7	2.2	336	17	3.7	1501
8	3.6	320	18	4.7	1527
9	6.7	139	19	3.8	1760
10	8.7	185	20	2.9	2266

Note. $^{+}$upstream direction

The statistically significant models that describe suspended sediment concentrations in surface waters as a function of reflectance bands 1 and 2 (Table 2), all show coefficient of determination values >0.88 and *p*-values below 0.01 (R^2>0.88, *p-value*<0.01). The predictive power and statistical properties of the models, as expressed by the RMSE and the AIC, respectively, pointed to Model 2 as the best mathematical representation of the relationship between suspended sediment concentrations in surface waters and band 1 and 2 reflectance values (Equation 1).

$$\mathrm{SSSC} = \exp^{(-1.085e{-}04+7.724e{+}01(\mathrm{RB1})-3.305e{+}02(\mathrm{RB1}^2)-5.118e{+}02(\mathrm{RB2}^2)}$$

Where SSSC is surface suspended sediment concentration (mg L^{-1}), RB1 is band 1 reflectance ($W{\cdot}sr^{-1}{\cdot}nm^{-1}$) and RB2 is band 2 reflectance ($W{\cdot}sr^{-1}{\cdot}nm^{-1}$).

Table 2. Models obtained for the estimation of the surface suspended sediment concentration at the mouth of the Magdalena River, with statistics. SSSC: surface suspended sediment concentration, RB1: band 1 reflectance, RB2: band 2 reflectance.

Model	Statistical Values			
	R^2	p-value	RMSE	AIC
$SSSC = exp^{(-2.641e-03+8.807e+01(RB1)-2.204e+01(RB2)-3.729e+02(RB1^2)+6.866e+02(RB2^2))}$	0.95	5.3e-11	364	21
$SSSC = exp^{(-1.085e-04+7.724e+01(RB1)-3.305e+02(RB1^2)-5.118e+02(RB2^2))}$	**0.96**	**3.9e-12**	**358**	**19**
$SSSC = exp^{(0.3066+44.2716(RB1)-368.86(RB2^2))}$	0.94	1.4e-11	574	27
$SSSC = exp^{(0.3066+44.2716(RB1)+368.86(RB2^2))}$	0.88	4.9e-10	679	40

The selected model showed generally good agreement between satellite-derived surface suspended sediment concentrations and field measurements (Figure 3). Most points were well distributed along the regression line. Statistical analysis showed an R^2 of 0.81 and a *p-value*<0.01, indicating that the satellite data can be used to predict accurately the surface suspended sediment concentrations. Although the dataset was small (20 sampling stations), data cover a wide range of surface suspended sediment concentrations and the model performs well under the entire range of suspended sediment concentrations.

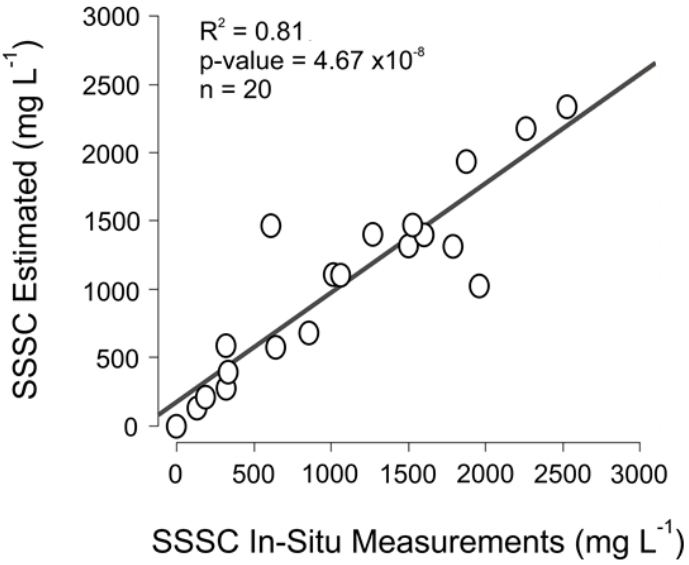

Figure 3. Scatter plot of the MODIS-derived surface suspended sediment concentrations (SSSC) vs. *in situ* measurements. The solid line is the regression line.

Estimated Surface Suspended Sediment Concentration

Surface suspended sediment concentrations of the Magdalena River estuary were estimated using the selected model (Table 2). A distinction was made between solid and diffuse plume suspended sediment concentration. For both types, suspended sediment concentration varied in time and space (Table 3). Suspended sediment concentrations in the solid plume showed a mean value of 178.6 ± 78.7 mg L^{-1} from 2003 to 2017. Upper extreme concentration was observed in August 2010 (1300 mg L^{-1}). No large variations were observed after September 2013 (Figure 4A). Estimated sea concentrations had a mean value of 6.3 ± 5.2 mg L^{-1}, with the upper extreme value in August 2010 (232 mg L^{-1}). The inter-annual series appears to show a decreasing trend for suspended sediment concentrations. The Mann-Kendall analysis, however, indicated that only sea concentration had a statistically significant decreasing trend through time ($p \leq 0.05$), with a confidence interval of 95% (Figure 4A). Also, the lowest monthly variability was observed in January, February and March (dry season) (Figures 4A and 4B). For April and May, large variability was observed in the solid plume (Table 3). Solid plume concentrations showed highest yearly estimated sediment variability and concentrations in September, i.e. the beginning of the wet season (Figure 4C). Likewise,

seasonal variability of estimated sea surface suspended sediment concentrations was highest in September and October (wet season) (Figure 4C).

Table 3. Surface suspended sediment concentrations (SSSC) calculated in the Magdalena River mouth with the selected model and turbid thresholds. Range of SSSC corresponds to the minimum and maximum value.

Characteristic		Plume Concentrations (mg L^{-1})	Sea Concentrations (mg L^{-1})
Mean value ± DE		178.6 ± 78.7	6.3 ± 5.2
Upper extreme value		1300.0	232.0
Lower extreme value		7.0	0.5
SSSC January-Range		7.0-15.0	1.0-1.2
SSSC February-Range		8.0-14.0	1.0-1.2
SSSC March-Range		10.0-32.0	1.0-1.4
SSSC April-Range		20.0-215.0	1.1-5.3
SSSC May-Range		14.0-215.0	1.0-7.3
SSSC June-Range		10.0-143.0	1.0-4.3
SSSC July-Range		12.0-98.0	1.0-3.9
SSSC August-Range		20.0-46.0	0.9-1.9
SSSC September-Range		11.0-237.0	1.2-14.0
SSSC October-Range		31.0-237.0	1.4-10.9
SSSC November-Range		12.0-47.0	1.0-2.0
SSSC December-Range		8.0-41.0	1.0-1.8
Year	**Month**	**Threshold SP (mg L^{-1})**	**Threshold DP (mg L^{-1})**
2003	January	9.5	1.2
	February	6.3	1.1
	March	18.6	1.4
	April	32.5	2.2
	May	115.2	15.9
	June	183.5	12.3
	July	10.1	1.5
	August	22.9	2.8
	September	455.9	37.0
	October	99.5	7.7
	November	39.8	1.7
	December	5.6	1.1
2004	January	7.8	1.2
	February	9.1	1.1
	March	11.5	1.3
	April	214.5	13.0

	May	214.5	17.8
	June	35.0	2.6
	July	78.7	14.8
	August	205.3	1.6
	September	43.9	2.0
	October	54.7	3.3
	November	13.4	1.4
	December	9.9	1.2
2005	January	9.6	1.1
	February	11.5	1.2
	March	20.7	1.7
	April	288.1	8.8
	May	112.7	28.9
	June	18.4	2.0
	July	9.9	1.7
	August	36.9	1.8
	September	78.5	18.4
	October	136.6	29.9
	November	38.6	2.5
	December	41.3	2.5
2006	January	36.6	2.2
	February	11.1	1.2
	March	31.5	1.2
	April	23.5	1.6
	May	70.9	8.8
	June	8.3	1.6
	July	18.6	1.8
	August	40.5	4.9
	September	21.2	2.2
	October	28.1	1.9
	November	24.8	2.3
	December	29.1	2.1
2007	January	10.5	1.1
	February	10.5	1.2
	March	130.5	8.8
	April	80.2	18.8
	May	598.5	83.6
	June	21.3	1.9
	July	42.7	2.8
	August	46.1	2.4
	September	236.8	12.6

	October	237.0	17.9
	November	11.4	1.1
	December	68.7	2.0
2008	January	12.6	1.1
	February	98.4	5.0
	March	15.9	1.2
	April	20.3	1.4
	May	48.0	2.4
	June	119.3	7.8
	July	89.3	16.4
	August	100.5	1.0
	September	587.2	178.0
	October	74.8	5.9
	November	26.1	3.3
	December	8.6	1.0
2009	January	10.2	1.2
	February	24.1	1.2
	March	14.0	1.3
	April	22.4	1.2
	May	20.1	1.7
	June	89.5	4.0
	July	27.6	1.7
	August	20.7	1.9
	September	11.5	1.5
	October	119.2	10.0
	November	11.2	1.0
	December	5.6	1.0
2010	January	6.9	1.2
	February	7.7	3.3
	March	111.3	6.3
	April	40.4	3.9
	May	54.7	5.3
	June	44.7	2.2
	July	275.8	19.3
	August	1930.2	1059.6
	September	495.0	32.8
	October	156.4	21.3
	November	46.6	2.7
	December	32.9	2.2
2011	January	8.2	1.2
	February	13.8	1.4

	March	25.5	1.2
	April	22.8	1.2
	May	1370.5	1000.2
	June	69.7	2.1
	July	64.8	2.7
	August	36.6	2.0
	September	73.9	5.2
	October	181.1	18.3
	November	118.8	37.7
	December	12.9	1.1
2012	January	14.5	1.7
	February	11.3	1.2
	March	20.1	1.2
	April	42.1	1.8
	May	13.3	1.5
	June	14.0	1.7
	July	39.9	1.8
	August	47.5	2.0
	September	41.5	2.3
	October	139.3	15.3
	November	31.6	2.7
	December	11.3	1.1
2013	January	6.6	1.1
	February	14.1	1.2
	March	30.8	1.4
	April	106.5	8.7
	May	49.4	1.8
	June	149.0	23.3
	July	19.4	1.7
	August	18.8	2.1
	September	146.3	60.9
	October	26.9	2.0
	November	11.2	1.1
	December	14.7	1.1
2014	January	9.8	1.0
	February	10.3	1.1
	March	32.8	1.2
	April	37.3	1.5
	May	18.7	1.2
	June	18.2	1.8
	July	13.6	1.2

	August	45.3	2.1
	September	53.5	2.2
	October	30.4	2.8
	November	12.7	1.4
	December	27.8	1.0
2015	January	8.2	1.0
	February	12.6	1.2
	March	28.3	1.2
	April	177.8	2.1
	May	21.0	1.5
	June	12.5	1.2
	July	27.8	1.8
	August	33.1	1.4
	September	42.4	1.7
	October	32.0	2.1
	November	25.0	1.4
	December	7.8	1.1
2016	January	6.1	1.2
	February	8.0	1.1
	March	9.9	1.1
	April	98.9	2.1
	May	38.5	1.7
	June	17.2	1.3
	July	32.8	1.7
	August	40.0	1.7
	September	107.1	11.4
	October	29.4	2.0
	November	22.4	1.7
	December	27.0	1.8
2017	January	33.8	1.9
	February	7.6	1.3
	March	12.4	1.2
	April	20.3	1.4
	May	65.2	7.8
	June	76.3	9.6
	July	100.3	8.9
	August	36.1	2.0
	September	125.1	17.8
	October	144.6	26.3
	November	20.3	1.8
	December	12.8	1.0

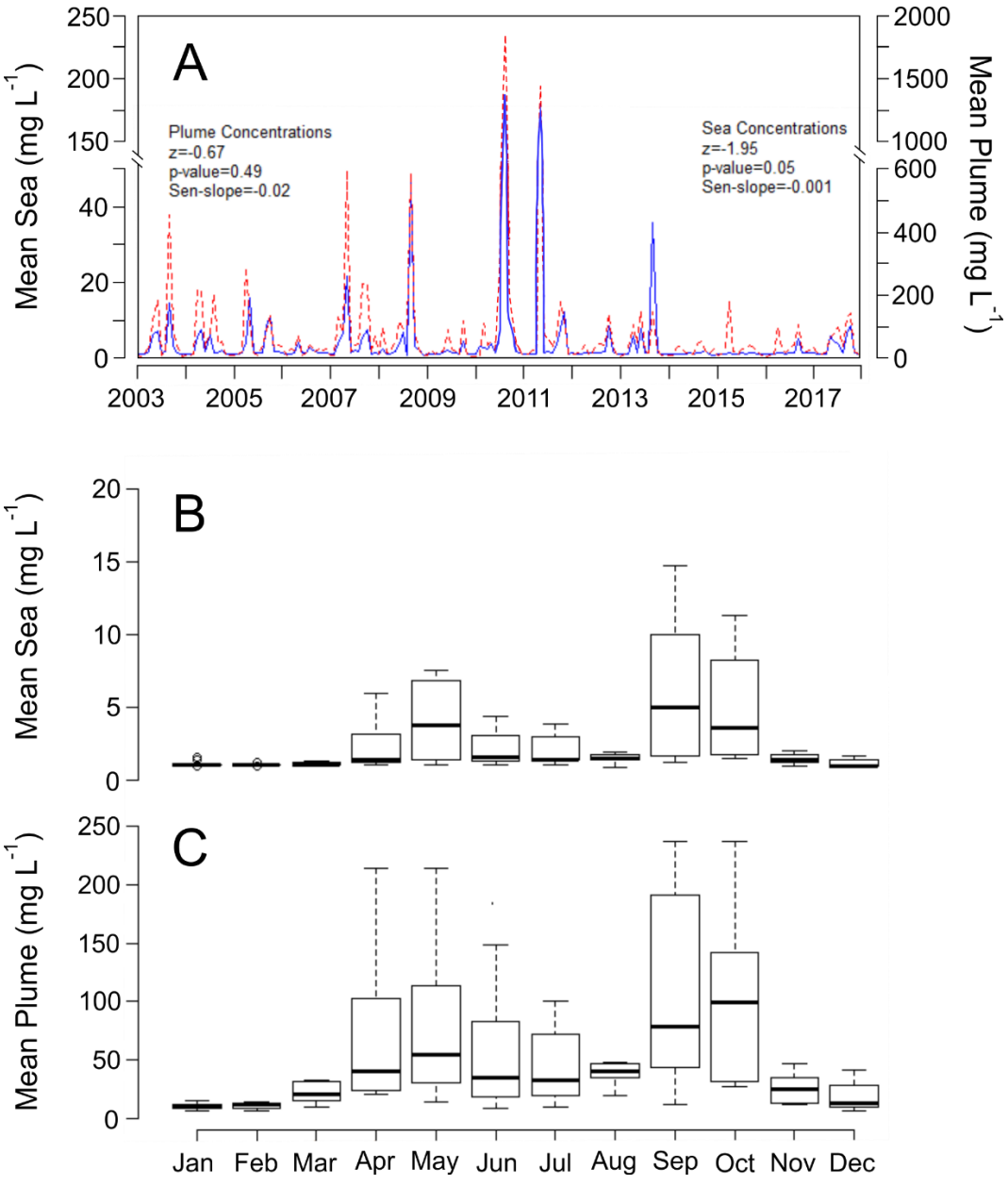

Figure 4. Surface suspended sediment concentrations in the Magdalena River mouth for the period 2003-2017. A) The blue line indicates the average of sea concentrations. The red dotted line indicates the average of plume concentrations. B) Monthly variability of sea surface suspended sediment concentration. C) Monthly variability of plume surface suspended sediment concentration.

Shape and Area of Solid and Diffuse Plumes

The shape of the solid and diffuse plumes changed throughout the year. The years 2006 and 2010 are used to illustrate intra-annual patterns in plume dynamics. In a typical year, e.g. 2006, the highest turbidity thresholds, defined using the mean solid plume concentration, were observed in January (dry season) and May (transition period), with concentrations of 36.6 mg L^{-1} and 70.9 mg L^{-1}, respectively. In January an elongated diffuse plume was observed. The diffuse and solid plumes were oriented toward the northwest. In May (transition period) and September (wet season), the diffuse plume was circular in shape, and directed toward the north and northeast, respectively (Figure 5). Conversely, in an anomalous year, e.g. 2010, the turbidity thresholds, defined using the mean solid plume concentration in January (dry season) and May (transition period) were 6.9 mg L^{-1} and 70.9 mg L^{-1}, respectively. In January, the diffuse plume had an irregular shape (Figure 6). The diffuse and solid plumes in May and September were larger than those found for a typical year like 2006. The upper confidence interval for suspended sediment concentration near the sea surface was 32.8 mg L^{-1}, and the mean of the solid plume concentrations was 495 mg L^{-1} for the wet 2010 season. These values are higher than those found in a typical year such as 2006.

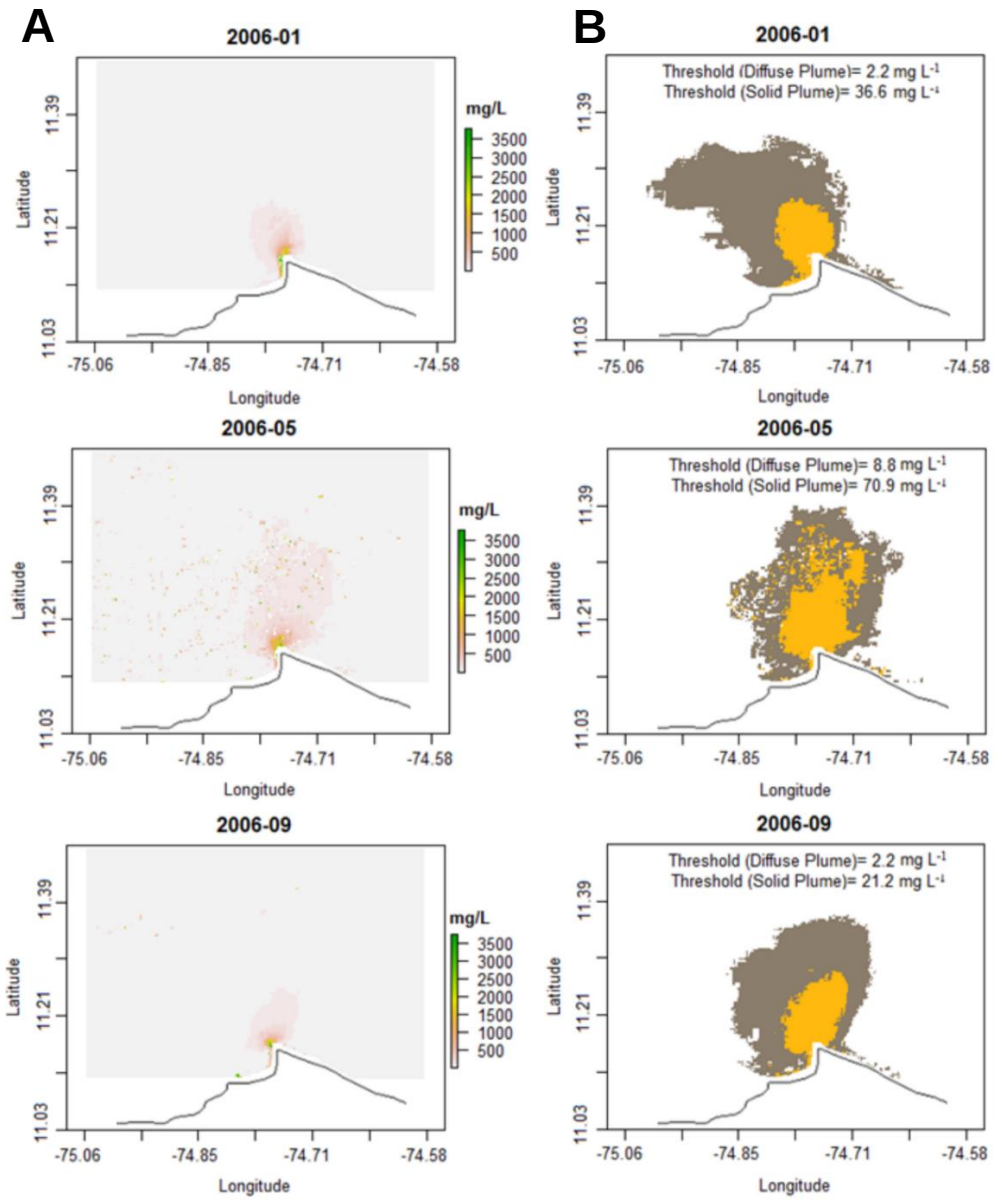

Figure 5. Surface suspended sediment concentrations and delimitation of the plumes for 2006 (typical year). A) Surface suspended sediment concentrations for January, May and September 2006 (typical year). Gray indicates the lowest concentrations (<100 mg L^{-1}), pink indicates concentrations close to 500 mg L^{-1}, and green indicates high concentrations (>2000 mg L^{-1}). B) Delimitation of the diffuse and solid plumes for January, May and September 2006. The dark brown area indicates the diffuse plume, which includes the solid plume, whereas the orange area indicates the solid plume only.

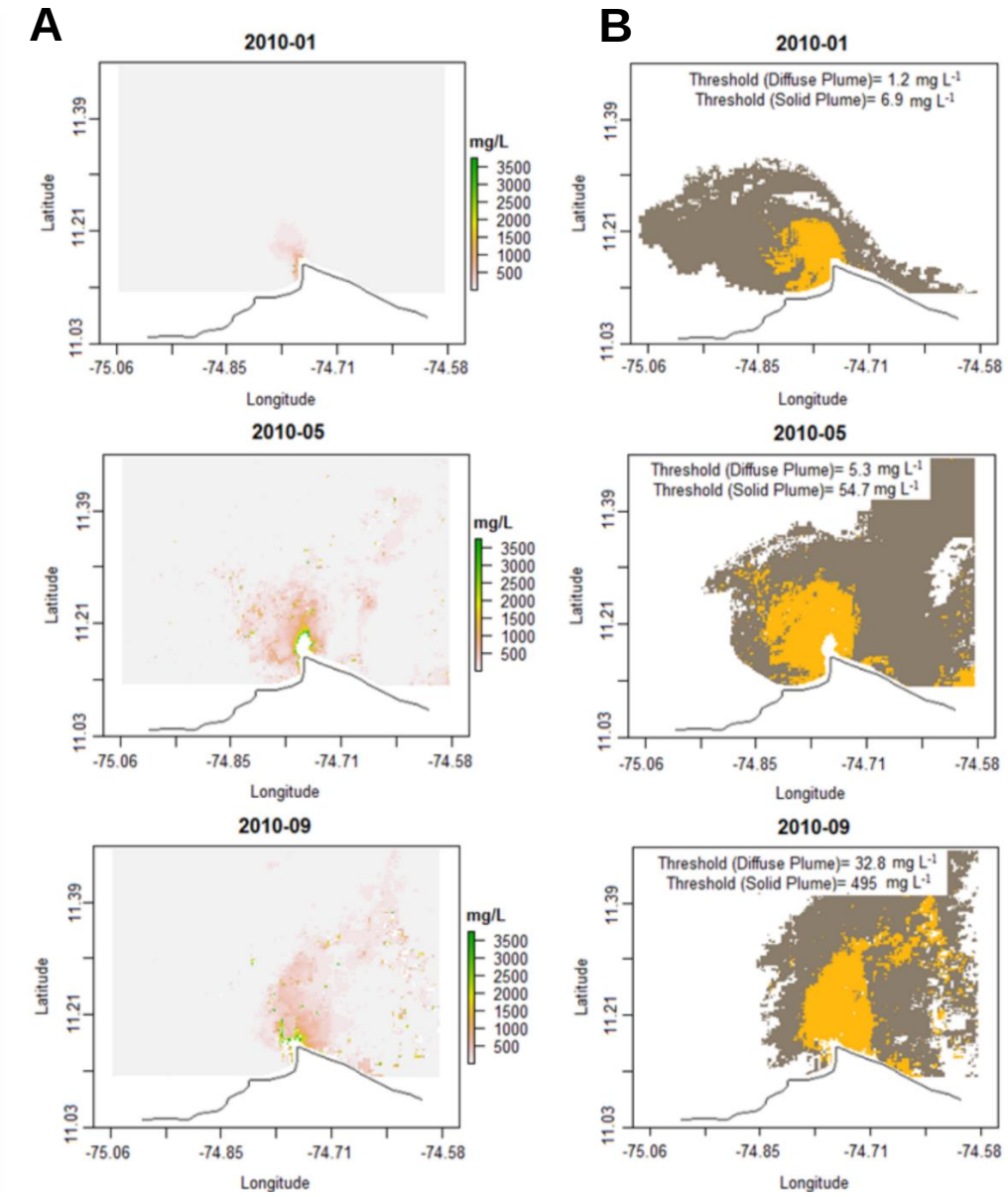

Figure 6. Surface suspended sediment concentrations and delimitation of the plumes for 2010 (anomalous year). A) Surface suspended sediment concentrations for January, May and September 2010 (anomalous year). Gray indicates the lowest concentrations (<100 mg L^{-1}), pink indicates concentrations close to 500 mg L^{-1}, and green indicates high concentrations (> 2000 mg L^{-1}). B) Delimitation of the diffuse and solid plumes for January, May and September 2010. The dark brown area indicates the diffuse plume, which includes the solid plume, whereas the orange area indicates the solid plume only.

The area of the solid and diffuse plumes varied throughout the analyzed months (Figure 7A). The diffuse plume had an average area of 1193 ± 516 km², whereas the solid plume had an average value of 184 ± 68 km² (Table 4). The mixing area had an average value of 1009 ± 478 km² (Figure 7B). Interannual values of the plume elongation ratio showed a predominantly elongated shape (Re<0.7), except for May 2011 and January 2017 when the plume was circular (Re=0.8) (Figure 8A). February and April, the dry season and transition period, respectively, were the months with less variability in the shape of the solid plume. The month with most variability was July (transition period). A more elongated shape was observed in September (wet season) (Figure 8B).

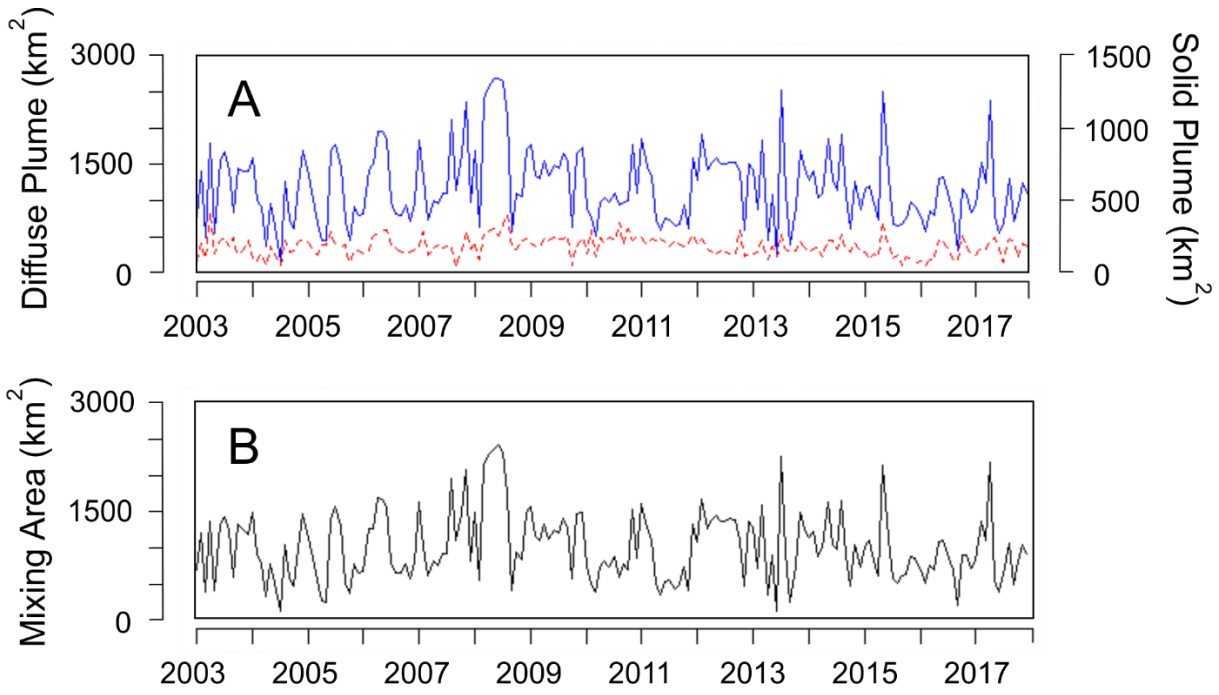

Figure 7. Diffuse and solid plume, and mixing area. A) Diffuse and solid plume in the Magdalena River mouth for the period 2003-2017. The blue line indicates the behavior of the diffuse plume, which includes the solid plume. The red dotted line indicates the behavior of the solid plume. B) Mixing area (diffuse plume – solid plume) in the Magdalena River mouth for the period 2003-2017.

Table 4. Characteristics of plumes delimited in the Magdalena River mouth. Range corresponds to the minimum and maximum value.

River Plume Attribute	Characteristic	
	Mean value ± SD	Range
Diffuse plume (km²)	1193 ± 516	170 – 2673
Solid plume (km²)	184 ± 68	43 – 419
Mixing area (km²)	1009 ± 478	119 – 2421
Elongation ratio (solid plume)	0.40 ± 0.14	0.06 -0.82

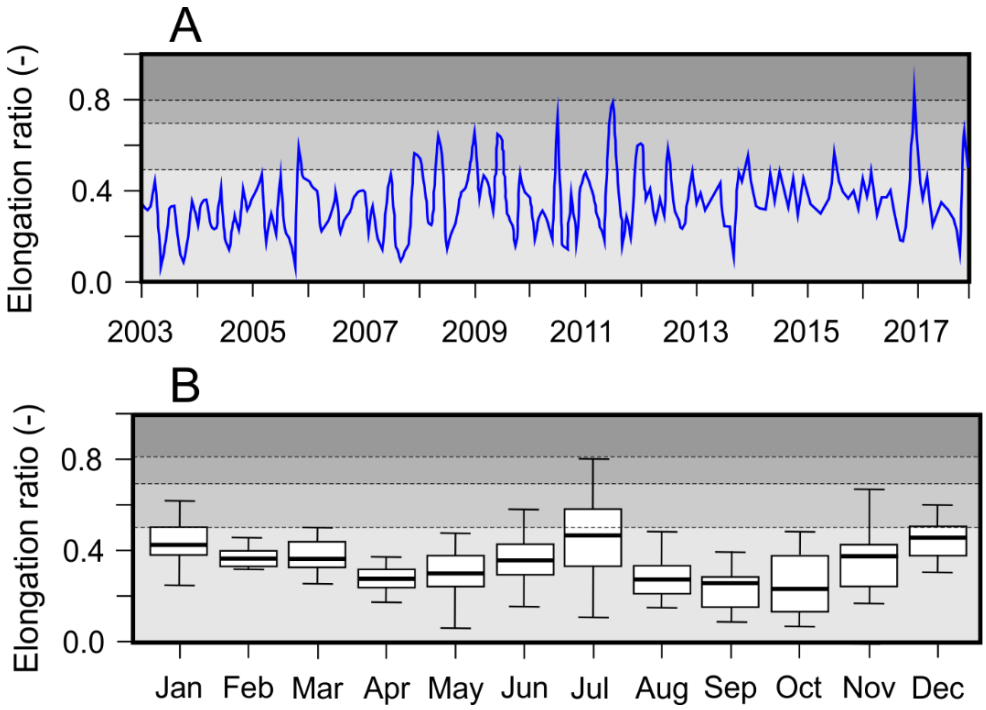

Figure 8. Elongation ratio in the Magdalena River mouth. A) Elongation ratio of the solid plume in the Magdalena River mouth for the period 2003-2017. B) Monthly elongation ratio for the solid plume in the Magdalena River mouth. In both cases, 0.5 corresponds to the limit for the more elongate shape, 0.7 to the limit of the elongate shape, 0.8 to the limit of the less elongate shape. Values between 0.8 and 1.0 indicate oval and circular shape, respectively.

Direction and Length of the Solid Plume

From December to March in all years, the direction of the solid plume showed little variability. In contrast, greatest variability in the length and direction of the solid plume was observed during the transition period (April, May, and June) and the wet season (September, October and November) (Figure 9A). The length and direction of the solid plume varied systematically through the months. The solid plume extended offshore to a maximum distance of 6.5 km (Figure 9B). According to monthly averages, the plume showed greatest length in May (transition period), September and October (wet season), between 6.0 and 6.5 km. The direction of the solid plume varied from northwest in January, to north in June, and northeast in October, and back again to northwest in December. Shorter solid plumes had a northwest direction and longer solid plumes had a northeast direction.

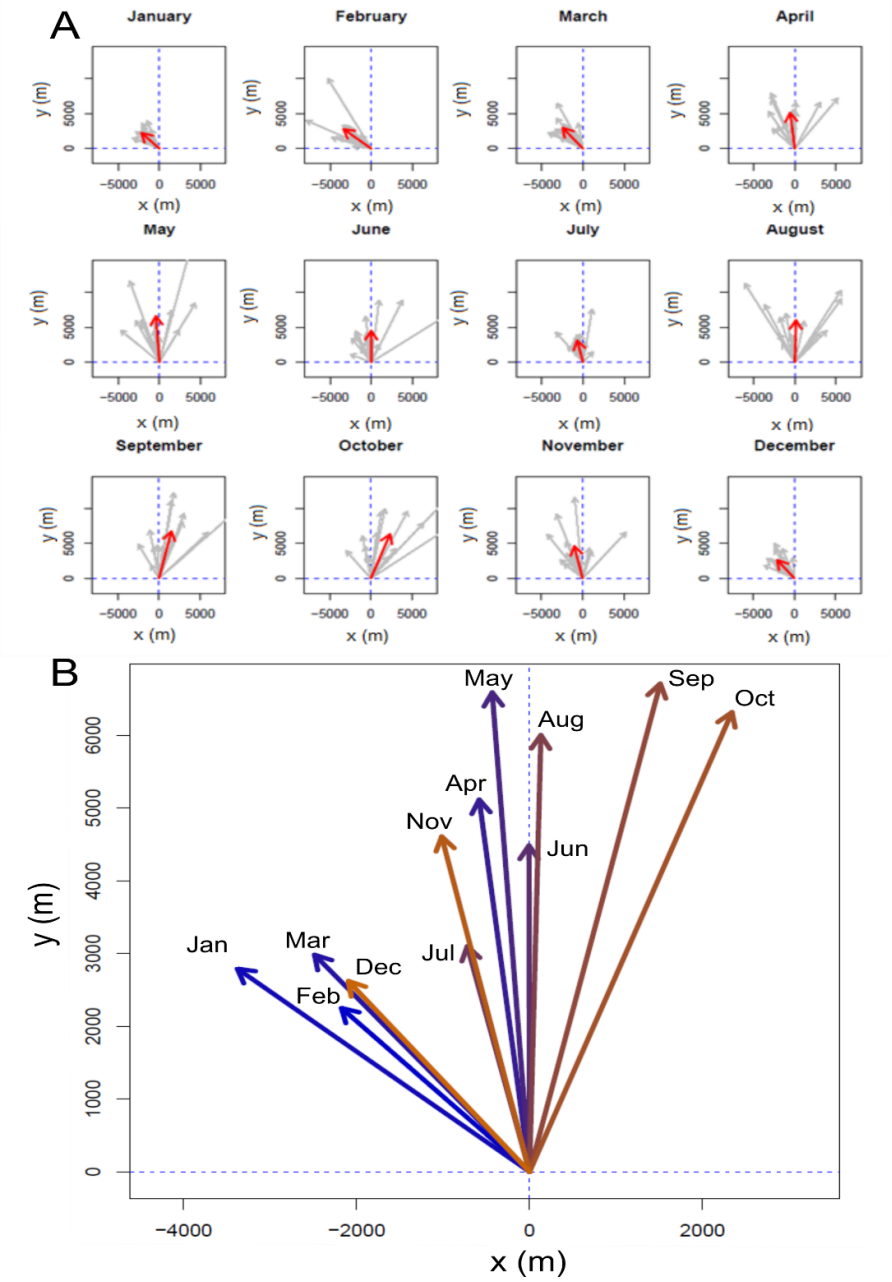

Figure 9. Solid plume in the Magdalena River for the period 2003-2017. A) Solid plume length and direction by month. B) Average monthly solid plume length and direction.

Influence of Fluvial and Oceanographic Factors

Seasonally, average streamflow varied from 5437 $m^3 s^{-1}$ to 9726 $m^3 s^{-1}$ during the dry and wet seasons, respectively. Suspended sediment transport showed a seasonal average during the dry season of 264 x 10^3 t d^{-1}, and 573 x 10^3 t d^{-1} during the wet season (Figure 10). Winds and ocean currents showed little variability. Winds had an average velocity of 6.0 m s^{-1}, with a southward direction during the dry season, and 2.0 m s^{-1}, with a southward direction during the wet season. Ocean currents had an average velocity of 0.3 m s^{-1} during the dry season, and 0.1 m s^{-1} during the wet season with a southward direction in both seasons.

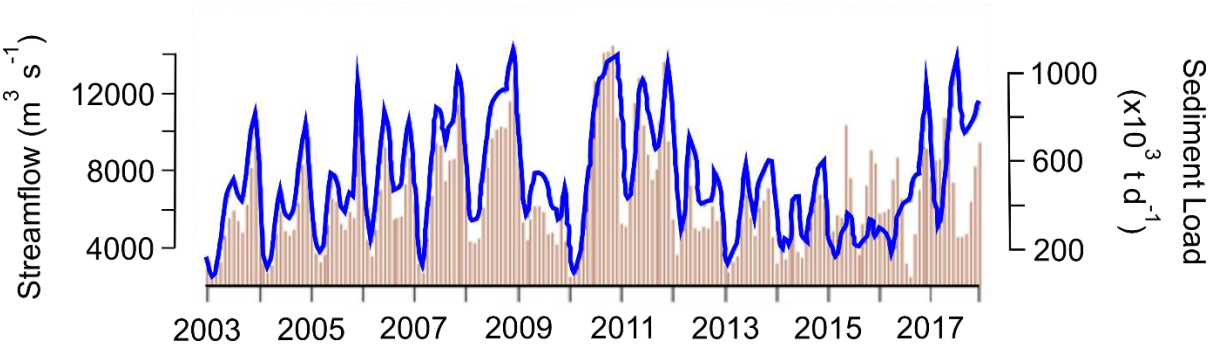

Figure 10. Streamflows and sediment transport in the Magdalena River (Calamar Station) for the period 2003-2017. The blue line indicates streamflow and dark bars indicate sediment load.

PCA Axes 1 and 2 explained 48% of the variability in the dataset, including attributes of the plume and independent explanatory variables (Axis 1 30.2% and Axis 2 17.8%) (Figure 11). According to the layout of vectors associated with the analyzed variables in the two first principal components, the solid plume length is influenced by water discharge and sediment transport. The solid plume length increases with increasing river streamflow and suspended sediment transport, whereas its direction is correlated with magnitude and direction of both wind and ocean currents. The diffuse and solid areas of the plume, however, were relatively independent from these variables. Wind and surface current magnitude showed a positive correlation. Our fitted explanatory models (Table 5) showed that the direction of the solid plume was influenced significantly by magnitude and wind direction, whereas the random component of the model, was best described by seasonal and autoregressive random components.

The solid plume longitude and area were influenced significantly by wind speed, streamflow, and a random autoregressive component, whereas the diffuse plume area was influenced significantly by wind speed, sediment transport, and a random component described by seasonal and random walk variability.

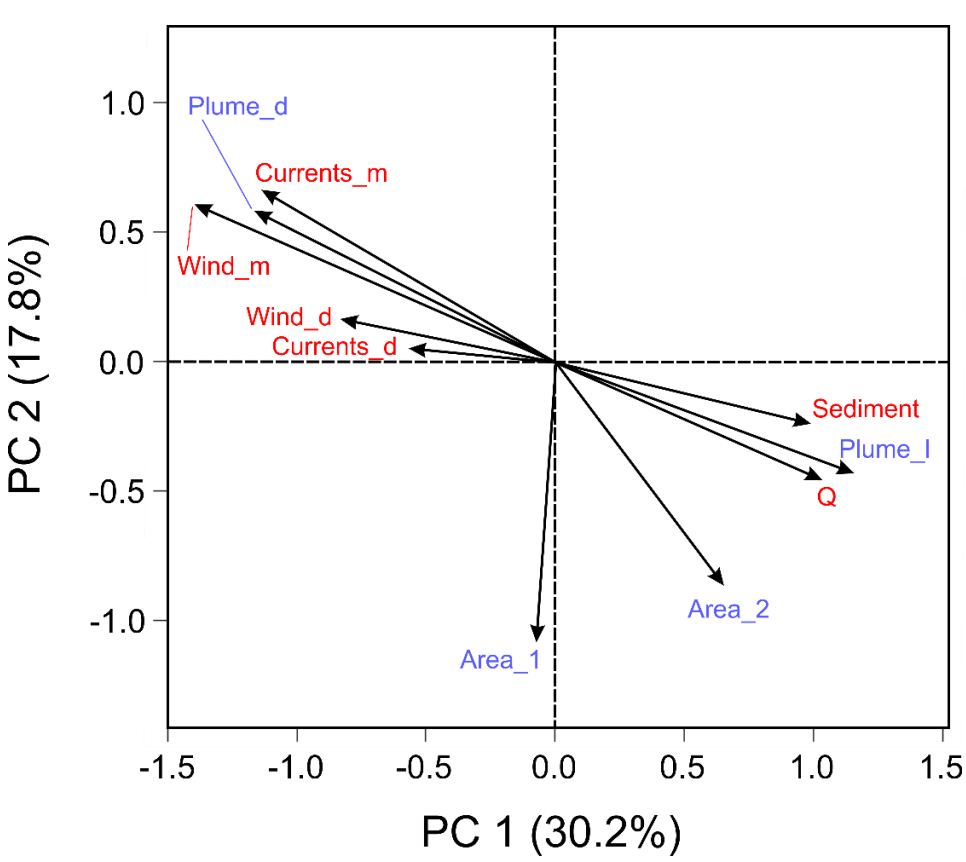

Figure 11. Principal Component Analysis (PCA) between the characteristics of the solid plume and the fluvial and oceanographic factors in the Magdalena River mouth. Plume_d= plume direction; Wind_d= wind direction; Currents_d= current direction; Wind_m= wind magnitude; Current_m= current magnitude; Sediment= sediment load; Q= caudal; Plume_l= plume length; Area_1= plume area; Area_2= diffuse plume.

Table 5. Summary statistics of fixed effects of the models obtained for the description of the behavior of the solid plume in the Magdalena River.

Model		Mean	SD	DIC
Solid_Plume_Direction ~ Wind_Direction + Wind_Magnitude + f(seasonal, 12) + f(time, ar, 1)	Intercept	65.1	10.5	1603
	Wind_Direction	0.07	0.03	
	Wind_Magnitude	4.30	1.36	
log_Solid_Plume_ length ~ Wind_Magnitude + Streamflow + f(time, ar, 1)	Intercept	9.36	0.19	-1040
	Wind_Magnitude	-0.10	0.01	
	Streamflow	-0.00	0.00	
Diffuse_Area ~ Wind_Magnitude + Sediment + f(seasonal, 12) + f(rw, rw1)	Intercept	192.3	68.6	-834
	Wind_Magnitude	-6.36	9.45	
	Sediment	0.08	0.04	
log_Solid_Plume_Area ~ Wind_Magnitude + Streamflow + f(time, ar, 1)	Intercept	6.48	0.21	-1042
	Wind_Magnitude	0.04	0.01	
	Streamflow	0.00	0.00	

Discussion

Calibration Model

Our training dataset allowed us to construct a model to estimate suspended sediment concentration in surface waters at the Magdalena River mouth, using the MODIS-Aqua data (R^2=0.96, *p-value*<0.05, RMSE=358 mg L^{-1}). The model incorporates the polynomial combination of an 8-day composite from bands 1 and 2 obtained from MODIS-Aqua images. Previous work showed the importance of a polynomial combination to improve predictions, particularly in rivers with high sediment loads, in which particle properties such as size, shape, and color, change significantly (Ondrusek et al., 2012; Martínez et al., 2015). Likewise, Chen et al. (2015) found for the Yangtze River Estuary that the quadratic model of the log-ratio was the most stable and acceptable model for estimation of surface suspended sediment concentrations under conditions of widely ranging values. The statistical values calculated for the model indicate that the model fits the data better than other models developed for the same study area, and for the mouths of rivers such as the Yangtze and Amazon (Restrepo et al., 2016b; Wang and Lu, 2010; Park and

Latrubesse, 2015). A model with higher calibration accuracy does not imply higher validation accuracy (Chen et al., 2015). The model proposed in this work, however, shows good validation (R^2=0.81, *p-value*<0.01), even with a small calibration dataset, i.e. 20 sampling stations. Also, we incorporated the statistical criterion AIC for best model selection (AIC). The AIC criterion has not been used in similar studies, and considers parsimony, simplicity and goodness of fit (Burnham et al., 2011).

We propose an innovative and statistically robust method to define turbidity thresholds and delimit turbidity plumes. The finite mixing model enabled identification of thresholds used to define areas with different properties, providing a reliable, systematic means to delimit turbidity plumes. The surface water in the study area was divided into three categories: (1) seawater regime (outside the diffuse plume), (2) river plume regime (solid plume), and (3) the unstable regime of the plume front (mixing area). Several studies have estimated suspended sediment concentrations in surface waters (Mendes et al., 2014; Chen et al., 2015; Gensac et al., 2016; Fernández-Nóvoa et al. 2017; Espinoza-Villar et al., 2018), but few have delimited the area of influence for the plume, because defining turbidity thresholds has proven difficult (Mendes et al., 2014). In previous studies, a fixed threshold value was employed (Mendes et al., 2014; Restrepo et al., 2016b; Fernández-Nóvoa et al. 2017). For example, Fernández-Nóvoa et al. (2017) delimited the turbidity plume of the Tagus River (Spain), using radiance values and two thresholds. The first threshold was defined with the maximum correlation between river discharge and plume length, and the second threshold was based on a histogram of radiance distribution. Restrepo et al. (2016b) delimited the turbidity plume in the Magdalena River mouth and the Canal del Dique, using a threshold of 10 mg L^{-1}, a value used to define waters suitable for coral reefs to thrive, because the objective of that study was to analyze the effect of sediment concentrations on those aquatic organisms. The choice of a fixed threshold assumes fixed sediment inputs and fluvial discharges. This assumption, however, is not appropriate to determine the net area of the river influence, especially in regions with marked seasonality (Mendes et al., 2014). Turbidity thresholds proposed in this study varied depending on specific background conditions. A proper definition of the turbidity limit is crucial to understand the process of sediment transfer from rivers to oceans, as well as to delimit areas of influence of the turbidity plume.

Turbidity Plume Features

Calculated suspended sediment concentrations indicate high turbidity in the Magdalena River plume (178.9 ± 78.7 mg L^{-1}), larger than previously reported values (Restrepo et al., 2016b; INVEMAR, 2017). Restrepo et al. (2016b) used field data from the Canal del Dique and Cartagena Bay to calibrate satellite images. The Canal del Dique generates an entirely separate plume with direct discharge in the bays of Barbacoas and Cartagena (Moreno-Madriñan et al., 2015). These environments are less turbid than the Magdalena River mouth (Restrepo et al., 2017b). Likewise, the Instituto de Investigaciones Marinas de Colombia (INVEMAR) reported sediment concentrations in Bocas de Ceniza <75 mg L^{-1} based on laboratory analyses of field samples (INVEMAR, 2017). Uncertainty in laboratory-based measurements of suspended sediment is high for turbid environments (Jago et al., 2006), as well as for those with a higher proportion of fine sediments. Spatial and temporal resolution is also limited in studies that rely on laboratory measurements. The usefulness of satellite images depends on the quality of data employed for calibration, particularly for high-turbidity zones and ecosystems in which sediment characteristics are highly variable (Chang et al., 2014).

This work showed that surface suspended sediment concentrations in the Magdalena River plume are of the same order of magnitude as those found in the Yangtze, Huang He and Amazon Rivers, despite the fact that these rivers exhibit much larger sediment fluxes and drainage areas and broader river mouths that have several distributary channels (Wang et al., 2010; Liu et al., 2011; Gensac et al., 2016). The data generated in this research enabled us to distinguish seasonal and inter-annual variations and/or modifications of suspended sediment concentration in the study area through time. It was possible to identify atypical suspended sediment concentrations in August 2010 and May 2011, linked to the 2010/2011 ENSO phase (La Niña), one of the strongest recorded in Colombia (Hoyos et al., 2013). There is a direct relationship between streamflow anomalies and the suspended sediment load in the Magdalena River (Restrepo and Kjerfve, 2000). In our study, concentrations were higher than 1300 mg L^{-1} in the turbidity plume and >200 mg L^{-1} for the ocean, and there was a northwest trend of the delimited plumes in August 2010 and May 2011. These atypical concentrations might have a negative impact on ecosystem services, particularly those related to productivity, because of their potential to inhibit ocean photosynthesis (Welch et al., 2014). In addition, plume direction during anomalous months might indicate greater impact on

the Ciénaga Grande de Santa Marta, a RAMSAR site. This potential impact has not been documented previously and might be critical given the profound hydrological modifications that have altered the ecosystem in the last few decades, thereby diminishing its resilience (Vilardy et al., 2011). High sediment discharges might obstruct waterways and increase siltation and pollutant concentrations in the ecosystem.

Large variations in the plume, from northwest to northeast, are observed in typical years. Our results suggest that the turbidity plume of the Magdalena River is directed away from the Rosario Islands (i.e. Cartagena Bay). The buoyancy and momentum that initiate a river plume are determined by estuarine processes, which are responsible for the initial transformation of river discharge (Horner-Devine et al., 2015). The calculated areas (diffuse, solid and mixing) and their shapes suggest that the Magdalena River plume has a limited area of influence. These areas and shapes denote the ability to generate a near-field area (the jet-like region of initial plume expansion), indicating the presence of a clear convergence front (Horner-Devine et al., 2015). Likewise, the use of shape coefficients (e.g. elongation ratio) is proposed to better describe the characteristics of turbidity plumes, expressing the overall form and dimensions of the plume (Gajbhiye, 2015). The elongation ratio might be one of the main geometric features of plumes, describing the degree of stretching with respect to its area. Thus, this geometric feature might reflect, or serve as a *proxy* for the effect of the physical drivers in the spreading and fate of the river plume. The Magdalena River plume generally showed an elongation ratio less than 0.5, which indicates a more elongated shape. This elongated shape could be related to the strong influence of the northeast trade winds.

Surface suspended sediment concentrations in the riverine section are greater during the low-flow season, as density gradients define the formation of a well-defined river plume, and riverine sediment inputs are much larger than marine sediment inputs. Large surface suspended sediment concentrations are commonly observed in the top of the water column (Geyer et al., 2004; Restrepo et al., 2018). In the Magdalena River mouth, however, the surface suspended sediment concentrations are controlled by estuarine morphology and by processes that influence the horizontal advection of water masses, leading to the formation of a clear convergent front (Restrepo et al., 2018). Our results suggest that the solid plume represents the area of the river plume where its influence, relative to the ocean, is more intense. Overall, these turbidity thresholds were lower during the dry period than in the wet season. In addition, short-term and rapid increases

in flow and suspended sediment load were observed in May of all years during the period of study. These increases might explain why the major length of the turbidity plume in May was comparable to that during the rainy months (September and October).

The plume length and direction, as well as the measured areas (diffuse, solid and mixing) exhibit a monthly pattern, related to conditions for each month, which are wind speed and direction, streamflow, and sediment transport. These results suggest that winds play a strong role in geomorphology and influence the spatial and temporal distribution of physical and chemical properties. Wind speed and direction are the most important variables, influencing the surface suspended sediment concentrations and the attributes of river plumes. The momentum added by wind stress is trapped in a relatively thin layer that has a low-level interchange with the oceanic layer because of density differences (Lentz and Largier, 2006). Winds cause shear stress on the surface layer that act in favor of or against the buoyant plume motion, promoting or hindering plume dispersion (Montoya et al., 2017). Upwelling winds tend to move the plume seaward because of offshore Ekman transport, whereas downwelling winds have the opposite effect, compressing the plume against the coast as a result of onshore transport (Jurisa and Chant, 2012). The study area is under the strong influence of the northeast trade winds (Andrade, 2001), with variations in magnitude and direction through the year. Previous studies in other areas (e.g. Columbia River, Chesapeake Bay, Ebro River) also identified the predominant influence of wind, particularly on plume direction (Jiang and Xia, 2016; Fernández-Nóvoa et al., 2015; Zhao et al., 2017). The dynamic characteristics of the ecosystem determine the quantity of transported sediment and mixing processes, all of which define the shape and length of the turbidity plume and the mixing zone (Horner-Devine et al., 2015).

References

Andrade, C.A. 2001. Las corrientes superficiales en la cuenca de Colombia observadas con boyas de deriva. Revista de la Academia Colombiana de Ciencias Exactas, Físicas y Naturales, 25(96), 321-335.

Benaglia, T., Chouteau, D., Hunter, D., Young, D. 2009. Mixtools: An R package for analyzing finite mixture models. Journal of Statistical Software, 32, 1-29.

Burnham, K. P., Anderson, D.R., Huyvaert, K.P. 2011. AIC model selection and multi-model inference in behavioral ecology: some background, observations and comparisons. Behavioral Ecology and Sociobiology, 65, 23–35. https://doi.10.1007/s00265-010-1029-6.

Celeux, G., Forbes, F., Robert, C. P., Titterington, D.M. 2006. Deviance Information Criteria for Missing Data Models. Bayesian Analysis, 1(4), 651–74.

Chang, N.B., Imen, S., Vannah, B. 2014. Remote sensing for monitoring surface water quality status and ecosystem state in relation to the nutrient cycle: a 40-year perspective. Critical Reviews in Environmental Science and Technology, 45(2), 101-166. https://doi.org/10.1080/10643389.2013.829981.

Chao, G., Qing, H., Leicheng, G., Winterwerp, J. 2017. A study of in-situ sediment flocculation in the turbidity maxima of the Yangtze Estuary, Estuarine, Coastal and Shelf Science, 191, 1-9. https://doi.org/10.1016/j.ecss.2017.04.001.

Chassignet, E.P., Hurlburt, H.E., Smedstad, O.M., Halliwell, G.R., Hogan, P.J., Wallcraft, A.J., Baraille, R., Bleck, R. 2006. The HYCOM (Hybrid Coordinate Ocean Model) data assimilative system. Journal of Marine Systems, 65(1-4), 60-83. https://doi.org/10.1016/j.jmarsys.2005.09.016.

Chen, S., Han, L., Chen, X., Li, D., Sun, L., Li, Y. 2015. Estimating wide range Total Suspended Solids concentrations from MODIS 250-m imageries: An improved method. ISPRS Journal of Photogrammetry and Remote Sensing, 99, 58-69. https://doi.org/10.1016/j.isprsjprs.2014.10.006.

Devlin, M., McKinna, L., Alvarez-Romero, J., Petus, C., Abott, B., Harkness, P., Brodie, J. 2012. Mapping the pollutants in surface riverine flood plume waters in the Great Barrier Reef, Australia. Marine Pollution Bulletin, 65(4), 224-235. https://doi.org/10.1016/j.marpolbul.2012.03.001.

Espinoza-Villar, R., Martínez, J.M., Armijos, E., Espinoza, J.C., Filizola, N., dos Santos, A., Willems, B., Fraizy, P., Santini, W., Vauchel, P. 2018. Spatio-temporal monitoring of suspended sediments in the Solimões River (2000–2014). Comptes Rendus Geoscience, 350 (1-2), 4-12. https://doi.org/10.1016/j.crte.2017.05.001.

Fernández-Nóvoa, D., Mendes, R., de Castro, M., Dias, J.M., Sánchez-Arcilla, A., Gómez-Gesteira, M. 2015. Analysis of the influence of river discharge and wind on the Ebro turbid plume using MODIS-Aqua and MODIS-Terra data. Journal of Marine Systems, 142, 40-46. https://doi.org/10.1016/j.jmarsys.2014.09.009.

Fernández-Nóvoa, D., Gómez-Gesteira, M., Mendes, R., de Castro, M., Vaz, N., Dias, J.M. 2017. Influence of main forcing affecting the Tagus turbid plume under high river discharges using MODIS imagery. Plos One, 12(10), e0187036. https://doi: 10.1371/journal.pone.0187036.

Gajbhiye, S. 2015. Morphometric analysis of a Shakkar river catchment using RS and GIS. International Journal of u- and e- Service, Science and Technology, 8(2), 11-24. http://dx.doi.org/10.14257/ijunesst.2015.8.2.02.

Fitzsimons, M.F., Lohan, M.C., Tappin, A.D., Millward, G.E. 2011. The Role of Suspended Particles in Estuarine and Coastal Biogeochemistry. In: Treatise on Estuarine and Coastal Science, vol. 4. Elsevier, Amsterdam, pp. 71-114.

Gao, S., Wang, Y., Gao, J. 2011. Sediment retention at the Changjiang sub-aqueous delta over a 57-year period, in response to catchment changes. Estuarine. Coastal Shelf Science, 95, 29-38. https://doi.org/10.1016/j.ecss.2011.07.015.

Gensac, E., Martinez, J.M., Vantrepotte, V., Anthony, E.J. 2016. Seasonal and inter-annual dynamics of suspended sediment at the mouth of the Amazon river: The role of continental and oceanic forcing, and implications for coastal geomorphology and mud bank formation. Continental Shelf Research, 118, 49-62. https://doi.org/10.1016/j.csr.2016.02.009.

Geyer, W., Hill, P., Kineke, G. 2004. The transport, transformation and dispersal of sediment by buoyant coastal flows. Continental Shelf Research, 24, 927–949. https://doi.org/10.1016/j.csr.2004.02.006.

González-Márquez, L.C., Torres-Bejarano, F.M., Rodríguez-Cuevas, C., Torregroza-Espinosa, A.C., Sandoval-Romero, J.A. 2018. Estimation of water quality parameters using Landsat 8 images: application to Playa Colorada Bay, Sinaloa, Mexico. Applied Geomatics, 10(2), 147–158. https://doi.org/10.1007/s12518-018-0211-9.

He, W., Chen, S., Liu, X., Chen, J. 2008. Water quality monitoring in a slightly polluted inland water body through remote sensing case study of the Guanting Reservoir in Beijing, China. Frontiers of Environmental Science and Engineering in China, 2(2), 163–171. https://doi.org/10.1007/s11783-008-0027-7.

Higgins, A., Restrepo, J.C., Ortiz, J.C., Pierini, J., Otero, L. 2015. Suspended Sediment Transport in the Magdalena River (Colombia, South America): Hydrologic Regime, Rating Parameters and Effective Discharge Variability. International Journal of Sediment Research, 31, 25-35. http://dx.doi.org/10.1016/j.ijsrc.2015.04.003.

Horner-Devine, A., Hetland, R.D., MacDonald, D.G. 2015. Mixing and Transport in Coastal River Plumes. Annual Review of Fluid Mechanics, 47, 569-594. https://doi.org/10.1146/annurev-fluid-010313-141408.

Hoyos, N., Escobar, J., Restrepo, J.C., Arango, A.M., Ortiz, J.C. 2013. Impact of the 2010-2011 La Niña phenomenon in Colombia, South America: The human toll of an extreme weather event. Applied Geography, 39, 16-25. https://doi.org/10.1016/j.apgeog.2012.11.018.

INVEMAR. 2017. Diagnóstico y evaluación de la calidad de las aguas marinas y costeras en el Caribe y Pacífico colombianos. Garcés, O. y L. Espinosa (Eds.). Red de vigilancia para la conservación y protección de las aguas marinas y costeras de Colombia – REDCAM: NVEMAR, MADS y CAR costeras. Informe técnico 2016. Serie de Publicaciones Periódicas No. 4 (2017) del INVEMAR, Santa Marta. 260 p.

Jago, C.F., Jones, S.E., Sykes, P., Rippeth, T. 2006. Temporal variation of suspended particulate matter and turbulence in a high energy, tide-stirred, coastal sea: relative contributions of resuspension and disaggregation. Continental Shelf Research, 26, 2019–2028. https://10.1016/j.csr.2006.07.009.

Jiang, L., Xia, M. 2016. Dynamics of the Chesapeake Bay outflow plume: Realistic plume simulation and its seasonal and interannual variability. Journal of Geophysical Research: Oceans, 12(2), 1424-1445. https://doi:10.1002/2015JC011191.

Jolliffe, I. 2002. Principal component analysis, Second edition edn. Springer, New York.

Jurisa, J.T., Chant, R. 2012. The coupled Hudson River estuarine-plume response to variable wind and river forcings. Ocean Dynamics, 62(5), 771–784.

Kim H.C., Son S., Kim Y.H., Khim J.S., Nam J., Chang W.K., Lee J.H., Lee C.H., Ryu, J. 2017a. Remote sensing and water quality indicators in the Korean West coast: Spatio-temporal structures of MODIS-derived chlorophyll-a and total suspended solids. Marine Pollution Bulletin, 121, 425-434. https://doi.org/10.1016/j.marpolbul.2017.05.026.

Kim, Y.H., Hong, S., Song, Y.S., Lee, H., Kim, H.C., Ryu, J., Park, J., Kwon, B.O., Lee, C.H., Khim, J.S. 2017b. Seasonal variability of estuarine dynamics due to freshwater discharge and its influence on biological productivity in Yeong san River Estuary, Korea. Chemosphere, 181, 390-399. https://doi: 10.1016/j.chemosphere.2017.04.085.

Lentz, S.J., Largier, J. 2006. The influence of wind forcing on the Chesapeake Bay buoyant Coastal Current. Journal of Physical Oceanography, 36: 1305-1316, https://doi:10.1175/JPO2909.1.

Li, P., Yang, S.L., Milliman, J.D., Xu, K.H., Qin, W.H., Wu, C.S., Chen, Y.P., Shi, B.W. 2012. Spatial, temporal, and human-induced variations in suspended sediment concentration in the surface waters of the Yangtze Estuary and adjacent coastal areas. Estuaries and Coasts, 35, 1316–1327. https://doi:10.1007/s12237-012-9523-x.

Liu, F., Chen, S.L., Peng, J., Chen, G.Q. 2011. Temporal variability of water discharge and sediment load of the Yellow River into the sea during 1950-2008. Journal of Geographical Sciences, 21(6), 1047–1061. https://doi.org/10.1007/s11442-011-0899-5.

McLachlan, G., Peel, D. 2000. Finite Mixture Models. John Wiley & Sons, Inc., New York.

Martínez, J.M., Espinoza-Villar, R., Armijos, E., Silva Moreira, L. 2015. The optical properties of river and floodplain waters in the Amazon River Basin: implications for satellite-based measurements of suspended particulate matter. Journal of Geophysics Research, 120(7), 1274–1287. http://dx.doi.org/10.1002/2014JF003404.

Mendes, R., Vaz, N., Fernández-Nóvoa, D., da Silva, J.C.B., de Castro, M., Gómez-Gesteira M., Dias, J.M. 2014. Observation of a turbid plume using MODIS imagery: The case of Douro estuary (Portugal). Remote Sensing of Environment, 154, 127–138. https://doi.org/10.1016/j.rse.2014.08.003.

Meng, J., Yu, Z., Yao, Q., Bianchi, S., Paytan, A., Zhao, B., Pan, H., Yao, P. 2015. Distribution, mixing behavior, and transformation of dissolved inorganic phosphorus and suspended particulate phosphorus along salinity gradient in the Changjiang Estuary. Marine Chemistry, 168, 124-134. https://doi.org/10.1016/j.marchem.2014.09.016.

Montoya, L.J., Toro-Botero, F.M., Gómez-Giraldo, A. 2017. Study of Atrato river plume in a tropical estuary: Effects of the wind and tidal regime on the Gulf of Urabá, Colombia. DYNA, 84(200), 367-375. https://dx.doi.org/10.15446/dyna.v84n200.55040.

Montoya-Sánchez, R.M., Devis-Morales, A., Bernal, G., Poveda, G. 2018. Seasonal and intraseasonal variability of active and quiescent upwelling events in the Guajira system, southern Caribbean Sea. Continental Shelf Research, *In press*. https://doi.org/10.1016/j.csr.2018.10.006.

Moreno-Madriñan, M., Rickman, D., Ogashawara, I., Irwin, D., Ye, J., Al-Hamdan, M. 2015. Using remote sensing to monitor the influence of river discharge on watershed outlets and adjacent coral reefs: Magdalena River and Rosario Islands, Colombia. International Journal of Applied Earth Observation and Geoinformation, 38, 204-215. https://doi.org/10.1016/j.jag.2015.01.008.

Morera, S.B., Condom, T., Crave, A., Steer, P., Guyot, J.L. The impact of extreme El Niño events on modern sediment transport along the western Peruvian Andes (1968-2012). Scientific Reports, 7, 11947. https://doi.10.1038/s41598-017-12220-x.

Ondrusek, M., Stengel, E., Kinkade, C. S., Vogel, R. L., Keegstra, P., Hunter, C., Kim, C. 2012. The development of a new optical total suspended material algorithm for the Chesapeake Bay. Remote Sensing of Environment, 119, 243–254. https://10.1016/j.rse.2011.12.018.

Ortiz, J., Otero, L., Restrepo, J.C., Ruiz, J., Cadena, M. 2013. Characterization of cold fronts in the Colombian Caribbean and their relationship to extreme wave events. Natural Hazards Earth System Science, 13, 2797–2804. https://doi:10.5194/nhess-13-2797-2013.

Osadchiev, A.A., Izhitskiy, A.S., Zavialov, P.O., Kremenetskiy, V.V., Polukhin, A.A., Pelevin, V.V., Toktamysova, Z.M. 2017. Structure of the buoyant plume formed by Ob and Yenisei river discharge in the southern part of the Kara Sea during summer and autumn.

Journal of Geophysical Research, 122(7), 5916-5935. https://doi.org/10.1002/2016JC012603.

Park, E., Latrubesse, E.M. 2015. Surface water types and sediment distribution patterns at the confluence of mega rivers: The Solimões-Amazon and Negro rivers junction. Water Resources Research, 51, 6197-6213. https://doi.org/10.1002/2014WR016757.

Poveda, G. 2004. La hidroclimatología de Colombia: una síntesis desde la escala inter-decadal hasta la escala diurna. Revista de la Academia Colombiana de Ciencias Exactas, Físicas y Naturales, 28(107), 201-222.

R Core Team. 2018 R: A Language and Environment for Statistical Computing. R Foundation for Statistical Computing.

Restrepo, J.C., Ortiz, J.C., Pierini, J., Schrottke, K., Maza, M., Otero, L., Aguirre, J. 2014. Freshwater discharge into the Caribbean Sea from the rivers of Northwestern South America (Colombia): magnitude, variability and recent changes. Journal of Hydrology, 509, 266-281. https://doi.org/10.1016/j.jhydrol.2013.11.045.

Restrepo, J.C, Schrottke, K., Traini, C., Ortiz, J., Orejarena, A., Otero, L., Higgins, A., Marriaga, L. 2016a. Sediment Transport and Geomorphological Change in a High-Discharge Tropical Delta (Magdalena River, Colombia): Insights from a Period of Intense Change and Human Intervention (1990–2010). Journal of Coastal Research, 32(3), 575-589. https://doi.org/10.2112/JCOASTRES-D-14-00263.1.

Restrepo J.C., Orejarena A., Torregroza-Espinosa A.C. 2017a. Suspended sediment load in northwestern South America (Colombia): A new view on variability and fluxes into the Caribbean Sea. Journal of South American Earth Sciences, 80, 340-352. https://doi.org/10.1016/j.jsames.2017.10.005.

Restrepo, J.C., Escobar, J., Otero, L., Franco, D., Pierini, J., Correa, I. 2017b. Factors Influencing the Distribution and Characteristics of Surface Sediment in the Bay of Cartagena, Colombia. Journal of Coastal Research, 33(1), 135-148. https://doi:10.2112/jocoastres-D-15-00185.1.

Restrepo, J.C., Schrottke, K., Traini, C., Bartholomaec, A., Ospino, A., Ortiz, J.C., Otero, L., Orejarena, A. 2018. Estuarine and sediment dynamics in a microtidal tropical

estuary of high fluvial discharge: Magdalena River (Colombia, South America). Marine Geology, 398, 86–98. https://doi.org/10.1016/j.margeo.2017.12.008.

Restrepo, J.D, Kjerfve, B. 2000. Magdalena river: interannual variability (1975–1995) and revised water discharge and sediment load estimates. Journal of Hydrology, 235(1), 137-149. https://doi.org/10.1016/S0022-1694(00)00269-9.

Restrepo, J.D., Syvitski, J.P.M. 2006. Assessing the effect of natural controls and land use change on sediment yield in a major Andean River: The Magdalena drainage basin, Colombia. Ambio: a Journal of the Human Environment, 35, 44-53.

Restrepo, J.D., Zapata, P., Díaz, J.M., Garzón-Ferreira, J., García, C.B. 2006. Fluvial fluxes into the Caribbean Sea and their impact on coastal ecosystems: The Magdalena River, Colombia. Global and Planetary Change, 50(1–2), 33-49. https://doi.org/10.1016/j.gloplacha.2005.09.002.

Restrepo, J.D. 2008. Applicability of LOICZ catchment–coast continuum in a major Caribbean basin: The Magdalena River, Colombia. Estuarine Coastal Shelf Science, 77(2), 214-229. https://doi:10.1016/j.ecss.2007.09.014.

Restrepo, J.D., Park, E., Aquino, S., Latrubesse, E. 2016b. Coral reefs chronically exposed to river sediment plumes in the southwestern Caribbean: Rosario Islands, Colombia. Science of The Total Environment, 553, 316-329. https://doi.org/10.1016/j.scitotenv.2016.02.140.

Slattery, M., Phillips, J. 2009. Controls on sediment delivery in coastal plain rivers. Journal of Environmental Management, 92, 284-289. https://doi.org/10.1016/j.jenvman.2009.08.022.

Syvitski, J.P.M., Kettner, A.J. 2011. Sediment flux and the anthropocene. Philosophical Transactions of the royal society a mathematical. Mathematical, Physical and Engineering Science, 369(1938), 957-975. https://doi.org/10.1098/rsta.2010.0329.

Tuck, S.L., Phillips, H., Hintzen, R.E., Scharlemann, J., Purvis, A., Hudson, L.N. 2014. MODISTools – downloading and processing MODIS remotely sensed data in R. Ecology and Evolution, 4(24), 4658–4668. https://doi.org/10.1002/ece3.1273.

Uninorte. 2019. Distribución espacio-temporal de la temperatura y la salinidad – Influencia sobre la estratificación, la concentración de nutrientes y la productividad

primaria en el frente deltaico del rio Magdalena. Proyecto BanRepública, 2018-40423. 32 p.

Vilardy, S.P., González, J.A., Martín-López, B., Montes, C. 2011. Relationships between hydrological regime and ecosystem services supply in a Caribbean coastal wetland: a social-ecological approach. Hydrological Sciences Journal, 56(8), 1423–1435. https://doi.org/10.1080/02626667.2011.631497.

Wang, J.J., Lu, X.X. 2010. Estimation of suspended sediment concentrations using terra MODIS: an example from the lower Yangtze river, China. Science of Total Environment, 408, 1131–1138. http://dx.doi.org/10.1016/j.scitotenv.2009.11.057.

Welch, M.J., Watson, S.A., Welsh, J.Q., McCormick, M.I., Munday, P.L. 2014. Effects of elevated CO^2 on fish behavior undiminished by transgenerational acclimation. Nature Climate Change, 4, 1086–1089. https://doi:10.1038/nclimate2400.

Wood, S. 2006. Generalized Additive Models: An introduction with R. Chapman and Hall/CRC.

Wu, G., Liu, L., Chen, F., Fei, T. 2014. Developing MODIS-based retrieval models of suspended particulate matter concentration in Dongting Lake, China. International Journal of Applied Earth Observation and Geoinformation, 32, 46-53. https://doi.org/10.1016/j.jag.2014.03.025.

Xu, H., Wolanski, E., Chen, Z. 2013. Suspended particulate matter affects the nutrient budget of turbid estuaries: modification of the LOICZ model and application to the Yangtze Estuary. Estuarine Coastal Shelf Science, 127, 59–62. https://doi.org/10.1016/j.ecss.2013.04.020.

Yap, B.P., Sim, C.H. 2011. Comparisons of various types of normality tests. Journal of Statistical Computation and Simulation, 81(12), 2141-2155. https://10.1080/00949655.2010.520163.

Yue, S., Pilon, P., Cavadias, G. 2002. Power of the Mann-Kendall and Spearman's rho test to detecting monotonic trends in hydrological series. Journal of Hydrology, 259, 254-271. https://doi.org/10.1016/S0022-1694(01)00594-7.

Zhao, J., Gong, W., Shen, J. 2017. The effect of wind on the dispersal of a tropical small river plume. Frontiers of Earth Science, 12(1), 170-190. https://doi.10.1007/s11707-016-0628-6.

CHAPTER 3

3. Nutrient Input and Net Ecosystem Productivity in the Mouth of the Magdalena River, Colombia

Abstract

Nutrient inputs and biogeochemical cycles in estuaries are strongly influenced by river discharge and suspended particulate matter (SPM). We evaluated seasonal differences in nutrient bioavailability and net ecosystem productivity (NEP) in the mouth of the Magdalena River, Colombia, using the stratified Muddy LOICZ model. Calculated water residence times in the estuary were low (~0.9-2.1 days), as were proportions of dissolved nitrogen (DIN) and phosphorus (DIP) forms (~10-30%) in the total nutrient pool. Dissolved nutrient proportions displayed differences between seasons (transition period [June 2018] and wet [November 2018]), and between the upper and lower, density-stratified water layers. Nutrient adsorption and desorption, associated with SPM in the estuary, determined bioavailable nutrient concentrations. When SPM was incorporated in the Muddy LOICZ model, output indicated that NEP in the estuary was positive, i.e. primary productivity exceeded community respiration, and that there was net retention of nitrogen and phosphorus in the estuary.

Introduction

Estuaries are productive, biodiverse ecosystems that provide multiple services (Raboubille et al., 2001; Ramesh et al., 2015). Physico-chemical characteristics and productivity in these coastal systems depend on interactions among fluvial discharge, tides and waves (Kjerfve, 1994; Gobler et al., 2005). Fluvial inputs, nutrients, and suspended sediments all influence biogeochemical processes in estuaries (Anthony et al., 2014). Thus, river water quality affects the health of coastal ecosystems (Ramesh et al., 2015). Anthropogenic activities in watersheds, including deforestation and consequent soil erosion, application of fertilizers, and discharge of domestic and industrial waste, modify the characteristics of fluvial discharge, and increase suspended sediment loads and contaminant inputs to estuaries (Anthony et al., 2014). Poor watershed management has caused environmental problems such as cultural eutrophication in some coastal aquatic ecosystems (Harvey et al., 2015).

Coastal eutrophication has become a critical problem in some areas (Glober et al., 2005) and the ecological consequences of nutrient enrichment have been documented worldwide (Nixon et al., 2001; Paerl et al., 2014; Karydis and Kitsiou, 2019). Eutrophication can lead to greater rates of primary production, oxygen depletion (hypoxia or anoxia), high mortality of aquatic organisms, and disruption of food webs (Karydis and Kitsiou, 2019). The relationship between nutrient loads and NEP in estuaries is complex and depends on which nutrient limits primary production (i.e., nitrogen or phosphorus) and the physical dynamics of the receiving ecosystem (Glibert et al., 2005). For instance, Goñi et al. (2009) found that biogeochemical cycling in Winyah Bay, South Carolina (USA) was strongly influenced by river discharge and sediment properties, as well as water circulation in the estuary. Changes in freshwater discharge to estuaries have large impacts on biogeochemical processes, mainly because of shifts in nutrient transport and the properties of SPM (Goñi et al., 2009). Knowledge of physical aspects of estuaries is required to fully understand nutrient dynamics and the drivers of primary productivity in these coastal aquatic ecosystems (Kasai et al., 2010).

SPM plays an important role in biogeochemical cycles, particularly in estuaries that receive water from rivers that transport large loads of fine grain suspended sediment, which may adsorb nutrients and thereby inhibit primary production (Suzumura et al., 2004; Xu et al., 2013). On the other hand, SPM can desorb nutrients into the sea, leading to enhanced productivity (Suzumura et al., 2004; Xu et al., 2013). Despite the realization

that SPM can have profound effects on nutrient loads, most studies have ignored nutrients delivered in particulate form, and have not considered nutrient adsorption and desorption by/from SPM (Gao et al., 2008). Evidence, however, suggests that ~20% of the nutrients in estuarine waters is in particulate form, and values can be as high as 60% to 80% in estuaries with high turbidity (100-1000 mg L^{-1}) (Xu et al., 2013). Biogeochemical mass balance is typically used to study nutrient loads, fluxes and sinks, and to estimate NEP, i.e., gross primary production (GPP) minus community respiration (R) (Kemp et al., 1997). The role of SPM must be incorporated into estuarine biogeochemical models to develop reliable estimates of biologically available nutrient loads, especially in turbid estuaries (Xu et al., 2013; Xu et al., 2015).

Many biogeochemical models use a mass balance approach (Rabouille et al., 2001; Mackenzie et al., 2011). One of the most widely used is the Land-Ocean Interactions in the Coastal Zone (LOICZ) model (Gordon et al., 1996; Smith et al., 2005; Swaney et al., 2011), which has been applied to >200 estuaries and coastal water areas worldwide (Smith et al., 2005; Swaney et al., 2011; Xu et al., 2013). It is useful to quantify nutrient transfer from rivers to estuaries and from estuaries to the ocean, as well as to estimate NEP in the estuary (Swaney et al., 2011). The LOICZ Model was modified recently to include the effect of SPM on nutrient bioavailability in estuarine and coastal waters (Muddy LOICZ Model), which involved parameterization of the SPM input using the partition (distribution) coefficient (K_d), a measure of the relative amount of a nutrient present in particulate form (Xu et al., 2013; Xu et al., 2015). Recent studies highlight the regional and global importance of tropical systems, regarding the transfer of nutrients to coastal zones (Araujo et al., 2014; Jiang et al., 2019). Additional comprehensive studies are needed to investigate biogeochemical dynamics in microtidal estuaries that receive large water and sediment inputs. We used the Muddy LOICZ model to evaluate seasonal nutrient bioavailability and NEP in the Magdalena River mouth (i.e. Bocas de Ceniza Estuary). Our specific objectives were to: (*i*) determine seasonal nutrient bioavailability and NEP in the estuary, and (*ii*) analyze the effect of SPM on nutrient availability and estuary NEP.

Study Zone

The Magdalena River is the largest fluvial system in Colombia and extends for 1,548 km. Its delta features a discharge channel (Bocas de Ceniza) that is defined by a stratified, turbid estuary, with a microtidal regime (Figure 1) (Restrepo et al., 2018a). A decline in

flow at the river mouth results in saline intrusion, reduced vertical water mixing, and consequent marked density stratification, with a well-defined halocline that contributes to the formation of a salt wedge (Restrepo et al., 2018a). Surface salinity ranges from 0 in the fluvial sector, to values of ~15 at the mouth, and up to 33 in the coastal zone (Restrepo et al., 2018a). Mixing and stratification occur during high- and low-flow periods, respectively. During the high-flow period, the water column in the river is completely mixed along its length until about 1 km from the river mouth. Farther downstream it is density-stratified at the inner delta front, to about 1 km below the mouth. In contrast, during the low-flow period, the water column is stratified as far as ~6 km upstream from the river mouth (Restrepo et al., 2018a). The Magdalena River mouth has been highly modified through engineered channelization. River discharge is currently limited by two breakwaters that extend for 7.40 km along the west shore and 1.40 km along the east shore (Restrepo et al., 2016). The river mouth is 430 m wide and at least 9.15 m deep in its deepest channel (Restrepo et al., 2018a).

Climate in the study area is influenced by latitudinal position of the Intertropical Convergence Zone (ITCZ), with two main seasons: 1) a wet season from September to November, when the ITCZ moves northward, and (2) a dry season from January to April, when the ITCZ is farthest south (Poveda, 2004). Northeast trade winds, with a dominant southward direction, have a strong influence in February and March, and account for the low rainfall during those months (Andrade, 2001). The average wind velocity is 6.0 m s^{-1} near the coast of Colombia (Montoya-Sánchez et al., 2018). From September through November, winds are relatively weak, with average velocities of 2.0 m s^{-1} (Montoya-Sánchez et al., 2018).

During the dry season, mean flow in the river is 4,361 m^3 s^{-1}, with a mean suspended sediment transport rate of 218 x 10^3 t d^{-1} (Restrepo et al., 2014) and high wave energy (H_s > 2.50 m) (Ortiz et al., 2013). In the wet season, the river's mean flow is 8,063 m^3 s^{-1}, its mean suspended sediment transport rate is 531 x 10^3 t d^{-1}, and its wave energy is low (H_s < 1.50 m) (Ortiz et al., 2013). The Magdalena River Estuary is turbid (4,000 mg L^{-1} < SPM_{max} <10,000 mg L^{-1}) in the high-flow period, and extremely turbid during the low-flow period (SPM_{max}> 10,000 mg L^{-1}) (Restrepo et al., 2018a). Predominant particle sizes for suspended sediment in the Magdalena River are coarse silt (d_{10}= 0.3 µm; d_{50}=14.1 µm; d_{90}= 45.9 µm) in the dry season and medium silt (d_{10}= 0.3 µm; d_{50}=7.8 µm; d_{90}= 23.8 µm) in the wet season (Restrepo et al., 2016). The Magdalena River transports ~30 million tons (Mt)

y^{-1} of total dissolved matter into the Caribbean Sea, with a specific (areal) transport rate of 117 t km^{-2} y^{-1} (Restrepo et al., 2018b), and total fluxes of NO_3 and PO_4 of ~186 × 10^3 t y^{-1} and 47 × 10^3 t y^{-1}, respectively (Restrepo and Kjerfve, 2004). Reported nutrient values correspond to averages calculated from monthly samples that span the three-year period 1998–2000 (Restrepo and Kjerfve, 2004). The Magdalena River receives nutrients from many sources, including, among others, drainage from croplands and cattle pastures, untreated wastewater discharge from rural and urban areas, and undisturbed areas in the watershed (Kjerfve 1994; Vivas-Aguas et al., 2017). Since the 1950s, nitrogen (N) and phosphorus (P) fertilizers have been used widely for agriculture in Colombia, and N and P concentrations are high in detergents and industrial products. Fluvial N and P fluxes now exceed background, pre-disturbance rates by an order of magnitude (Restrepo, 2008).

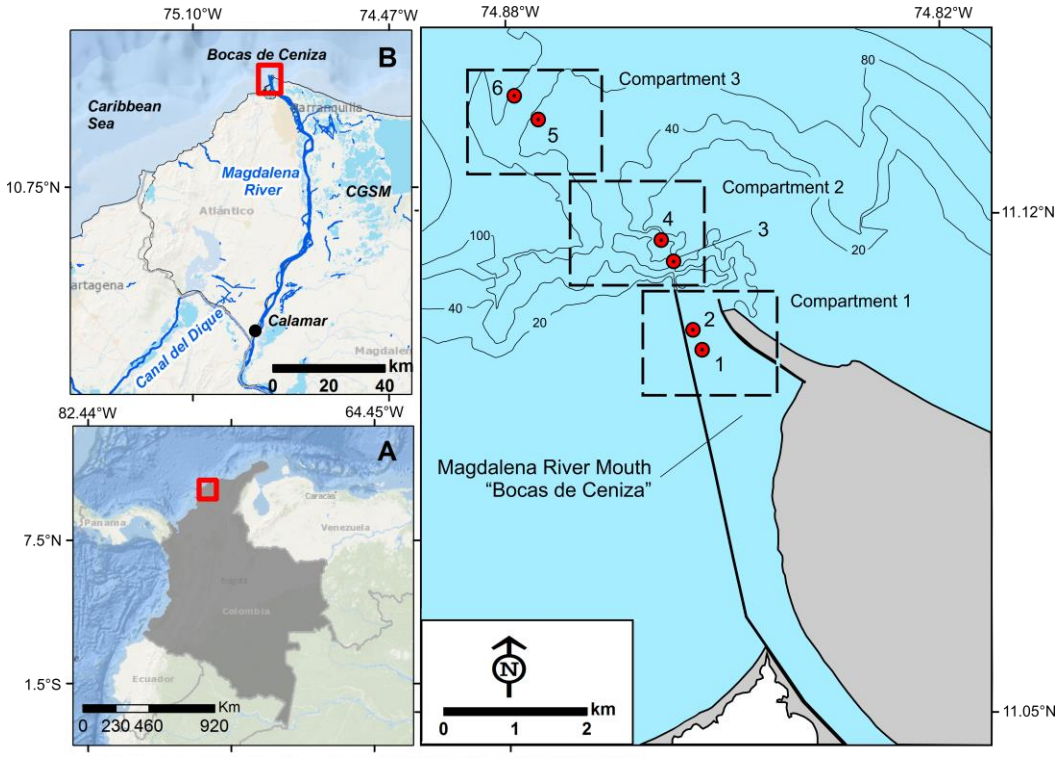

Figure 1. Study area. A) Location of the Magdalena River mouth in northern South America. B) View of the northern coast of Colombia and the location of the Magdalena River mouth. C) Close-up of the Magdalena River mouth, showing the sampling stations and water compartments used in the Muddy LOICZ model. The compartments were defined by the model requirements.

Methods

Data Collection and Laboratory Analysis

Six stations in the Magdalena River mouth were selected for sampling (Figure 1). The study area was divided into three compartments. Compartment 1 encompasses the area in the Magdalena River, 1 to 3 km upstream from the mouth. It possesses characteristics of a fluvial system and has salinities near 0 (Restrepo et al., 2018a). Compartment 2 is farther downstream and includes the Bocas de Ceniza, an estuarine system with intermediate salinities (~15-18) (Restrepo et al., 2018a). Compartment 3 is the ocean area adjacent to the river mouth and is a fully marine system with salinities > 33 (Restrepo et al., 2018a) (Figure 1C). Measurements of salinity and SPM were taken in the three compartments in the transition period (June 2018) and the wet season (November 2018).

Water temperature and salinity profiles were measured with a CTD Castaway (YSI) at a sampling rate of 5 Hz. SPM concentration profiles (sediment concentrations) were measured with a Backscatter Turbidity Sensor (OBS 3A, Campbell Scientific), and grain size distribution was determined with a Diffraction-based Particle Size Analyzer (LISST-200X, Sequoia), both at a sampling rate of 1 Hz. The LISST-200X enables measurement of volumetric concentrations of particles based on 36 logarithmically spaced size classes between 0 and 500 µm (Sequoia, 2016). The OBS 3A was calibrated previously for conditions in the study area. Surface and bottom water samples were collected with a Horizontal Niskin bottle. In the field, water samples were kept in amber glass bottles at 4°C, then transported to the laboratory where they were maintained at 4°C (Quamrul et al., 2016). Samples were filtered using 24-mm-diameter, 0.45-µm Whatman GF/C fiberglass filters, before measuring DIN and DIP concentrations. DIN forms (NH_4, NO_2, NO_3) and DIP (PO_4) were determined by colorimetric analysis (Parsons et al., 1984), using a UV spectrophotometer.

Additional Model Requirements

The stratified Muddy LOICZ model requires specific hydrological and meteorological information (Table 1). Monthly fluvial and meteorological data (streamflow, precipitation and evaporation) for 2018 were collected by the Calamar Hydrological and Meteorological Station and provided by the Colombian Hydrology and Meteorology Institute (IDEAM-Colombia, http://www.ideam.gov.co). The Calamar station was chosen because it is the closest station (~100 km) to the Magdalena River mouth. The area and

volume of the estuary were estimated following the method of Ospino et al. (2018). The estimated area of the estuary was verified with MODIS images downloaded from the NASA Ocean Color website (http://oceancolor.gsfc.nasa.gov). Sewage data (nutrient concentrations, SPM and flows) were obtained from technical reports produced by the Magdalena River Environmental Regional Corporation (CORMAGDALENA-Colombia, http://www.cormagdalena.gov.co).

Table 1. Additional information required for the Muddy-LOICZ model. Values are for the transition period (TP - June 2018) and wet season (WS - November 2018), and data sources are provided.

Additional Information	TP	WS	Source
*Streamflow (10^6 m^3 y^{-1})	190,000	306,670	IDEAM, http://www.ideam.gov.co
Precipitation (m)	0.14	0.27	IDEAM, http://www.ideam.gov.co
Evaporation (m)	0.29	0.12	IDEAM, http://www.ideam.gov.co
Area (10^6 m^2)	130	146	Ospino et al. (2018)
Volume (10^6 m^3)	365	402	Ospino et al. (2018)
Sewage Flow (10^6 m^3 y^{-1})	897	897	CORMAGDALENA, http://www.cormagdalena.gov.co
DIP Sewage (µM L^{-1})	0.1	0.1	CORMAGDALENA, http://www.cormagdalena.gov.co
DIN Sewage (µM L^{-1})	0.01	0.01	CORMAGDALENA, http://www.cormagdalena.gov.co
SPM Sewage (mg L^{-1})	90	90	CORMAGDALENA, http://www.cormagdalena.gov.co

DIP: Dissolved inorganic phosphorus, DIN: Dissolved inorganic nitrogen, SPM: Suspended particle matter. *Streamflow values are expressed on an "annual" basis, using the monthly value within each season.

Stratified Muddy LOICZ model

The Muddy LOICZ model has been used extensively to understand the role of coastal subsystems in the behavior of world oceans, including the role of coastal zones in the cycling of C, N and P (Gordon et al., 1996; Smith et al., 2005; Swaney et al., 2011; Xu et al., 2013). The Muddy LOICZ model is based on mass balance of water and materials (Gordon et al. 1996). Water and salts do not undergo biogeochemical transformations in the system, whereas nutrients do, and thus behave like non-conservative elements (Gordon et al. 1996). The water and salt budgets provide information on the exchange of water between the river and adjacent ocean, by advection, diffusion and mixing. The water budget was estimated using volume measurements of freshwater river discharge (V_r), precipitation (V_t), sewage input (V_{se}), and evaporative loss (V_e). The objective of these budget calculations is the determination of residual flow (V_s) (Gordon et al. 1996). The

seawater volume necessary to maintain the salinity in the system (mixing flow, V_x) was estimated using the conservative salt budget. The salt budget was calculated using the salinity difference between the estuary and the adjacent sea. DIP and DIN budgets were calculated using stoichiometric linkages between fluxes. P and N budgets were used to calculate NEP, i.e., gross primary production (GPP) minus community respiration (R), and N fixation minus denitrification (Nfix-denitr), respectively (Gordon et al. 1996).

We used the stratified Muddy LOICZ model, which is applicable to estuaries with a salt wedge and high concentrations of suspended sediment (Xu et al., 2013; Xu et al., 2015). The model requires clearly labeled entry data to calculate water and material (salts, SPM and nutrient) balances (Gordon et al. 1996). To better represent stratified systems, the model accommodates additional compartments, distributed both vertically and horizontally (Swaney et al., 2011). The estuary (compartment 2) and adjacent ocean (compartment 3) (Figure 1) were divided into two layers (surface and bottom), yielding the following divisions: surface estuary, bottom estuary, surface ocean and bottom ocean. The model also calculates the partition (distribution) coefficient K_d, which indicates the fraction of nutrients present in the particulate phase (Xu et al., 2013).

Results

Nutrient Concentrations

In the Magdalena River (compartment 1), concentrations of DIP and DIN were slightly higher in the wet season than in the transition period (Table 2). In Bocas de Ceniza (compartment 2), the highest DIP concentration was obtained in the wet season for both layers (1.92 ± 0.11 µM L^{-1} surface layer, and 1.77 ± 0.09 µM L^{-1} bottom layer), whereas highest DIN concentration was obtained in the transition period in the surface layer (0.88 ± 0.02 µM L^{-1}) (Table 2). Nutrient concentrations in Bocas de Ceniza were higher than those observed in the Magdalena River. In the adjacent ocean, DIP and DIN concentrations in the surface layer were similar in the transition period and wet season (2.00 ± 0.02 µM L^{-1} DIP and 0.16 ± 0.01 µM L^{-1} DIN in the transition period, and 2.10 ± 0.01 µM L^{-1} DIP and 0.18 ± 0.01 µM L^{-1} DIN in the wet season) (Table 2). DIP values in the ocean (compartment 3) were higher than those in the Magdalena River and Bocas de Ceniza.

Table 2. Averages and standard deviations of dissolved inorganic nutrient concentrations (µM L^{-1}) in compartments of the study area during the transition period (TP – June 2018) and wet season (WS – November 2018).

Compartment	DIP (µM L^{-1})		DIN (µM L^{-1})	
	TP	WS	TP	WS
MR (S)	1.13 ± 0.05	1.53 ± 0.08	0.11 ± 0.02	0.15 ± 0.01
MR (B)	1.32 ± 0.12	1.82 ± 0.10	0.20 ± 0.01	0.25 ± 0.01
BC (S)	1.77 ± 0.09	1.92 ± 0.11	0.88 ± 0.02	0.22 ± 0.02
BC (B)	1.46 ± 0.06	1.77 ± 0.05	0.18 ± 0.01	0.26 ± 0.01
CS (S)	2.00 ± 0.02	2.10 ± 0.01	0.16 ± 0.01	0.18 ± 0.01
CS (B)	1.48 ± 0.01	2.08 ± 0.01	0.01 ± 0.00	0.09 ± 0.01

DIP = Dissolved inorganic phosphorus, DIN = Dissolved inorganic nitrogen, MR(S) = Magdalena River (surface), MR(B) = Magdalena River (bottom), BC(S) = Bocas de Ceniza (surface), BC(B) = Bocas de Ceniza (bottom), CS(S) = Caribbean Sea (surface), CS(B) = Caribbean Sea (bottom).

Salinity and SPM Gradients

A marked salinity gradient was observed in the Bocas de Ceniza (Figure 2). Surface salinity increased gradually from ~0.06 in the river to ~35 in the open sea, ~20 km from the river mouth. Surface salinities in Bocas de Ceniza were lower during the wet season (~6) than during the transition period (~15). Salinities in the bottom layer of the estuary were higher than those in the surface during both periods, ~32 during the transition period and ~18 during the wet season. SPM concentrations in the surface and bottom layers ranged from ~2,600 mg L^{-1} in the Magdalena River to 0 mg L^{-1} in the adjacent ocean during both sampling periods. The estuary at Bocas de Ceniza is turbid, with surface concentrations of 539 mg L^{-1} during the transition period and 624 mg L^{-1} during the wet season. Bottom concentrations at Bocas de Ceniza were around 300 mg L^{-1} during the transition period and 400 mg L^{-1} during the wet season (Figure 2). Salinity profiles in Bocas de Ceniza indicated a stratified water column with a well-defined halocline from about 2-10 m depth during both sampling periods (Figure 3A). SPM measurements in both periods indicated that the highest sediment concentrations were found in the surface layer of the Magdalena River (Figure 3B). In the ocean compartment there was no difference between salinity and sediment concentration in the two monitoring periods. The surface salinity was ~35 in the open sea and the SPM was close to 0 mg L^{-1} (Figure 3C and 3D).

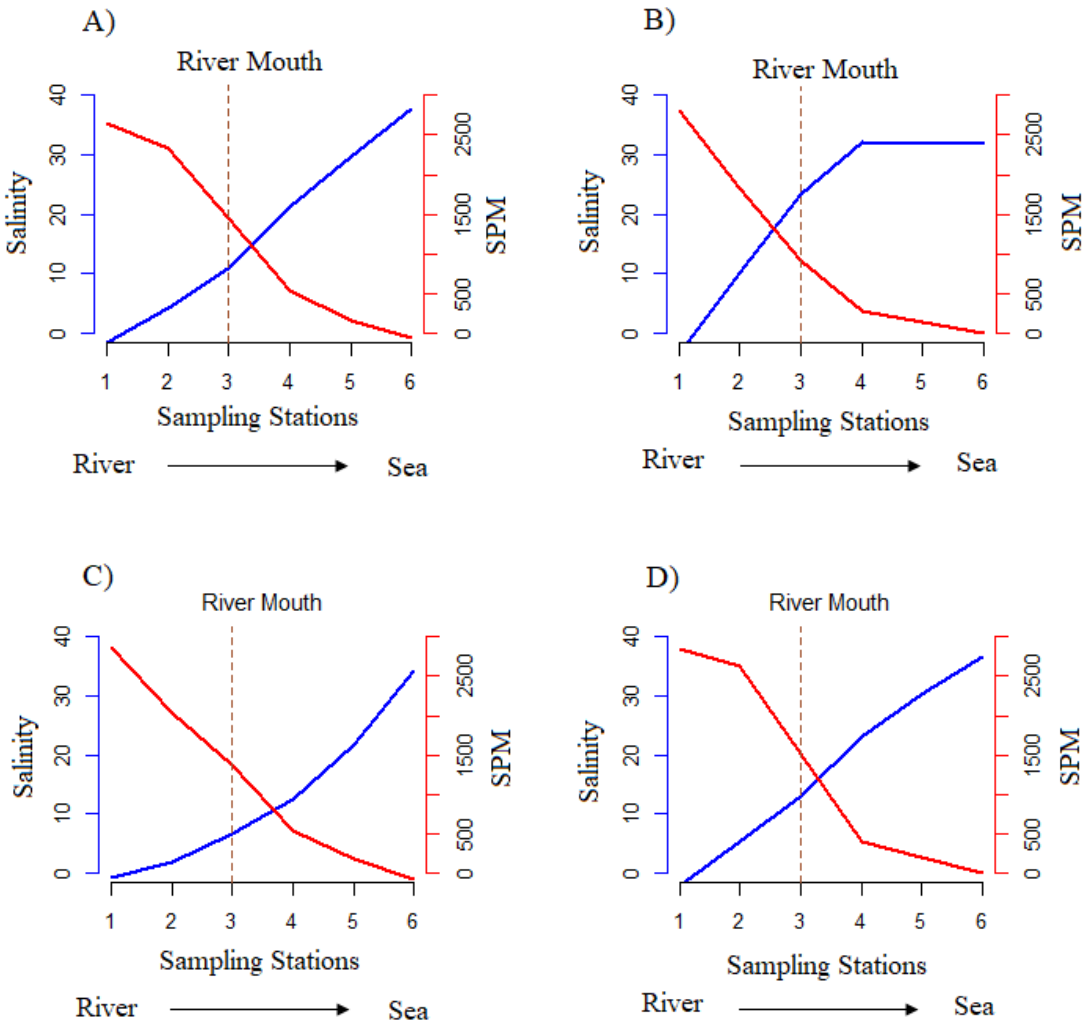

Figure 2. Salinity (blue) and SPM (mg L^{-1}, red) concentrations in upper and lower water layers from the Magdalena River to the open Caribbean Sea. A) Transition Period (June 2018), upper layer; B) Transition Period (June 2018), bottom layer; C) Wet season (November 2018), upper layer; D) Wet season (November 2018), bottom layer. The river mouth, station 3, is indicated by the dashed vertical line.

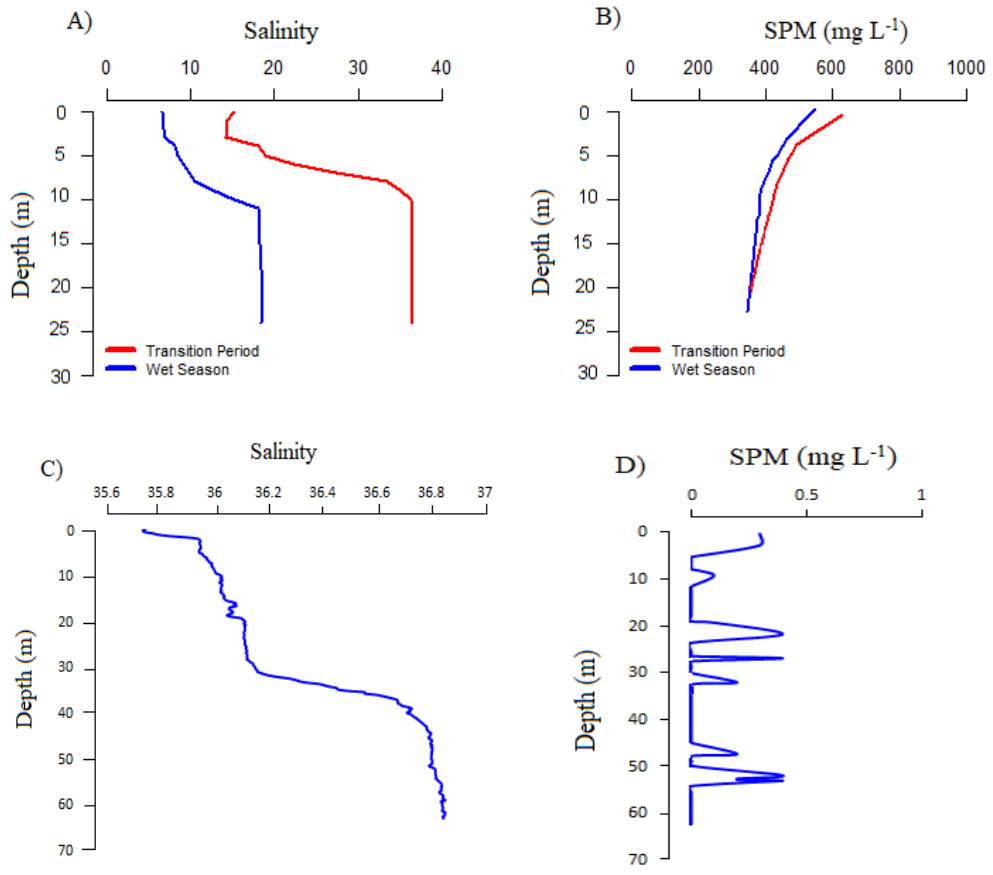

Figure 3. Vertical salinity and SPM. A) Vertical salinity profiles in Bocas de Ceniza (compartment 2) during the transition period (red line) and wet season (blue line). B) Vertical SPM profiles during the transition period (red line) and wet season (blue line) in Bocas de Ceniza. C) Vertical salinity profiles in Caribbean Sea (compartment 3) during the transition period. D) Vertical SPM profiles during the transition period in the Caribbean Sea.

Grain size distribution in both sampling periods indicated differences between the Magdalena River and Bocas de Ceniza compartments (Figures 4 and 5). The Magdalena River water column exhibited a high percentage of particles <63 µm, up to~48% in the transition period and ~47% during the wet season. Particles <63 µm represented ~39% during the transition period and ~35% in the wet season in Bocas de Ceniza. The adjacent ocean had very low concentrations of suspended sediment (near 0), of which ~50-67% was <63 µm. A difference in grain size between the surface and bottom layer was found only in the Magdalena River compartment, where ~87% of suspended sediment in the surface layer was <63 µm, but only ~25% was <63 µm in the bottom layer. In Bocas de Ceniza and the adjacent ocean, compartments 2 and 3, the grain size distributions in the surface and bottom layers were similar. In Bocas de Ceniza, ~32% of the suspended sediment in the surface layer and ~35% in the bottom layer was <63 µm. In the adjacent ocean, ~52% of the suspended sediment in the surface layer and ~50% in the bottom layer was <63 µm. In Bocas de Ceniza, although there was no difference in the proportion of particles <63 µm in the surface and bottom water layers, highest concentrations of particles >63 µm were observed in the surface layer.

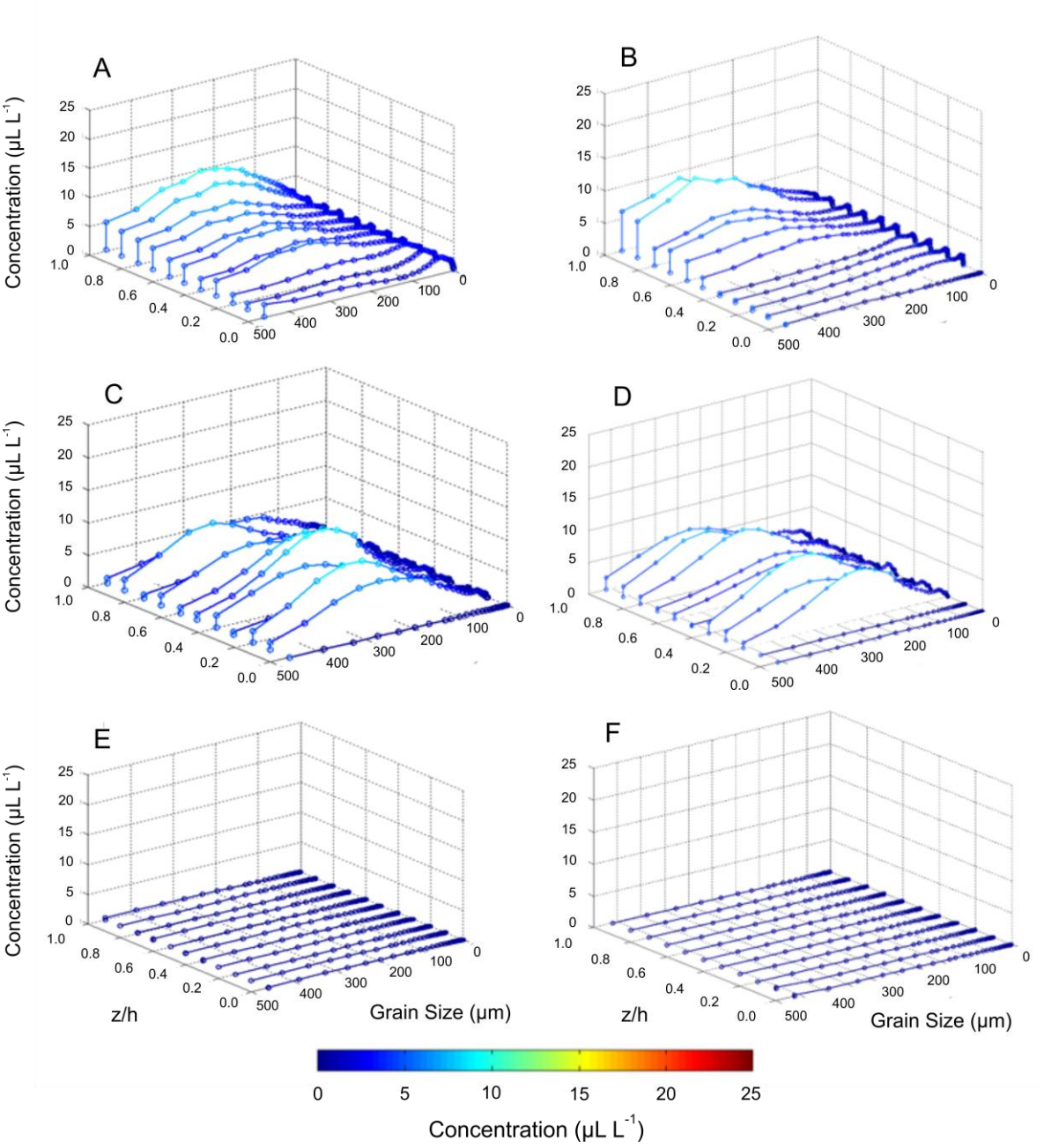

Figure 4. Concentrations of particles of different grain size in the water column during the transition period (June 2018). A) Magdalena River (sampling station 1), B) Magdalena River (sampling station 2), C) Bocas de Ceniza (sampling station 3), D) Bocas de Ceniza sampling station 4), E) Caribbean Sea (sampling station 5), F) Caribbean Sea (sampling station 6).

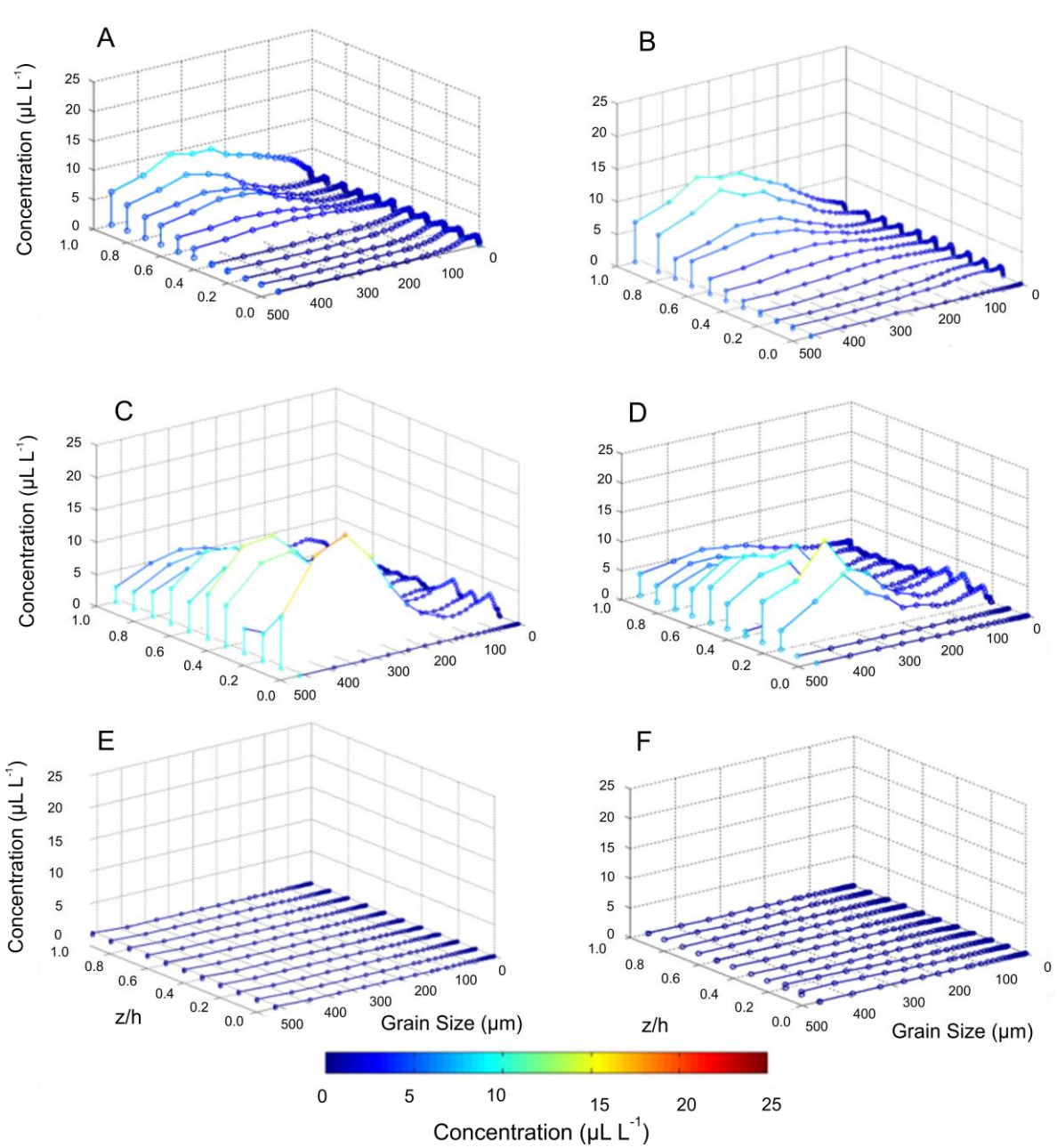

Figure 5. Concentrations of particles of different grain size in the water column during the wet season (November 2018). A) Magdalena River (sampling station 1), B) Magdalena River (sampling station 2), C) Bocas de Ceniza (sampling station 3), D) Bocas de Ceniza sampling station 4), E) Caribbean Sea (sampling station 5), F) Caribbean Sea (sampling station 6).

Stratified Muddy LOICZ Model

Water-Salt Balance

Residual volumes (V_s) discharged into the ocean were ~907 x 10^6 m^3 d^{-1} and 1,036 x 10^6 m^3 d^{-1} during the transition period and the wet season, respectively (Figure 6). In both cases, this volume was greater than the river discharge during the wet season (843 x 10^6 m^3 d^{-1}), and the transition period (523 x 10^6 m^3 d^{-1}). The mixed volume between the surface and bottom layers by diffusive turbulent flux (V_z) inside the estuary was 89 x 10^6 m^3 d^{-1} during the transition period, and 283 x 10^6 m^3 d^{-1} during the wet season. The advective flux (V_{ent}) from the bottom layer of the estuary to the surface layer was 384 x 10^6 m^3 d^{-1} and 193 x 10^6 m^3 d^{-1} during the transition period and the wet season, respectively (Table 3). Diffusive flow (V_z) during the wet season was three times greater than during the transition period. Advective flux, however, was approximately two times greater in the transition period compared to the wet season.

Salinity measurements show the formation of a salt convergence front and salt wedge penetration upriver (Figure 6). The area calculated for the estuary varied between the two sampling periods, with an area of 130 km^2 in the transition period and 146 km^2 in the wet season. Residence time during the transition period was 1.2 days for the upper layer of the estuary and 0.9 days for the bottom layer. Residence time during the wet season in the Bocas de Ceniza estuary was 1.5 days for the upper layer and 2.1 days for the bottom layer.

Table 3. Hydrologic variables for the Magdalena River Estuary (Bocas de Ceniza).

Output	Units	TP	WS
Inflow from land (V_r)	10^6 m^3 d^{-1}	523	843
Turbulent diffuse flow between two layers (V_z)	10^6 m^3 d^{-1}	89	283
Advective inflow estuary bottom to surface layer (V_{ent}, V_{deep})	10^6 m^3 d^{-1}	384	193
Advective outflow estuary surface layer to sea (V_s)	10^6 m^3 d^{-1}	907	1,036
Area (A)	km^2	130	146
Residence time surface layer (T_s)	d	1.2	1.5
Residence time bottom layer (T_b)	d	0.9	2.1

TP=Transition period (June), WS=Wet season (November).

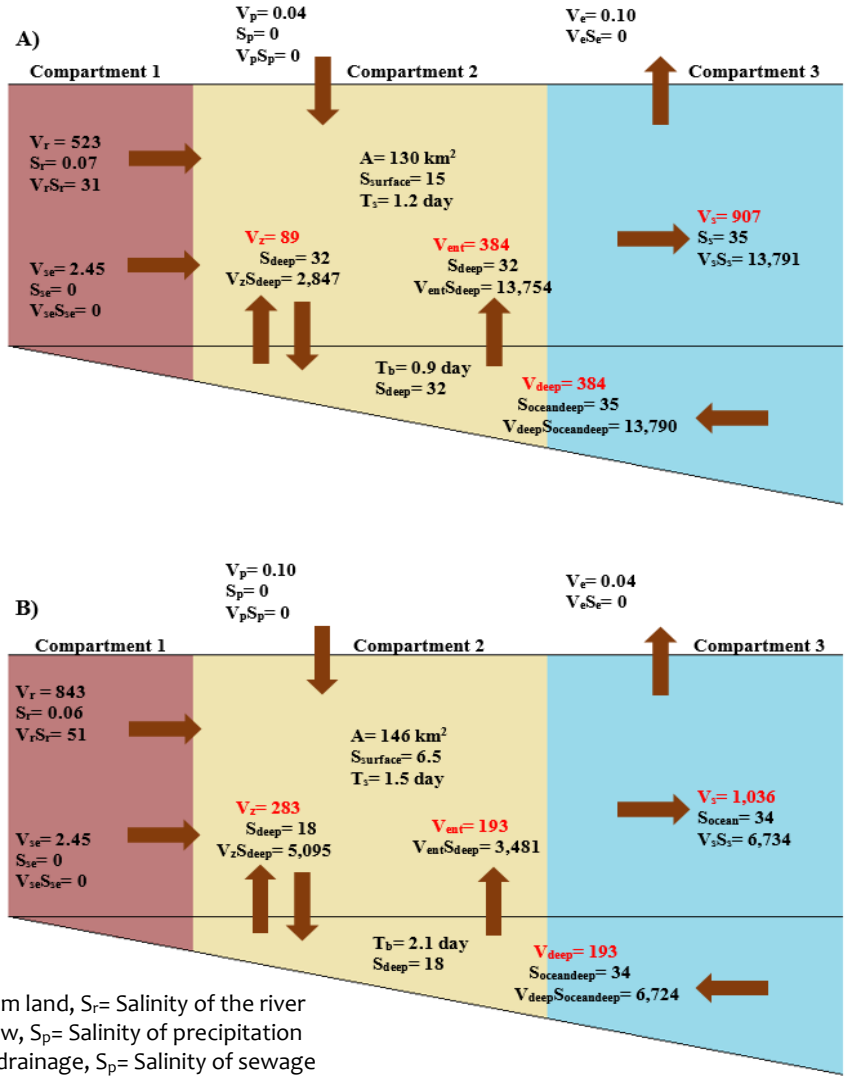

V_r= Inflow from land, S_r= Salinity of the river
V_p= Rain Inflow, S_p= Salinity of precipitation
V_{se}= Sewage drainage, S_p= Salinity of sewage
V_e=Water loss to evaporation
V_z= Turbulent diffuse flow between the two layers in the estuary
S_{deep}= Salinity of estuary (bottom layer)
$S_{surface}$= Salinity of estuary (surface layer)
V_{ent}= V_{deep}= Advective inflow from estuary bottom layer to surface layer
$S_{oceandeep}$= Salinity of ocean (bottom layer)
V_s= Advective outflow from estuary surface layer to the sea
S_{ocean} = Salinity of ocean (surface layer)
A= Area of estuary
T= Residence Time

Figure 6. Water-Salt Balance. A) Transition period (June). B) Wet season (November). The units for water fluxes are 10^6 m^3 d^{-1}, and for salinity fluxes are 10^3 ton d^{-1}.

Dissolved Inorganic Phosphorus (DIP) Transport

DIP fluxes and NEP varied seasonally and show the importance of phosphorus adsorption-desorption in the nutrient balance (Figure 7). The river compartment represented the largest contribution of phosphorus to the estuary during both the transition period and the wet season. Regardless of adsorption-desorption processes, the Magdalena River contributed DIP fluxes (DIP_r) to the estuary (Bocas de Ceniza) at rates of 588 x 10^3 moles d^{-1} during the transition period, and 1,285 x 10^3 moles d^{-1} during the wet season. Under these conditions, the model indicates that the Bocas de Ceniza estuary transported to the ocean 1,605 x 10^3 moles d^{-1} (DIP_s) during the transition period, and 1,989 x 10^3 moles d^{-1} during the wet season. The transport of DIP by advective flux in both periods was considerably lower than contributions from diffusive flux and turbulent mixing. Net DIP flux (ΔDIP) inside the estuary was 483 x 10^3 moles d^{-1} for the transition period, and 403 x 10^3 moles d^{-1} for the wet season. Positive ΔDIP values indicate loss of phosphorus. NEP values were negative for both the transition period (-394 mmol C m^2 d^{-1}), and wet season (-293 mmol C m^2 d^{-1}), indicating that the estuary behaved like a heterotrophic system (Table 4).

The model estimated partition (distribution) coefficients (K_d) for all compartments, considering adsorption-desorption processes related to suspended particle matter (SPM) (Table 5). These coefficients indicated low dissolved nutrient fractions in the River and Bocas de Ceniza Estuary (~10 to ~30%). These results indicated a significant increase in the flux of phosphorus coming from the river, with 1,921 x 10^3 moles d^{-1} in the transition period, and 4,078 x 10^3 moles d^{-1} in the wet season (Table 6). Overall, the estuary behaved like a phosphorus sink, showing storage of -1,241 x 10^3 moles d^{-1} and -3,578 x 10^3 moles d^{-1} for the transition period and wet season, respectively. NEP values were positive for both periods, with values of 1,012 mmol C m^2 d^{-1} during the transition period, and 2,592 mmol C m^2 d^{-1} during the wet season. Changes in SPM values from one compartment to another, and the high partition (distribution) coefficients (K_d) made the estuary an important sink or source of nutrients through adsorption-desorption with suspended sediment. Productivity was greater than respiration when the model considered SPM (Figure 7).

Table 4. Seasonal variation of dissolved inorganic phosphorus (DIP) and net ecosystem productivity (NEP), without considering nutrient adsorption and desorption.

Output	Units	TP	WS
Effective inflow DIP from river (DIP_r)	10^3 mol d^{-1}	588	1,285
Effective DIP inflow by turbulent mixing (DIP_z)	10^3 mol d^{-1}	-27	-42
Effective advective DIP inflow from bottom (DIP_{ent})	10^3 mol d^{-1}	561	342
Advective DIP loss from the estuary (DIP_s)	10^3 mol d^{-1}	1,605	1,989
Net budget (ΔDIP)	10^3 mol d^{-1}	483	403
Net ecosystem productivity (NEP)	mmol C m^2 d^{-1}	-394	-293

TP=Transition period (June), WS=Wet season (November).

Table 5. Seasonal difference in the partition (distribution) coefficient (K_d) in the study zone.

Output	Units	TP	WS
Partition coefficient river	%	97	98
Partition coefficient estuary surface layer	%	70	72
Partition coefficient estuary bottom layer	%	85	88
Partition coefficient estuary surface layer	%	23	25
Partition coefficient estuary bottom layer	%	33	38

TP=Transition period (June), WS=Wet season (November).

Table 6. Seasonal difference in dissolved inorganic phosphorus (DIP) and net ecosystem productivity (NEP), when nutrient adsorption and desorption are considered.

Output	Units	TP	WS
Effective inflow DIP from river (DIP_r)	10^3 mol d^{-1}	1,921	4,078
Effective DIP inflow by turbulent mixing (DIP_z)	10^3 mol d^{-1}	10	13
Effective advective DIP inflow from bottom (DIP_{ent})	10^3 mol d^{-1}	-205	-109
Net budget (ΔDIP)	10^3 mol d^{-1}	-1,241	-3,578
Net ecosystem productivity (NEP)	mmol C m^2 d^{-1}	1,012	2,592

TP=Transition period (June), WS=Wet season (November).

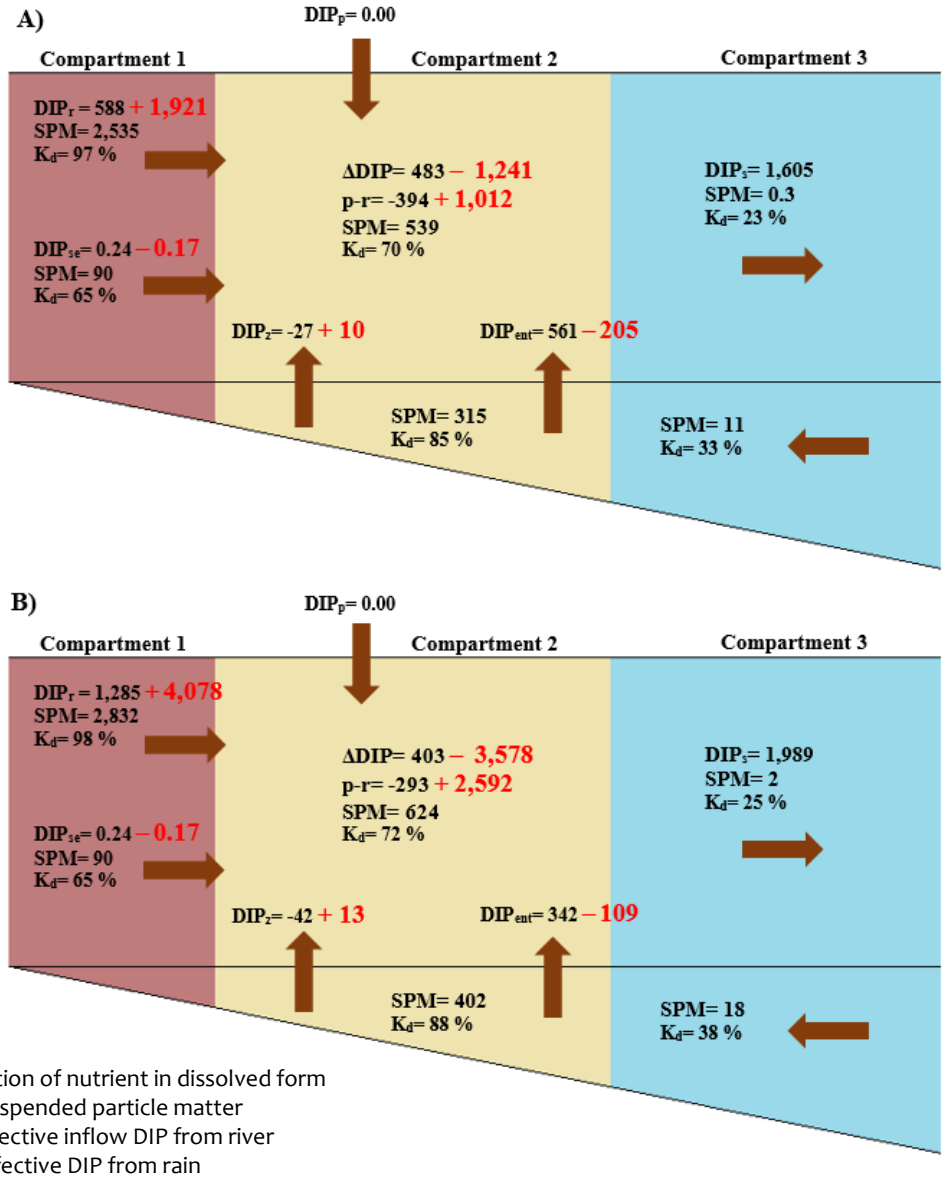

K_d= Fraction of nutrient in dissolved form
SPM= Suspended particle matter
DIP_r= Effective inflow DIP from river
DIP_p= Effective DIP from rain
DIP_{se}= Effective inflow DIP from sewage
DIP_z= Effective DIP inflow from bottom by turbulent mixing
DIP_{ent}= Effective advective DIP inflow from bottom
DIP_s= Advective DIP loss from estuary surface
ΔDIP= Net budget (Delta DIP for estuary surface layer)
p-r= Net ecosystem productivity

Figure 7. DIP Budget. A) Transition period (June). B) Wet season (November). Units for variables are 10^3 mol d^{-1} (DIP); mmol C m^2 d^{-1} (p-r); mg L^{-1} (SPM). DIP flux through the estuary was calculated both with adsorption-desorption (red), and without it (black).

Net DIN Transport

The most important nitrogen inputs for both study periods were those from the river (DIN_r) and through diffusive flux (DIN_{ent}) (Figure 8). Turbulent input of nitrogen was low, about 8 x 10^3 mol d^{-1} during the transition period, and 11 x 10^3 mol d^{-1} during the wet season. When SPM input is not considered, the Bocas de Ceniza Estuary exported 72 x 10^3 moles d^{-1} of nitrogen during the transition period, and 227 x 10^3 moles d^{-1} of nitrogen during the wet season. Net DIN flux within the estuary was -62 x 10^3 moles d^{-1} of nitrogen in the transition period, and -40 x 10^3 moles d^{-1} of nitrogen during the wet season. Nitrogen metabolism, expressed as nfix-denit, was negative for both cases, with -60 mmol DIN m^2 d^{-1} during the transition period, and -43 mmol DIN m^2 d^{-1} during the wet season. These results indicate that denitrification prevailed in both study periods (Table 7).

DIN fluxes and nitrogen metabolism changed considerably when adsorption-desorption processes were included in the model (Table 8). Results indicated a significant increase in nitrogen flux from the river, 187 x 10^3 moles d^{-1} in the transition period and 399 x 10^3 moles d^{-1} in the wet season, with increases of 65 and 43%, when adsorption-desorption processes were included in the model. The estuary behaved as a nitrogen sink during both study periods, with -158 x 10^6 moles d^{-1} in the transition period, and -339 x 10^6 moles d^{-1} in the wet season. Nitrogen metabolism (nfix-denit) turned positive when adsorption-desorption processes were considered, with 151 mmol DIN m^2 d^{-1} in the transition period, and 389 mmol DIN m^2 d^{-1} in the wet season (Figure 8). This indicates that nitrogen fixation prevailed when SPM was considered, whereas denitrification prevailed when SPM was not considered.

Table 7. Seasonal variation of dissolved inorganic nitrogen (DIN) without considering nutrient adsorption and desorption.

Output	Units	WS	TP
Effective inflow DIN from river (DIN_r)	10^3 mol d^{-1}	126	57
Effective DIN inflow by turbulent mixing (DIN_z)	10^3 mol d^{-1}	11	8
Effective advective DIN inflow from bottom (DIN_{ent})	10^3 mol d^{-1}	50	69
Advective DIN loss from the estuary (DIN_s)	10^3 mol d^{-1}	227	72
Net budget (ΔDIN)	10^3 mol d^{-1}	-40	-62
Nitrification – denitrification (nfix-denit)	mmol DIN m^2 d^{-1}	-43	-60

TP=Transition period (June), WS=Wet season (November).

Table 8. Seasonal variation of dissolved inorganic nitrogen (DIN), when nutrient adsorption and desorption are considered.

Output	Units	TP	WS
Effective inflow DIN from river (DIN_r)	10^3 mol d^{-1}	187	399
Effective DIN inflow by turbulent mixing (DIN_z)	10^3 mol d^{-1}	-3	-3
Effective advective DIN inflow from bottom (DIN_{ent})	10^3 mol d^{-1}	-25	-16
Advective DIN loss from the estuary (DIN_s)	10^3 mol d^{-1}	72	227
Net budget (ΔDIN)	10^3 mol d^{-1}	-158	-339
Nitrification – denitrification (nfix-denit)	mmol DIN m^2 d^{-1}	151	389

TP=Transition period (June), WS=Wet season (November).

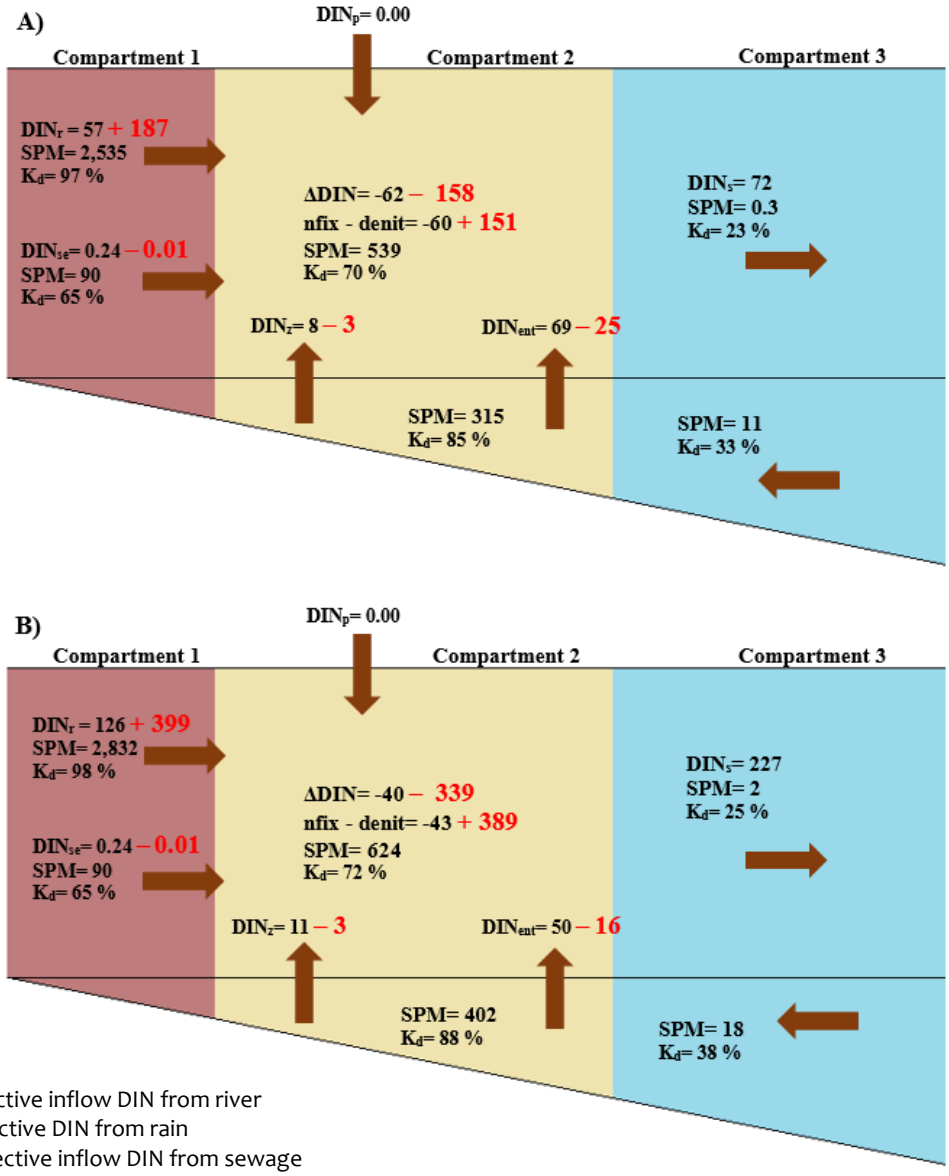

DIN_r= Effective inflow DIN from river
DIN_p= Effective DIN from rain
DIN_{se}= Effective inflow DIN from sewage
DIN_z= Effective DIN inflow from bottom by turbulent mixing
DIN_{ent}= Effective advective DIN inflow from bottom
DIN_s= Advective DIN loss from estuary surface
ΔDIN= Net budget (Delta DIN for estuary surface layer)
nfix-denit= Nitrification – denitrification

Figure 8. DIN Budget. A) Transition period (June). B). Wet season (November). Units are 10^3 mol d^{-1} (DIN); mmol DIN m^2 d^{-1} (nfix-denit). The DIN flux through the estuary was calculated without adsorption-desorption (black), and with it (red).

Discussion

Biogeochemical Dynamics in the Magdalena River Estuary

This study elucidates the biogeochemistry of the Bocas de Ceniza Estuary, which is dependent on (1) seasonal river discharge, which varies from ~4,361 m^3 s^{-1} in the transition period to ~8,063 m^3 s^{-1} in the wet season, and (2) the concentration of SPM transported by the Magdalena River (~2,400 mg L^{-1} in the transition period and ~2,600 mg L^{-1} in the wet season) (Restrepo et al., 2014). Changes in river flux lead to variations in the sediment and nutrient transport into the estuary, and the formation of convergent fronts (surface and vertical), which determine productivity in coastal waters (Dittmar and Kattner, 2003; Watanabe et al., 2014). Conservative nutrient mixing is associated with water residence time, which controls biotic and abiotic processes that can modify the concentration of incoming nutrients (Wolanski et al., 2004). Water residence time determines, to a large extent, the sensitivity of coastal systems to nutrient contamination (Wolanski et al., 2004). This depends on the morphology and oceanographic conditions in the study zone (e.g. drainage area, water density, streamflow, density stratification, mixing conditions, tidal variations, winds, among others) (Kenov et al., 2012), and is critical to the health of a water body subjected to human-induced stresses (Watanabe et al., 2014). The Muddy LOICZ model used in this study estimated residence times for the Bocas de Ceniza Estuary. There was little difference in water residence time between seasons: 1.2 days (surface layer) and 0.9 days (bottom layer) in the transition period, and 1.5 (surface layer) and 2.1 days (bottom layer) in the wet season (Figure 6). Residence time in the Bocas de Ceniza Estuary surface layer was slightly higher in the wet season than in the transition period. On the other hand, there was a difference in water residence time across seasons for the bottom layer, which could be related to the salt wedge penetration in the study zone. Residence times obtained by this study are lower and less different between seasons compared to those reported for other stratified estuaries in the world, with values of ~7-8 days during low-flow seasons and ~0.5-3 days in high-flow seasons for the Yangtze (China) and Wami (Tanzania) Estuaries, respectively (Xu et al., 2013; Kiwango et al., 2018). It is important to note that those estuaries are characterized by greater water fluxes and drainage areas (Xu et al., 2013; Kiwango et al., 2018). Likewise, the low residence times found at the Bocas de Ceniza Estuary can be associated with the anthropogenic activities (i.e. constructed channels). Estuaries with low water residence times inhibit algae blooms

because the water residence time is shorter than the doubling time of algal cells (Kenov et al., 2012).

Our results corroborate the claim that the Magdalena River carries high concentrations of suspended sediment, so that the estuary at its mouth is highly turbid (Restrepo et al., 2018a). Sediment concentrations in the Magdalena River mouth are of the same magnitude as those reported for rivers with greater fluxes and drainage areas (e.g, the Yangtze, Yellow and Amazon Rivers) (Li et al., 2012; Liu et al., 2011; Gensac et al., 2016). Several recent studies showed that SPM properties and concentrations directly influence nutrient concentrations and distributions (Gao et al., 2008; Mbaye et al., 2016). Nutrient budgets in most studies, however, have not accounted for nutrients in particulate form (Xu et al., 2013). The calculated partition (distribution) coefficient (K_d) for upper waters in the Bocas de Ceniza Estuary ranged from 70% in the transition period to 72% in the wet season, whereas in the bottom layer it varied from 85% during the transition period to 88% in the wet season. These K_d values indicate low fractions (~10-30 %) of dissolved nutrients. In this case, K_d values differed significantly between seasons, which could be related to the slight difference in the amount of sediment transported by the Magdalena River during the two time periods analyzed. These results are consistent with those of Middelburg and Herman (2007), and Xu et al. (2013), who suggested that 20% of the nutrients in estuarine waters are in particulate form, a fraction that rises to 60-80% in highly turbid estuaries (100-1000 mg L^{-1}). Sediments in deltaic systems are subject to resuspension, so particle sinks may not be permanent. This implies that (re)-transport and remineralization of organic matter (OM) in sediment may contribute bioavailable nutrients to the water column (Chao et al., 2017), particularly if hydrodynamic factors promote chemical interchange between the sediment and water. Depending on the physical characteristics of ecosystems (e.g. density stratification, streamflow, water residence time, etc.), and reaction times, processes involving SPM can become even more complex, e.g. if flocculation occurs (Chao et al., 2017). Flocculation may occur in the estuary of the Magdalena River mouth, as suggested by the high proportion of cohesive sediment (Figure 4 and 5), together with the density stratification and salinities typical for the area (Figure 3). The prevalence of fine sediment (Restrepo et al., 2016) with high OM content in the Magdalena River (Restrepo and Kjerfve, 2004), and the role of turbulence in vertical mixing, suggest a system prone to flocculation (Wu et al., 2012; Restrepo et al., 2018; Papenmeier et al., 2014).

DIP and DIN concentrations in the Bocas de Ceniza Estuary reflect strong DIP and DIN retention there. That is, the estuary is a sink for both phosphorus and nitrogen. NEP is a useful indicator of trophic state in estuaries and can differ depending on the physico-chemical characteristics of ecosystems (Caffrey, 2003; Swaney et al., 2011). If NEP is positive, the system is autotrophic, suggesting that internal production of OM dominates, whereas if NEP is negative, the system is heterotrophic and depends on external sources of OM (Cafrey, 2003; Swaney et al., 2011). Consistent with the NEP results, the Bocas de Ceniza Estuary functions as a heterotrophic system in which denitrification prevails, if the SPM contribution is not considered. Net heterotrophic ecosystems, i.e. P<R, imply that allochthonous OM inputs contribute to high ecosystem respiration rates (Moore et al., 2008). Conversely, when SPM was considered, the Bocas de Ceniza Estuary functions as an autotrophic system, with nitrogen fixation. A net autotrophic ecosystem (P>R) has surplus primary production to feed higher trophic levels (Moore et al., 2008). Results indicated that SPM influence on NEP is greater during the wet season, possibly because of higher sediment concentrations during the wet season than during the transition period. SPM must be included in estimates of nutrient loads in turbid environments (Xu et al., 2013). In the Bocas de Ceniza Estuary, SPM sequesters riverine DIP and DIN, which affects the estimate of NEP to such an extent that the respective roles of primary production and biological respiration would have been wrongly interpreted if SPM were ignored. Likewise, fine sediment particles (silt and clay) transported by rivers carry the major proportion of nutrients in adsorbed form. Thus, sediment deposition removes nutrients from the water column (Chao et al., 2017).

A large proportion of the Colombian population depends on the Magdalena River for potable water, agricultural activities, or as a protein source (Tejeda-Benítez et al., 2016). The Magdalena River basin has experienced major human disturbances in the last few decades (Restrepo and Syvitski, 2006). Perturbations include poor land use practices, agrochemical overuse, deforestation, mining, and increasing urban development and wastewater discharge (Restrepo and Syvitski, 2006; Olivero-Verbel, 2012; Caballero-Gallardo et al., 2015). Thirty-eight million inhabitants, ~79% of the Colombian population, live in the largest cities (Bogotá, Medellin, Cali and Barranquilla) of the country, within the zone influenced by the Magdalena River (Tejeda-Benítez et al., 2016). The Bogota River, one of the most contaminated rivers in Colombia, flows into the Magdalena River, and is the largest contributor of heavy metals to the Magdalena River (Olivero-Verbel, 2012). In the city of Barranquilla, wastewater from the city water and sewer company is

discharged approximately 3 km from the Magdalena River mouth (Vivas-Aguas et al., 2017). Some houses have no connection to the sewage network, resulting in direct waste discharge into water bodies (Magdalena River and Ciénaga de Mallorquín) (Tejeda-Benítez et al., 2016). All the aforementioned human activities have modified the natural function of this ecosystem, leading, in some cases, to the deterioration of critical habitats and loss of biodiversity (Caballero-Gallardo et al., 2015; Restrepo and Syvitski, 2006; Restrepo, 2008). Nevertheless, our results suggest that despite the high contaminant load that the Magdalena River receives, low water residence times in the estuary imply that only biogeochemical processes with rapid reaction rates (e.g., SPM adsorption-desorption), influence ecological functions in the estuary and its assimilation capacity (Kenov et al., 2012). The assimilation capacity defines the ability of an estuary to absorb and use a discharged substance, without water quality impairment, without harm to the aquatic biota, and without compromising the water body's designated use (Watson et al., 2012). Simulations of water quality in the area close to the Magdalena River mouth revealed a hydrology altered by human activities, but also highlighted the large assimilation capacity of the Magdalena River (Torres-Bejarano et al., 2015). Nevertheless, other types of contamination (e.g. heavy metals, pesticides) occur in the study area, from urban and industrial wastewaters, constant dredging of the navigable channel, and sediment settling.

Field measurements of dissolved oxygen (DO) and pH showed that DO concentrations differ between compartments, with an average value of 4.2 mg L^{-1} in the river, 6.9 mg L^{-1} in Bocas de Ceniza and 7.0 mg L^{-1} in the adjacent ocean (Uninorte, 2019). Differences in DO concentrations among compartments could be related to hydrodynamics, which influence mixing and transport processes, concentrations of nutrient and non-nutrient substances, and oxygenation of the water column (Horner-Devine et al., 2015). pH varied from 7.1 to 7.8 in all compartments (Uninorte, 2019). Reported DO and pH values are within the permitted ranges for conservation of fauna and flora (>4.0 mg L^{-1} and 6.0-8.5 mg L^{-1}, respectively), according to legal regulations in Colombia (MinAmbiente, decree 1598 of 1984). Nevertheless, DO values in the Magdalena River are low, which might be a consequence of low light penetration and low rates of photosynthesis caused by high SPM concentrations.

Stratified Muddy LOICZ Model

One recent human modification of coastal zones is the increase in nutrient input from the continent. At the global scale, nutrient inputs increased dramatically during the 20th century, mainly because of human activities and climate change (Swaney et al., 2011). Efforts to understand biogeochemical functioning of ecosystems have generally used linear models to discern global trends in dissolved inorganic nutrient loads (Talaue-McManus et al., 2003). The LOICZ model is one of the simplest and most realistic box models that enables identification of the path taken by nutrients (Swaney et al., 2011). The LOICZ model has been applied to more of 200 estuaries and coastal waters around the world (Xu et al., 2013; Swaney et al., 2011; Xu et al., 2015; Kiwango et al., 2016). Nutrient budgets calculated with the LOICZ model are useful to understand the function of coastal systems and how they respond to natural and anthropogenic pressures (Smith et al., 2005).

The Muddy LOICZ model is also simple and provides reliable estimates of biogeochemical processes in coastal ecosystems (Xu et al., 2013). This model was used to estimate net ecosystem productivity in the Magdalena River mouth during the two study periods, i.e. the wet season and transition period. Implementation of this model enabled us to determine that (*i*) the fluvial contribution of nutrients into the estuary differed between seasons, (*ii*) function of the estuary ecosystem changes considerably when SPM adsorption-desorption processes were included, (*iii*) most nutrients are in particulate form, with only a small percentage in dissolved form, and (*iv*) the estuary is an autotrophic nutrient sink. The LOICZ model is mainly predictive and cannot be verified unless specific biophysical studies are undertaken, which require extensive field work and data sampling. Nutrient concentration values obtained with the LOICZ model may be inaccurate, as additional (e.g. nonpoint) nutrient sources are not considered (Kiwango et al., 2016). Likewise, the model ignores the role of detritus and the processing of nutrients in the food web above the trophic level of phytoplankton (Kiwango et al., 2016). Additional nutrient sources and the role of detritus are not considered, in large part because of the lack of data that encompass the high spatial and temporal variability of coastal ecosystems, and because of the high complexity of physical and chemical processes that occur in these systems (Kiwango et al., 2016).

Information related to other nutrient input sources in the Magdalena River mouth is scarce, limiting available data for the model. In Colombia there are no reliable

discharge/volume databases regarding runoff, groundwater, and wastewater (urban or industrial), or their physico-chemical properties. Some data used for the implementation of the model were taken from technical reports from the Environmental Regional Corporations (CRA and CORMAGDALENA). We believe that changes in input data would not alter our results dramatically, as runoff water volume is very low, given the low rainfall in the study area.

References

Andrade, C.A. 2001. Las corrientes superficiales en la cuenca de Colombia observadas con boyas de deriva. Revista de la Academia Colombiana de Ciencias Exactas, Físicas y Naturales, 25(96), 321-335.

Anthony, E., Marriner, N., Morhange, C. 2014. Human influence and the changing geomorphology of Mediterranean deltas and coast over last 6000 years: from progradation to destruction phase?. Earth Science Reviews, 139, 336-361. https://doi.org/10.1016/j.earscirev.2014.10.003.

Araujo, M., Noriega, C., Lefèvre, N. 2014. Nutrients and carbon fluxes in the estuaries of major rivers flowing into the tropical Atlantic. Frontiers Marine Sciences, 1(10), 1-16. https://doi.org/10.3389/fmars.2014.00010.

Bianchi, T. 2007. Biogeochemistry of estuaries. New York: Oxford University Press, 689 p.

Caballero-Gallardo, K., Guerrero-Castilla, A., Johnson-Restrepo, B., Olivero-Verbel, J. 2015. Chemical and toxicological characterization of sediments along a Colombian shoreline impacted by coal export terminals. Chemosphere, 138, 837-846. https://doi.org/10.1016/j.chemosphere.2015.07.062.

Caffrey, J.M. 2003. Production, respiration and net ecosystem metabolism in U.S. estuaries. Environmental, Monitoring and Assessment, 81, 207–219. https://doi.org/10.1023/A:1021385226315.

Chao, G., Qing, H., Leicheng, G., Winterwerp, J. 2017. A study of in-situ sediment flocculation in the turbidity maxima of the Yangtze Estuary. Estuarine, Coastal and Shelf Science, 191, 1-9. https://doi.org/10.1016/j.ecss.2017.04.001.

Dittmar, T., Kattner G. 2003. The biogeochemistry of the river and shelf ecosystem of the Arctic Ocean: a review. Marine Chemistry, 83, 103-120. https://doi.org/10.1016/S0304-4203(03)00105-1.

Gao, L., Li, D. J., Ding, P. X. 2008. Variations of nutrients in response to the highly dynamic suspended particulate matter in the Changjiang (Yangtze River) plume. Continental Shelf Research, 28(17), 2393-2403. https://doi.org/10.1016/j.csr.2008.05.004.

Gensac, E., Martinez, J.M., Vantrepotte, V., Anthony, E.J. 2016. Seasonal and inter-annual dynamics of suspended sediment at the mouth of the Amazon river: The role of continental and oceanic forcing, and implications for coastal geomorphology and mud bank formation. Continental Shelf Research, 118, 49-62. https://doi.org/10.1016/j.csr.2016.02.009.

Glibert, P.M., Seitzinger, S., Heil, C.A., Burkholder, J.A., Parrow, M.W., Codispoti, L.A., Kelly, V. 2005. The role of eutrophication in the global proliferation of harmful algal blooms: new perspectives and new approaches. Oceanography, 18, 198-209. https://doi.org/10.5670/oceanog.2005.54.

Glober, C., Cullison, L.A., Koch, F., Harder, T.M., Krause, J.W. 2005. Influence of freshwater flow, ocean exchange, and seasonal cycles on phytoplankton – nutrient dynamics in a temporally open estuary. Estuarine, Coastal and Shelf Science, 65, 275-288. https://doi.org/10.1016/j.ecss.2005.05.016.

Goñi, M.A., Voulgaris, G., Kim, Y.H. 2009. Composition and fluxes of particulate organic matter in a temperate estuary (Winyah Bay, South Carolina, USA) under contrasting physical forcings. Estuarine, Coastal Shelf Science, 85, 273-291. https://doi.org/10.1016/j.ecss.2009.08.013.

Gordon, D.C., Boudreau, P.R., Mann, K.H., Ong, J.E., Silvert, W.L., Smith, S.V., Wattayakorn, G., Wulff, F., Yanagi, T. 1996. LOICZ Biogeochemical Modelling Guidelines. LOICZ Reports and Studies No. 5, 96 p.

Harvey, E., Kratzer, S., Philipson, P. 2015. Satellite-based water quality monitoring for improved spatial and temporal retrieval of chlorophyll-a in coastal waters. Remote Sensing Environment, 158, 417–430. https://doi.org/10.1016/j.rse.2014.11.017.

Horner-Devine, A., Hetland, R.D., MacDonald, D.G. 2015. Mixing and Transport in Coastal River Plumes. Annual Review of Fluid Mechanics, 47, 569-594. https://doi.org/10.1146/annurev-fluid-010313-141408.

Jiang, S., Müller, M., Jin, J., Wu, Y., Zhu, K., Zhang, G., Mujahid, A., Rixen, T., Muhamad, M. F., Sia, E. S. A., Jang, F. H. A., Zhang, J. 2019. Dissolved inorganic nitrogen in a tropical estuary at Malaysia: transport and transformation. Biogeosciences, 16, 2821–2836. https://doi.org/10.5194/bg-16-2821-2019.

Karydis, M., Kitsiou, D. 2019. Marine Eutrophication: A Global Perspective. 1st Edition, CRC Press. 194 p.

Kasai, A., Kurikawa, Y., Ueno, M., Robert, D., Yamashita, Y. 2010. Salt-wedge intrusion of seawater and its implication for phytoplankton dynamics in the Yura Estuary, Japan. Estuarine, Coastal and Shelf Science, 86, 408-414. https://doi:10.1016/j.ecss.2009.06.001.

Kenov, I.A., García, A.C., Neves, R. 2012. Residence time of water in the Mondego estuary (Portugal). Estuarine, Coastal and Shelf Science, 106, 13-22. https://doi.org/10.1016/j.ecss.2012.04.008.

Kemp, W., Smith, E., Marvin-DiPascuale, M., Boynton, W. 1997. Organic carbon balance and net ecosystem metabolism in Chesapeake Bay. Marine Ecology Progress Series, 150, 229-248. https://doi:10.3354/meps150229.

Kiwango, H., Njau, K.N., Wolanski, E. 2018. The application of nutrient budget models to determine the ecosystem health of the Wami Estuary, Tanzania. Ecohydrology & Hydrobiology, 18(2), 107-119. https://doi.org/10.1016/j.ecohyd.2017.10.002.

Kjerfve, B. 1994. Coastal lagoons process. Elsevier Oceanography Series 60. Elsevier Science, 576 p.

Li, P., Yang, S.L., Milliman, J.D., Xu, K.H., Qin, W.H., Wu, C.S., Chen, Y.P., Shi, B.W. 2012. Spatial, temporal, and human-induced variations in suspended sediment concentration in the surface waters of the Yangtze Estuary and adjacent coastal areas. Estuaries and Coasts, 35, 1316–1327. https://doi.org/10.1007/s12237-012-9523-x.

Liu, F., Chen, S.L., Peng, J., Chen, G.Q. 2011. Temporal variability of water discharge and sediment load of the Yellow River into the sea during 1950-2008. Journal of Geographical Sciences, 21(6), 1047–1061. https://doi.org/10.1007/s11442-011-0899-5.

Mackenzie, F.T., Lerman, A., DeCarlo, E.H. 2011. Coupled C, N, P and O biogeochemical cycling at the land–ocean interface. Treatise Estuarine Coastal Science, 5, 317–342. http://doi:10.1016/B978-0-12-374711-2.00512-X.

Mbaye, M., Gaye, A., Spitsy, A., Dahnke, K., Afouda, A., and Gaye, B. 2016. Seasonal and spatial variation in suspended matter, organic carbon, nitrogen, and nutrient concentrations of the Senegal River West Africa. Limnologica, 57, 1-13. https://doi.org/10.1016/j.limno.2015.12.003.

Middleburg, J.J., Herman, P.M.J. 2007. Organic matter processing in tidal estuaries. Marine Chemistry, 106, 127-147. https://doi.org/10.1016/j.marchem.2006.02.007.

Ministerio de Ambiente y Desarrollo Sostenible. Decreto 1594 de 1984. Usos del agua y residuos líquidos. http://www.minambiente.gov.co/images/normativa/app/resoluciones/18-res%20883%20de%202018.pdf.

Moore, J.W., Schindler, D.E. 2008. Biotic disturbance and benthic community dynamics in salmon-bearing streams. Journal of Animal Ecology, 77(2), 275–284. https:// DOI: 10.1111/j.1365-2656.2007.01336.x.

Montoya-Sánchez, R.M., Devis-Morales, A., Bernal, G., Poveda, G. 2018. Seasonal and intraseasonal variability of active and quiescent upwelling events in the Guajira system, southern Caribbean Sea. Continental Shelf Research, 171, 97-112. https://doi.org/10.1016/j.csr.2018.10.006.

Nixon, S., B. Buckley, S. Granger, Bintz, J. 2001. Responses of very shallow marine ecosystems to nutrient enrichment. Human and Ecological Risk Assessment: An International Journal, 7, 1457–1481. https://doi.org/10.1080/20018091095131.

Ortiz, J., Otero, L., Restrepo, J.C., Ruiz, J., Cadena, M. 2013. Characterization of cold fronts in the Colombian Caribbean and their relationship to extreme wave events.

Natural Hazards Earth System Science, 13, 2797–2804. https://doi:10.5194/nhess-13-2797-2013.

Olivero-Verbel, J. 2012. Colombia: environmental health issues Reference Module in Earth Systems and Environmental Sciences, from Encyclopedia of Environmental Health, 740-754 p.

Ospino, S., Restrepo, J.C., Otero, L., Pierini, J., Álvarez-Silva, O. 2018. Saltwater Intrusion into a River with High Fluvial Discharge: A Microtidal Estuary of the Magdalena River, Colombia. Journal of Coastal Research, 34(6), 1273 – 1288. https://doi.org/10.2112/JCOASTRES-D-17-00144.1.

Paerl, H. W., Hall, N. S., Peierls, B. L., Rossignol, K. L. 2014. Evolving paradigms and challenges in estuarine and coastal eutrophication dynamics in a culturally and climatically stressed World. Estuaries and Coasts, 37, 243–258. https://doi.org/10.1007/s12237-014-9773-x.

Parson, T. R., Maitia, Y., Lalli, C.M. 1984. A manual of Chemical and Biological Methods for Sea Water Analysis. Pergamonn Press, Oxford. 135 p.

Poveda, G. 2004. La hidroclimatología de Colombia: una síntesis desde la escala inter-decadal hasta la escala diurna. Revista de la Academia Colombiana de Ciencias Exactas, Físicas y Naturales, 28, 201-222.

Quamrul, A., Benson, B., Visser, J., Gang, D. 2016. Response of estuarine phytoplankton to nutrient and spatio temporal pattern of physico-chemical water quality parameters in little vermilion bay, louisiana. Ecological informatics, 32, 79-90. https://doi.org/10.1016/j.ecoinf.2016.01.003.

Rabouille, C., Mackenzie, F., Ver, L. 2001. Influence of the human perturbation on carbon, nitrogen, and oxygen biogeochemical. Geochimica et Cosmochimica Acta, 65, 3615-3641. https://doi.org/10.1016/S0016-7037(01)00760-8.

Ramesh R., Chen, Z., Cummins, V., Dayd, J., D'Elia, C., Dennison, B., Forbes, D.L., Glaeser, B., Glaser, M., Glavovic, B., Kremer, H., Lange, M., Larsen, J.N., Le Tissier, M., Newton, A., Pelling, M., Purvaja, R., Wolanski, E. 2015. Land– Ocean Interactions in the Coastal Zone: Past, present & future. Anthropocene, 12, 85–98. https://doi.org/10.1016/j.ancene.2016.01.005.

Restrepo, J.C., Schrottke, K., Traini, C., Bartholomaec, A., Ospino, A., Ortiz, J.C., Otero, L., Orejarena, A. 2018a. Estuarine and sediment dynamics in a microtidal tropical estuary of high fluvial discharge: Magdalena River (Colombia, South America). Marine Geology, 398, 86–98. https://doi.org/10.1016/j.margeo.2017.12.008.

Restrepo J.C., Orejarena A., Torregroza-Espinosa, A.C. 2017. Suspended sediment load in northwestern South America (Colombia): A new view on variability and fluxes into the Caribbean Sea. Journal of South American Earth Sciences, 80, 340-352. https://doi.org/10.1016/j.jsames.2017.10.005.

Restrepo, J.C, Schrottke, K., Traini, C., Ortiz, J., Orejarena, A., Otero, L., Higgins, A., Marriaga, L. 2016. Sediment Transport and Geomorphological Change in a High-Discharge Tropical Delta (Magdalena River, Colombia): Insights from a Period of Intense Change and Human Intervention (1990–2010). Journal of Coastal Research, 32(3), 575-589. https://doi.org/10.2112/JCOASTRES-D-14-00263.1.

Restrepo, J.C., Ortiz, J.C., Pierini, J., Schrottke, K., Maza, M., Otero, L., Aguirre, J. 2014. Freshwater discharge into the Caribbean Sea from the rivers of Northwestern South America (Colombia): magnitude, variability and recent changes. Journal of Hydrology, 509, 266-281. https://doi.org/10.1016/j.jhydrol.2013.11.045.

Restrepo, J.D., Escobar, R., Tosic, M. 2018b. Fluvial fluxes from the Magdalena River into Cartagena Bay, Caribbean Colombia: Trends, future scenarios, and connections with upstream human impacts. Geomorphology, 302, 92-105. https://doi.org/10.1016/j.geomorph.2016.11.007.

Restrepo, J.D., Kettner, A.J., Syvitski, J.P.M. 2015. Recent deforestation causes rapid increase in river sediment load in the Colombian Andes. Anthropocene, 10, 13-28. https://doi.org/10.1016/j.ancene.2015.09.001.

Restrepo, J.D. 2008. Applicability of LOICZ catchment–coast continuum in a major Caribbean basin: The Magdalena River, Colombia. Estuarine, Coastal Shelf Science, 77(2), 214-229. https://doi.org/10.1016/j.ecss.2007.09.014.

Restrepo, J.D., Syvitski, J.P.M. 2006. Assessing the effect of natural controls and land-use change on sediment yield in a major Andean river: The Magdalena drainage basin, Colombia. Ambio, 35(1), 44–53.

Restrepo, J.D., Kjerfve, B. 2004. The Pacific and Caribbean Rivers of Colombia: Water Discharge, Sediment Transport and Dissolved Loads. En: Lacerda, L.; Santelli, R.; Duursma, E.; Abrao, J., (Eds.). Environmental Geochemistry in Tropical and Subtropical Environments. Springer Verlag, Berlín, 169-187 p.

Papenmeier, S., Schrottke, K., Bartholomä, A. 2014. Over time and space changing characteristics of estuarine suspended particles in the German Weser and Elbe estuaries. Journal Sea Research, 85, 104-115. https://doi.org/10.1016/j.seares.2013.03.010.

Sequoia Scientific. 2016. LISST-ABS acoustic backscatter sensor user's manual, version 1.2, 35 p.

Suzumura, M., Kokubun, H., Arata, N. 2004. Distribution and characteristics of suspended particulate matter in a heavily eutrophic estuary, Tokyo Bay, Japan. Marine Pollution Bulletin, 49, 496–503. https://doi.org/10.1016/j.marpolbul.2004.03.002.

Smith, S.V., Swaney, D.P., Buddemeier, R.W., Scarsbrook, M.R., Weatherhead, M.A., Humborg, C., Eriksson, H., Hannerz, F. 2005. River nutrient loads and catchment size. Biogeochemistry, 75, 83-107. https://doi.org/10.1007/s10533-004-6320-z.

Swaney, D., Smith, S., Wulff, F. 2011. The LOICZ biogeochemical modeling protocol and its application to estuarine ecosystems. Treatise on Estuarine and Coastal Science, 9, 136-159. https://doi:10.1016/B978-0-12-374711-2.00907-4.

Syvitski, J. P. M., Saito, Y. 2007. Morphodynamics of deltas under the influence of humans. Global Planetary Change, 57, 261–282. https://doi.org/10.1016/j.gloplacha.2006.12.001.

Talaue-McManus, L., Smith, S.V., Buddemeier, R.W. 2003. Biophysical and socio-economic assessment of the coastal zone: the LOICZ approach. Ocean and Coastal Management, 46,2 323-333. https://doi.org/10.1016/S0964-5691(03)00011-5.

Tejeda-Benitez, L., Russell, Flegal., Kingsley, Odigie., Olivero-Verbel, J. 2016. Pollution by metals and toxicity assessment using Caenorhabditis elegans in sediments from the Magdalena River, Colombia. Environmental Pollution, 212, 238-250. https://doi.org/10.1016/j.envpol.2016.01.057.

Torres-Bejarano, F.M., Ramírez-León, H., Rodríguez Cuevas, C., Tejera González, M.P, Vásquez Jaraba, M.C. 2015. Validación de un modelo hidrodinámico y calidad del

agua para el Río Magdalena, en el tramo adyacente a Barranquilla, Colombia. Hidrobiológica, 25(1), 7-23.

Uninorte. 2019. Distribución espacio-temporal de la temperatura y la salinidad – Influencia sobre la estratificación, la concentración de nutrientes y la productividad primaria en el frente deltaico del rio Magdalena. Proyecto BanRepública, 2018-40423. 32 p.

Vivas-Aguas, L., Ibarra, K., Sánchez, J., Martínez, M., Nieto, Y., Moreno, Y., Cuadrado, I., Obando, P., Garces, O., Sánchez, D., Villarraga, M., Sierra, O. 2017. Diagnóstico y evaluación de la calidad de las aguas marinas y costeras del Caribe y Pacífico Colombianos. Santa Marta: Serie de publicaciones periódicas del INVEMAR. REDCAM. INVEMAR.

Wang, J.J., Lu, X.X. 2010. Estimation of suspended sediment concentrations using terra MODIS: an example from the lower Yangtze river, China. Science of Total Environment, 408, 1131–1138. https://doi.org/10.1016/j.scitotenv.2009.11.057.

Watanabe, K., Kasai A., Antonio, E., Kentaro, S., Ueno, M., Yamashita, Y. 2014. Influence of salt-wedge intrusion on ecological processes at lower trophic levels in the Yura Estuary, Japan. Estuarine, Coastal and Shelf Science, 139, 67-77. https://doi.org/10.1016/j.ecss.2013.12.018.

Watson, B.J., Wyss, J., Booth, E.A., Sousa, G. 2012. Assimilative capacity modeling using integrated watershed and lake models in support of the Georgia comprehensive state wide water management plan. International Journal of Design and Nature and Ecodynamics., 7(2), 155–165. https://doi:10.2495/DNE-V7-N2-155-165.

Wolanski, E., Boorman, L.A., Chicharo, L., Langlois-Saliou, E., Lara, R., Plater, A.J., Uncles, R.J., Zalewski, M. 2004. Ecohydrology as a new tool for sustainable management of estuaries and coastal waters. Wetlands Ecology and Management, 12, 235–276. https://doi.org/10.1007/s11273-005-4752-4.

Wu, J., Liu, J., Wang, X. 2012. Sediment trapping of turbidity maxima in the Changjiang estuary. Marine Geology, 303–306, 14-25. https://doi.org/10.1016/j.margeo.2012.02.011.

Xu, H., Wolanski, E., Chen, Z. 2013. Suspended particulate matter affects the nutrient budget of turbid estuaries: modification of the LOICZ model and application to the Yangtze Estuary. Estuarine, Coastal and Shelf Science, 127, 59–62. http://dx.doi.org/10.1016/j.ecss.2013.04.020.

Xu, H., Newton, A., Wolanski, E., Chen, Z. 2015. The fate of phosphorus in the Yangtze (Chiangjiang) Estuary, China, under multi-stressors: hindsight and forecast. Estuarine, Coastal and Shelf Science, 163(B), 1–6. https://doi.org/10.1016/j.ecss.2015.05.032.

CHAPTER 4

4. Spatio-temporal Variability of Temperature, Salinity and Chlorophyll a in the Magdalena River Mouth

Abstract

Variations in the physical characteristics in estuaries (e.g. sea surface salinity and sea surface temperature) lead to the establishment gradients, tightly related with the distribution of nutrients and suspended sediment, and with the penetration of light, which in turn influences primary productivity (Chlorophyll-a). We used MODIS imagery to identify spatio-temporal patterns of physical (e.g. sea surface salinity and sea surface temperature) and biological (Chlorophyll-a) parameters from 2003-2017, and to analyze the relationship between these features and oceanographic factors (e.g. streamflows, winds and currents) in the Magdalena River mouth. The results indicated sea surface salinity (SSS) in the study zone varied in time and space (estuarine and marine). The average SSS value was 10.8 ± 3.4 at Bocas de Ceniza, and 28.4 ± 0.4 in the Caribbean Sea. This horizontal salinity gradient is evidence of the formation of a saline plume. The monthly inter-annual average sea surface temperature (SST) was 27.6 ± 1.5 °C at Bocas de Ceniza, and 27.6 ± 1.3 °C in the Caribbean Sea. Additionally, a significant increasing trend was observed throughout the study period in temperature. Average Chl-a values were 3.3 ± 1.4 mg m^{-3} at Bocas de Ceniza, and 1.5 ± 1.2 mg m^{-3} in the Caribbean Sea and calculated average Trophic State Index (TSI) for Bocas de Ceniza showed the estuary trophic state varied between mesotrophic ($40<TSI\leq50$) and oligo-mesotrophic ($30<TSI\leq40$). The highest concentrations of Chl-a were found in intermediate salinities in the estuarine zone. Outside the saline plume there is a considerable decrease of Chl-a concentrations (<0.5 mg m^{-3}). Finally, in the study zone, winds play the most important role in the spatio-temporal distribution of chemical and physical features.

Introduction

Physicochemical and biological conditions of estuaries are the result of the equilibrium between continental water discharge coming from rivers and the marine realm (Kjerfve, 1994). Estuaries are controlled by inertia, buoyancy, winds and tide strength (Valente and da Silva, 2009). River plume dynamics is a key element for this balance since rivers deliver freshwater and sediments, but also nutrients, pollutants and other constituents (Wysocki et al., 2006; Kouame et al., 2009), influencing circulation and mixing processes, as well as the physicochemical and biological properties of estuaries (Horner-Devine et al., 2015). River plumes are generated by buoyant river water flowing into the coastal zone (Lentz and Largier, 2006). It is difficult to generalize their behavior, which varies both in space and time, depending on river flow, estuarine dynamics and the morphology of the receiving basin (Horner-Devine et al., 2015). In Neotropical estuaries/deltas, river flow variation depends mainly on the migration of the Intertropical Convergence Zone (ITCZ) and other climate oscillations that occur at different frequencies (i.e. ENSO, NAO, PDO). Thus, physicochemical gradients tend to be marked and abrupt (Restrepo et al., 2014; 2018). During the last decade, research efforts have significantly improved our understanding of estuarine dynamics and mixing processes (e.g. Espinosa-Garzón et al., 2001; Obeso-Nieblas et al., 2012; Moskalski and Torres, 2012; Wu et al., 2012; Horner-Devine et al., 2015; Wafar et al., 2016). Although these studies have clarified many specific processes related to variations in the physicochemical characteristics of these ecosystems, studies are still required to understand the influence of river plumes on estuary conditions, particularly in tropical, stratified and turbid estuaries. More studies on the spatio-temporal variability of sea surface salinity (SSS), sea surface temperature (SST), and chlorophyll-a (Chl-a) will increase our understanding of Neotropical marine-coastal ecosystems (Moradi and Kabiri, 2015).

Variations in SSS and SST lead to the establishment of horizontal gradients, strongly associated with the distribution of nutrients and suspended sediment, and with light penetration, which in turn influence phytoplankton distribution and concentration, and primary productivity (He et al., 2008). Variability of phytoplankton is strongly influenced by light intensity, patterns of river discharge that bring nutrients and organic matter from continental runoff, tidal pumping and wind-induced currents, and biological factors such as grazing by aggregated zooplankton and other organisms (Lihan et al., 2011; Quamrul et al., 2016). Chl-a concentration, a pigment proxy for phytoplankton

abundance, is also considered an important indicator of trophic state in marine-coastal ecosystems, which affects ecosystem services (e.g. ecotourism, transport, human consumption of aquatic protein, fisheries, among others) (Raboubille et al., 2001; Moradi and Kabiri, 2015). The dynamic structure of phytoplankton communities is a direct reflection of the health of aquatic ecosystems (Quamrul et al., 2016). It is thus necessary to acquire detailed information on the physical and ecological dynamics of estuarine ecosystems. Studies on the extent and features of the saline convergence zone, primary productivity, and the interaction between physical and ecological processes are necessary as well (Espinosa-Garzón et al., 2001; Geyer, 2010; Moskalski and Torres, 2012; Quamrul et al., 2016; Daqamseh et al., 2019). The variable nature of estuaries, however, makes it difficult to survey and monitor these coastal ecosystems. Long periods of time, and rigorous sampling are required to accumulate sufficient data, particularly if the aim is to observe broad spatial and temporal (intra- and inter-annual) variations (Urquhart et al., 2013; González-Márquez et al., 2018). Remote sensing techniques have been very useful for the study of water quality in coastal ecosystems, including for the estimation of SSS, SST and Chl-a variability at different spatial and time scales (Urquhart et al., 2013; Chen et al., 2015; Kim et al., 2017; González-Márquez et al., 2018; Coronado-Franco et al., 2018).

Previous research in the Caribbean region has employed remote sensing techniques in the monitoring of physicochemical (SST and sediments) and biological (Chl-a) parameters (e.g. Ruiz-Ochoa et al., 2012; Sakuno et al., 2014; Moreno-Madriñan et al., 2015; Restrepo et al., 2016b; Torregroza-Espinosa et al., 2020). Additional studies to analyze links between the physical and biological variables are needed, especially for estuaries with both high discharge and sediment load. We used MODIS imagery to determine the physical and biological parameters in the mouth of the Magdalena River, Colombia. Specifically, we sought to: (*i*) identify spatio-temporal (intra- and inter-annual) patterns of SSS, SST and Chl-a in the Magdalena River mouth; (*ii*) determine the temporal variation of trophic state index in the Magdalena River mouth; and (*iii*) analyze the relationship between SSS, SST, and Chl-a and oceanographic factors (e.g. streamflow, winds and ocean currents) in the Magdalena River mouth.

Study Zone

The Magdalena River is the main fluvial system of Colombia, with a length of 1540 km (Restrepo et al., 2016a). The area of the estuary at the Magdalena River mouth (Bocas

de Ceniza) is approximately 146 km^2. The main channel morphology has changed, as two breakwaters were built in 1936 to prevent sediment deposition in the river mouth and promote commercial navigation into the port of Barranquilla. The current width of the river mouth is 430 m, with a minimum depth of 9.15 m in the deep channel. The west and east breakwater extend for 7.4 and 1.4 km, respectively (Figure 1) (Restrepo et al., 2016a). According to morphological classifications of deltaic systems, the Magdalena River Delta is classified as being of mixed domain, influenced by fluvial input and wave action (Restrepo et al., 2016a). Northeast trade winds have the largest influence on the study zone, with an average speed of 6 m s^{-1} during the dry period, 2 m s^{-1} in the wet period, and a prevailing southward direction (Andrade, 2001). General circulation within the Colombian Caribbean Basin is dominated by the Caribbean current, the Guajira upwelling center and the Panama-Colombia cyclonic gyre (Andrade, 2001). Close to the Magdalena River mouth, ocean currents have an average velocity of 0.3 m s^{-1} during the dry season, and 0.1 m s^{-1} during the wet season and maintain a southward direction in both seasons (Chassignet et al., 2006). Mixing conditions are predominantly caused by the river discharge, and therefore, tied to the hydrological cycle (Restrepo et al., 2016a). Additionally, a maximum turbidity zone (TMZ) forms (SSC> 4500 mg l^{-1}) at the mouth of the Magdalena River, and displays strong seasonal variation in size and structure. Its location is generally associated with the convergence front demarcated by saline intrusion (Restrepo et al., 2018). A gradual seaward salinity increase has been reported, with values ranging from 0 at the fluvial portion of the estuary, to intermediate values (~15-18) at the river mouth, to 33 in the coastal zone (Restrepo et al., 2018).

Through delimitation of the Magdalena River plume using a turbidity threshold, surface waters in the study area can be divided into three categories: (1) seawater, (2) river plume (with high sediment concentrations), and (3) the unstable mixing area (Torregroza-Espinosa et al., 2020). The drainage basin shows two well-defined seasons, influenced by the position of the ITCZ (Poveda, 2004). During the dry period, from January to April, the mean river flux is 4360.5 m^3 s^{-1}, with a mean sediment transport rate of 218 x 10^3 t d^{-1} (Restrepo et al., 2014), and high wave energy state (Hs > 2.5 m) (Ortiz et al., 2013). In the wet period, from September to November, the mean river flux is 8063.1 m^3 s^{-1}, the mean sediment transport rate is 531 x 10^3 t d-1, and wave energy is low (Hs < 1.5 m) (Ortiz et al., 2013). Calculated suspended sediment concentrations indicate high turbidity in the Magdalena River Estuary (178.6 ± 78.7 mg L^{-1}) (Torregroza-Espinosa et al., 2020). These values are of the same order of magnitude as those reported for the

mouths of the Yangtze, Huang He and Amazon Rivers (Wang et al., 2010; Liu et al., 2011; Gensac et al., 2016).

During the last few decades, changes in river flow and sediment transport rates have been observed, as a consequence of deforestation, erosion and mining activities within the Magdalena River Basin (Restrepo and Syvitski, 2006; Restrepo et al., 2014). Evidence for recent changes in the Magdalena River hydrology has been reported (Restrepo et al., 2014), particularly in relation to significant increases in the occurrence of extreme flood (e.g. 2011) and drought (e.g. 2015) events. These changes have influenced sediment dispersal, nutrient transfer into the ocean, and biological function of coastal ecosystems. Torregroza-Espinosa et al. (2020) reported that concentrations were higher than 1300 mg L^{-1} in the Magdalena River turbidity plume and >200 mg L^{-1} for the ocean in August 2010 and May 2011. These concentrations are atypical, and may be linked to the 2010/2011 ENSO phase (La Niña), one of the strongest recorded in Colombia (Hoyos et al., 2013). Previous work in the Colombian Caribbean (Cartagena Bay) reported low Chl-a concentrations of 1.20 mg m^{-3} during the wet season (September-November), related to various sources of continental waters (input from the Magdalena River and Canal del Dique), and even lower concentrations (0.06 mg m^{-3}) in the dry season (December-February) (Orejarena et al., 2004). Coronado-Franco et al. (2018) detected, using MODIS images, that between 2003 and 2013, the mouth of the Magdalena River had persistently high algal bloom values (Fluorescence Line Height > 0.04 W m^{-2} μm^{-1} sr^{-1}), and results obtained suggest that the La Niña events could have favored algal blooms in the Colombian Caribbean Sea of higher magnitudes because of increases in continental precipitation and sediment transport. Studies indicate that diatoms are the most dominant group in the micro-phytoplankton community, followed by dinoflagellates (Ramírez-Barón et al., 2010) in the Colombian Caribbean Sea. The Caribbean is considered an oligotrophic sea, a consequence of strong thermal stratification that hinders the entry of nutrients into the photic layer (Müller-Karger et al., 1989). However, more fertile and productive zones can be found in coastal areas (Margalef, 1969; Melo et al., 1995).

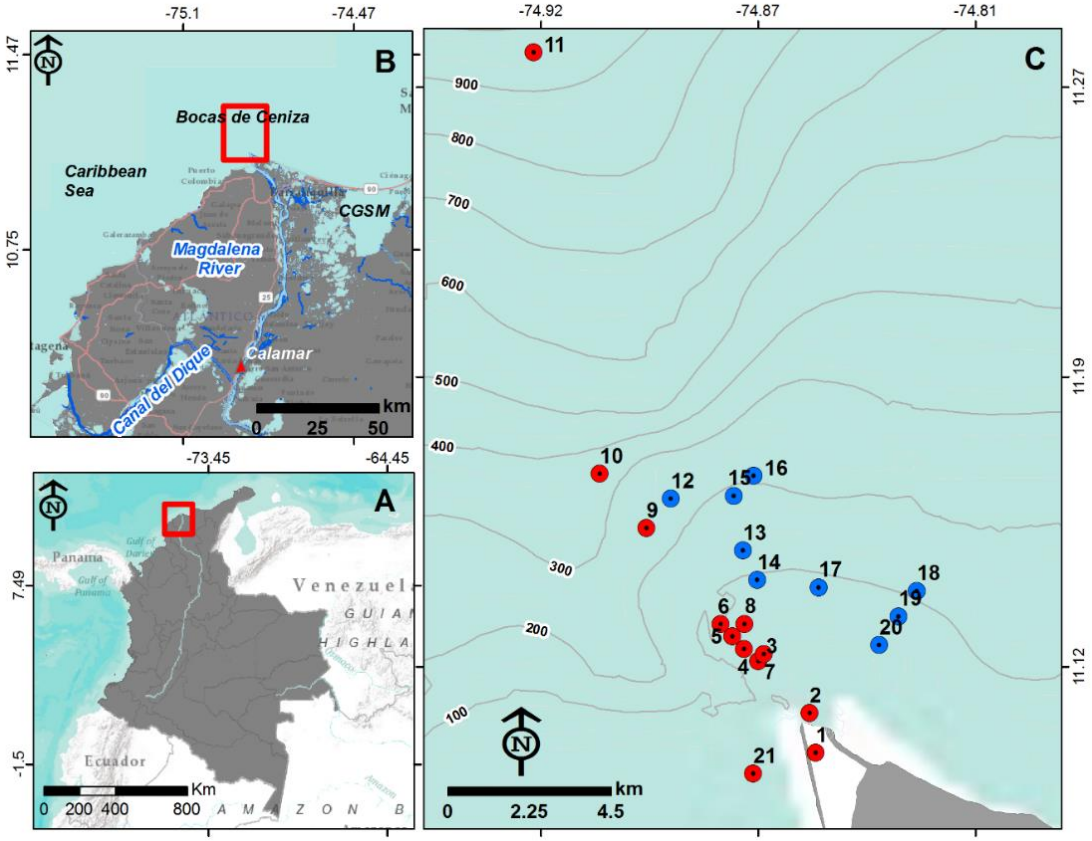

Figure 1. Magdalena River mouth. General location and sampling stations. Red points indicate the sampling stations in November 2017, and blue points indicate the sampling stations in August 2018. Depth contours in meters (m).

Methods

Data acquisition

We used MODIS-Aqua images, downloaded from the NASA Ocean Color website, for the period 2003-2017 (http://oceancolor.gsfc.nasa.gov). For SSS, we used MODIS product MYD09A1 500-m spatial resolution Level-3 Surface Reflectance 8-day composites. These MODIS products use a global atmospheric correction algorithm, which corrects for the effects of gaseous and aerosol scattering and absorption, as well as adjacency effects caused by variation of land cover, Bidirectional Reflectance Distribution Function (BRDF) and atmosphere coupling effects, and contamination by thin cirrus clouds (Vermote and Vermeulen, 1999). The images contain reflectance information from band 1 to band 7 (B1:

620 – 670 nm; B2: 841 – 876 nm; B3: 459 – 479 nm; B4: 545 – 565 nm; B5: 1230 – 1250 nm; B6: 1628 – 1652 nm; B7: 2105 – 2155 nm) (Vermote and Vermeulen, 1999). We cropped images to the deltaic front of the Magdalena River (Figure 1B) and then calculated monthly averages for band reflectance.

We took field measurements of SSS with a CTD (Castaway) at 21 stations (Figure 1C) in November 2017 and August 2018. To calibrate the model, we used MODIS images (MYD09A1) obtained on the same day's samples were collected in the field. (21 November 2017 and 8 August 2018). We fitted a statistical model, using field measurements of SSS as the dependent variable, and reflectance values of bands 1 to 7 as independent variables. To test the assumption of normally distributed data, we performed a Shapiro-Wilk Test (Yap and Sim, 2011). We assessed the calibration of the model through simple linear regression analysis, using the salinity values obtained from the MODIS spectral information and field measurement results. Finally, using the best-fit model, we calculated estimated values of SSS values in the study area for the period 2003-2017. To map the salinity plume, a mask was applied, which defined threshold salinity values. The mask was in a range from 0 to 20, in accordance with salinities reported in Bocas de Ceniza (Restrepo et al., 2018).

For SST and Chl-a concentration data, we downloaded, from the NASA Ocean Color website (http://oceancolor.gsfc.nasa.gov) the processed products L-3 thermal Daily and L-3 CHL, respectively, for the period 2003-2017. We then calculated the monthly average SST and Chl-a, both with spatial resolution of 1 km. We used the R program (R Core Team, 2018) for image processing. We obtained monthly wind (magnitude and direction) data from WaveWatch III (http://polar.ncep.noaa.gov), and monthly surface current data from the Hybrid Coordinate Ocean Model (https://hycom.org). Wind and surface current data encompass the same time interval (2003-2017), at coordinates close to the river mouth (11.30 N - 74.78 W). We downloaded monthly river flow and suspended sediment load data from the Colombian Institute of Hydrology, Meteorology and Environmental Studies (IDEAM-Colombia, http://www.ideam.gov.co) for the same time period (2003-2017). We used data taken at Calamar, IDEAM's closest station (100 km) to the Magdalena River mouth. Additionally, data on laboratory measurements of Chl-a in the study zone were acquired from a research project developed by the Universidad del Norte (Uninorte, 2019).

Processing and Data Analysis

We determined the spatio-temporal variation and identified trends of SSS, SST and Chl-a values in the Magdalena River mouth using the Mann-Kendall Test (MKT) (Yue et al., 2002). The MKT is a non-parametric statistical test, based on ranges, used to detect monotonous trends and evaluate their importance within time series (Yue et al., 2002). The influence of the freshwater river plume was determined for three different climate scenarios: (1) a La Niña year (2011), (2) a neutral year (2013), and (3) an El Niño year (2015). The 12-month periods were divided into four quarters, as follows: December, January and February (DJF); March, April and May (MAM); June, July and August (JJA); September, October and November (SON). We calculated Carlson's Trophic State Index (TSI) from Chl-a concentrations obtained from satellite images (Carlson, 1977). The TSI has been used widely in numerous water quality studies of lakes and estuaries and varies between 0 and 100 (Table 1) (O'Boyle et al., 2013; Marreto et al., 2017). We also performed a Principal Component analysis (PCA) to determine the influence of oceanographic and/or fluvial variables (streamflow, suspended sediment load, wind and surface currents) on physical and biological patterns (SSS, SST y Chl-a). The PCA was done with the complete data set to explore relationships between variables, and avoid multiple co-linearity between them (Jolliffe, 2002). As dependent variables, we used SSS, SST and Chl-a. Monthly values of wind magnitude and direction, streamflow, surface current magnitude and direction, and suspended sediment load were used as independent variables.

Table 1. Trophic State Index (TSI) (Carlson, 1977).

Range	Trophic State
0 < TSI≤30	oligotrophic
30 < TSI≤40	oligo-mesotrophic
40 < TSI≤50	mesotrophic
50 < TSI≤60	slightly eutrophic
60 < TSI≤70	moderately eutrophic
70 < TSI	hypereutrophic

Results

SSS: Calibration Model

The model obtained for SSS calibration was highly significant (R^2=0.83, p-value ≤ 0.05). The relationship between SSS and reflectance values for bands 1, 2, 3, 4, 5 and 7, in the mouth of the Magdalena River, is mathematically represented by Equation 1.

$$\boldsymbol{SSS = 54.3 + 1,184\ RB1 - 733\ RB2 - 330\ RB3 - 981\ RB4 - 550\ RB5 + 827\ RB7}$$

(*Equation 1*)

Where SSS is surface salinity, and RB1, RB2, RB3, RB4, RB5, and RB7 are the reflectance values (W sr^{-1} nm^{-1}) for bands 1, 2, 3, 4, 5, and 7, respectively.

The obtained model showed generally good agreement between satellite-derived SSS and field measurements (Figure 2). Most points were well distributed along the regression line. Statistical analysis showed an R^2 of 0.76 and a p-value ≤ 0.01, indicating that the satellite data can be used to predict SSS accurately.

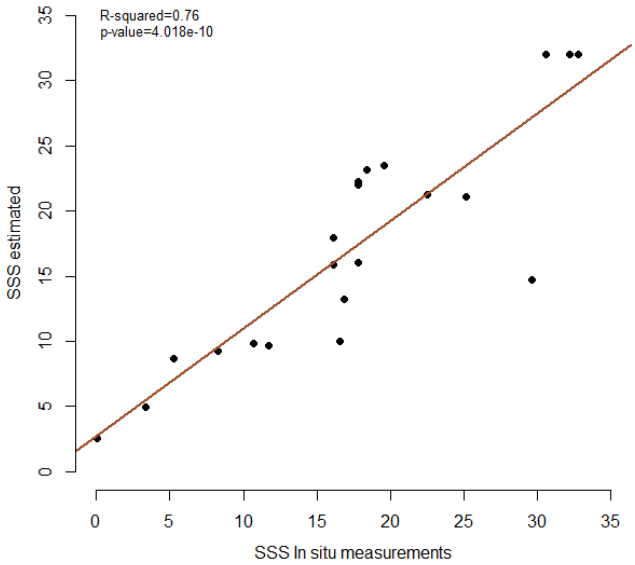

Figure 2. Scatter plot of the MODIS-derived SSS vs. *in situ* measurements. The solid line shows a regression line.

Spatio-temporal Distribution of SSS, SST and Chl-a

The influence of the freshwater river plume is shown in Figure 3. In La Niña year 2011 the greatest influence of the freshwater river plume area was observed in MAM (Figure 3B). In neutral year 2013 and El Niño year 2015, the largest freshwater river plume area of influence was observed in SON, during with the wet season (Figure 3H and 3L). The smallest freshwater river plume area of influence area was found in DJF and JJA, in the neutral and El Niño year (Figure 3E, 3G, 3I and 3K). The freshwater river plume area of influence during the DJF and JJA quarters had a similar pattern under all three climate scenarios.

There was not a marked SST spatial gradient at Bocas de Ceniza (Figure 4). However, a strong influence of cold waters moving westward from the Guajira Peninsula was observed along the littoral zone in months DJF, and these lower temperatures (~25°C) were recorded at the study area. Highest temperatures (between ~28 and 29°C) were found in the study area during SON. This pattern was found in a La Niña year 2011 (Figure 4D), in neutral year 2013) (Figure 4H), and in El Niño year 2015 (Figure 4L).

Greater Chl-a concentrations were found within the zone influenced by fluvial discharge, with concentrations between 3.0 and 4.2 mg m^{-3} at Bocas de Ceniza (Figure 5). Outside the area influenced by the Magdalena River discharge, observed concentrations were <0.5 mg m^{-3}. During La Niña year 2011, more heterogenous concentration values were observed along the Colombian Caribbean coast (Figure 5A, 5B, 5C and 5D). In neutral year 2013 concentrations displayed a strong SE-NW decreasing trend through the entire year (Figure 5E, 5F, 5G and 5H). Conversely, during El Niño year 2015, the influence of river discharge on Chl-a concentration was more limited (Figure 5I, 5J, 5K and 5L).

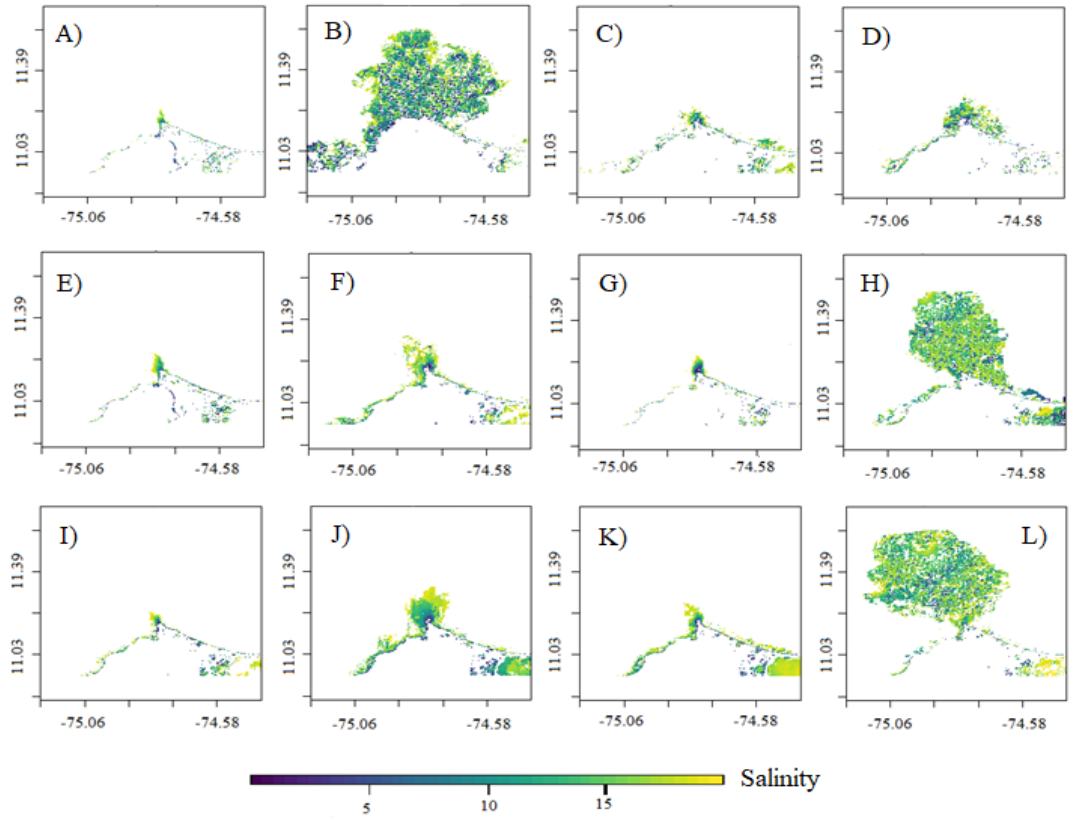

Figure 3. Quarterly Average of SSS in the Magdalena River mouth for three years: La Niña year (2011), neutral year (2013) and El Niño year (2015). A) December 2010 to February 2011. B) March to May 2011. C) June to August 2011. D) September to November 2011. E) December 2012 to February 2013. F) March to May 2013. G) June to August 2013. H) September to November 2013. I) December 2014 to February 2015. J) March to May 2015. K) June to August 2015. L) September to November 2015.

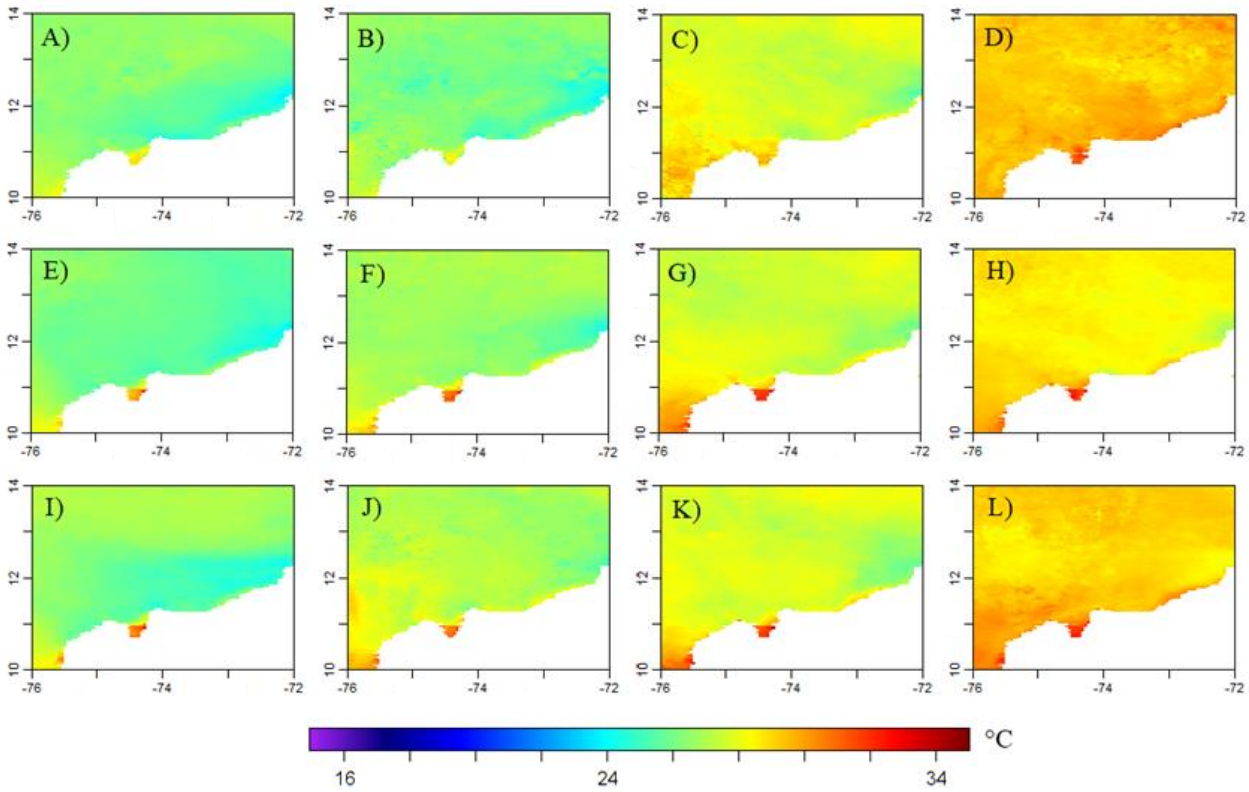

Figure 4. Quarterly Average of SST in the Magdalena River mouth for three years: La Niña year (2011), neutral year (2013) and El Niño year (2015). A) December 2010 to February 2011. B) March to May 2011. C) June to August 2011. D) September to November 2011. E) December 2012 to February 2013. F) March to May 2013. G) June to August 2013. H) September to November 2013. I) December 2014 to February 2015. J) March to May 2015. K) June to August 2015. L) September to November 2015.

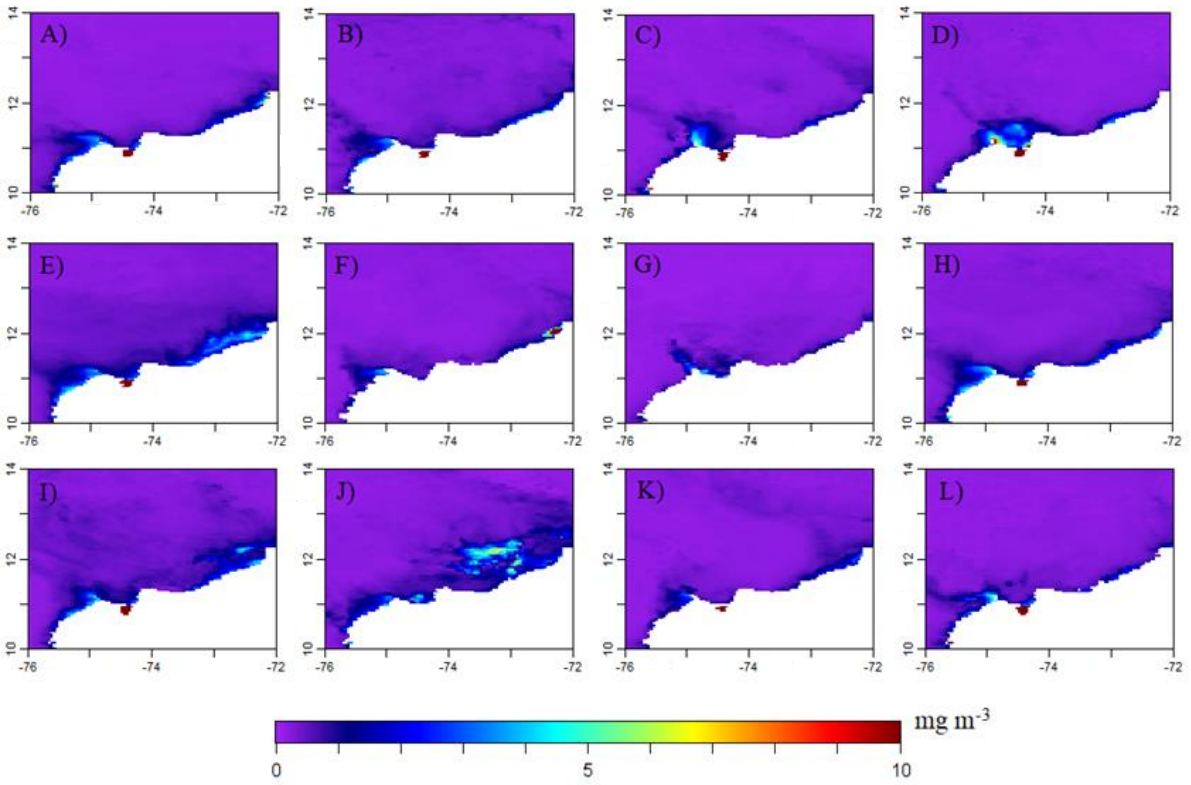

Figure 5. Quarterly Average of Chl-a in the Magdalena River mouth for three years: La Niña year (2011), neutral year (2013) and El Niño year (2015). A) December 2010 to February 2011. B) March to May 2011. C) June to August 2011. D) September to November 2011. E) December 2012 to February 2013. F) March to May 2013. G) June to August 2013. H) September to November 2013. I) December 2014 to February 2015. J) March to May 2015. K) June to August 2015. L) September to November 2015.

Inter-annual Patterns of Monthly SSS, SST and Chl-a

SSS of the Magdalena River mouth were estimated using the fitted model (equation 1). Figure 6 shows SSS in the Magdalena River mouth (sampling stations 2, 3, 17, 21 and 10) for the period 2003-2017. SSS in the study zone varied in time and space (estuarine and marine) (Figure 6). The average SSS value was 10.8 ± 3.4 at Bocas de Ceniza (sampling station 2), and 28.4 ± 0.4 in the Caribbean Sea (sampling station 10). The greatest SSS variability was observed in Bocas de Ceniza (estuarine zone sampling station 2). Inter-annual SSS series appeared to show a slight increasing trend through time at Bocas de Ceniza (Figures 6A and 6B), whereas the points east and west of the Magdalena River mouth, as well as the point in the Caribbean Sea (sampling stations 17, 21, and 10), exhibited a slightly decreasing trend (Figures 6C, 6D and 6E). However, the Mann-Kendall analysis indicated no significant trend for SSS in Bocas de Ceniza (sampling stations 2, 3 and 17) and in the ocean zone (sampling station 10) (*p-value* ≥ 0.05, Sen-slope between -0.001 and 0.008). A significant decreasing trend through time was, however, observed at the sampling station located to the northwest (sampling station 21) (*p-value* ≤ 0.05, Sen-slope=-0.001).

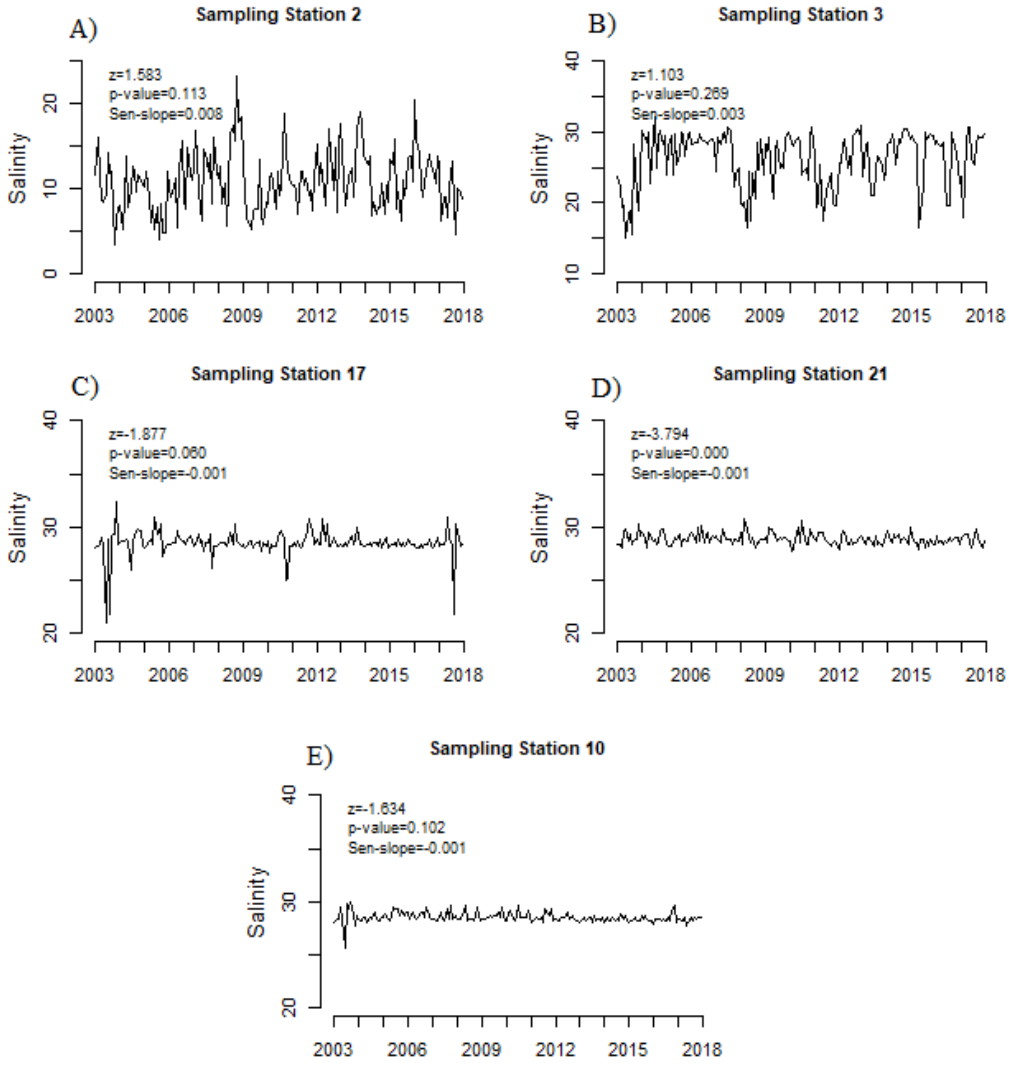

Figure 6. SSS in the Magdalena River mouth for the period 2003-2017. A) Sampling stations 2. B) Sampling stations 3. C) Sampling station 17. D) Sampling station 21. E) Sampling station 10.

SST inter-annual series displayed an increasing trend in the study area (Figure 7). The monthly inter-annual average SST was 27.6 ± 1.5 °C at Bocas de Ceniza (sampling station 2) (Figure 7A), and 27.6 ± 1.3 °C in the Caribbean Sea (sampling station 10) (Figure 7E). A similar pattern was observed in the series across different (estuarine and marine) areas of the study region. A marked seasonality was observed, with two annual peaks. The

Mann-Kendall Test indicated a significant increasing trend at all sampling stations (*p-value* ≤ 0.05, Sen-slope between 0.005 and 0.038) (Figure 7).

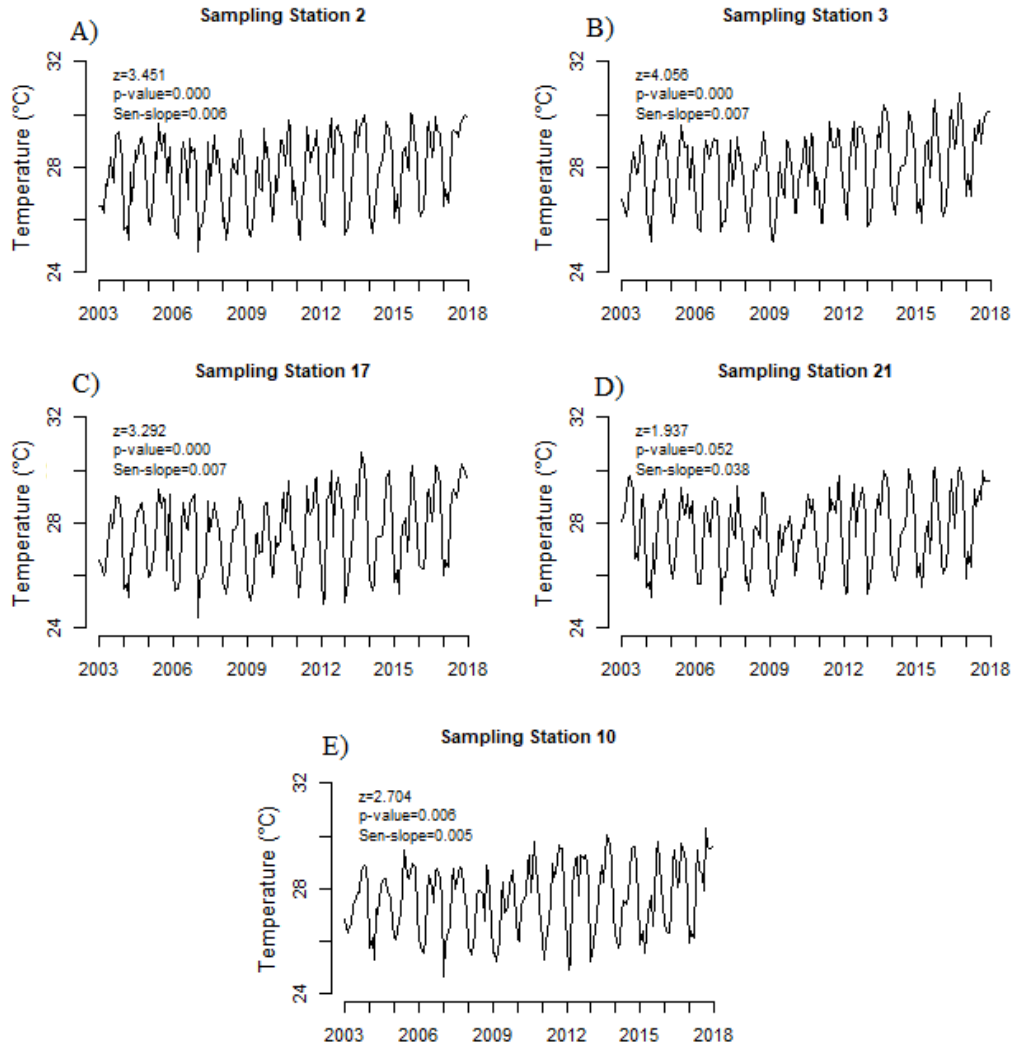

Figure 7. SST in the Magdalena River mouth for the period 2003-2017. A) Sampling station 2. B) Sampling station 3. C) Sampling station 17. D) Sampling station 21. E) Sampling station 10.

Chl-a inter-annual monthly series showed a decreasing trend at Bocas de Ceniza (sampling station 3) and the Caribbean Sea (sampling station 10) (Figures 8A and 8D). Average Chl-a values were 3.3 ± 1.4 mg m^{-3} at Bocas de Ceniza, and 1.5 ± 1.2 mg m^{-3} in the

Caribbean Sea (Figures 8). A larger fluvial influence was observed in the east (sampling station 17), with an average concentration of 2.3 ± 1.5 mg m^{-3} (Figure 8B). Chl-a concentrations were difficult to extract from MODIS images, specifically from the estuarine section with the most fluvial influence (sampling station 2). Fluctuations within the series at different sites in the study area (estuarine and marine) exhibited similar behaviors (Figure 8). The Mann-Kendall Test indicated a significantly decreasing trend in Chl-a concentration in the study area over time (*p-value* ≤ 0.05, Sen-slope between 0.000 and 0.004).

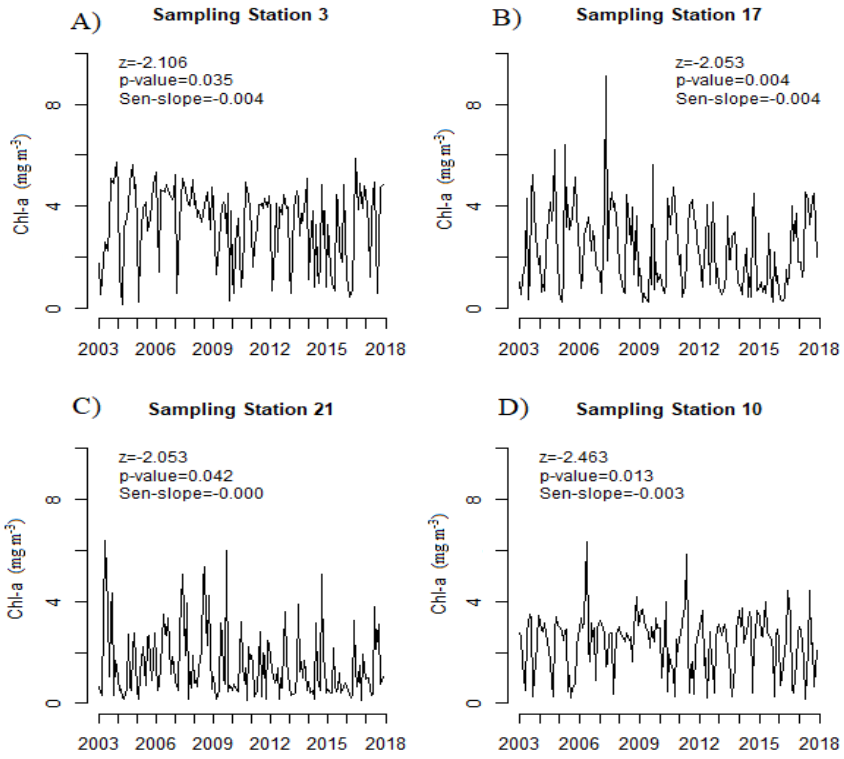

Figure 8. Chl-a in the Magdalena River mouth for the period 2003-2017. A) Sampling stations. B) Sampling station 17. C) Sampling station 21. D) Sampling station 10.

Monthly Patterns of SST, SSS and Chl-a

At Bocas de Ceniza (sampling station 2), the highest average SSS was observed in January (12.5 ± 3.3), coinciding with the dry season, whereas the lowest average SSS was observed in May during transition period (7.9 ± 2.0) (Figure 9A). The greatest monthly

variability was seen in October (wet season) with an average value of 11.6 ± 5.3, a minimum of 3.4, and a maximum of 23.3 (Figure 9A). The highest SSS in the Caribbean Sea was observed in October, during the wet season (28.6 ± 0.4), and the lowest in January, during the dry season (28.2 ± 0.2) (Figure 9B). The highest monthly variability for the Caribbean Sea was observed in June (28.2 ± 0.8) and the lowest in February (28.3 ± 0.2). Maximum and minimum SSS values were observed in September (29.9) and June (25.6) (Figure 9B).

Monthly average SST showed a significant monthly trend, similar to that observed in Bocas de Ceniza (sampling station 2) and the Caribbean Sea (sampling station 10) (Figure 9C and 9D). At Bocas de Ceniza, the lowest average SSTs were observed during January, February and March, coinciding with the dry season. SST variability was highest during June (transition period), with an average value of 28.7 ± 0.9 °C, a minimum of 27.5 °C and a maximum of 30.1°C. The highest average SST was observed in October (29.3 ± 1.0 °C), coinciding with the wet season (Figure 9C). For the Caribbean Sea, February (dry season) was the month with the lowest average value and variability of SST (26.1 ± 0.6 °C) (Figure 9D). The highest average SST was 29.3 ± 0.8 °C, observed in October (wet season), whereas the highest variability was reported in September, coinciding with the wet season (Figure 9D).

Chl-a concentrations at Bocas de Ceniza showed marked monthly variation. The highest average value was observed in December (4.3 mg m^{-3}), and the lowest average value (1.6 mg m^{-3}) in February (Figure 9E). The highest monthly variability (3.2 ± 1.5 mg m^{-3}) was also observed in January, and the lowest (4.1 ± 0.9 mg m^{-3}) in October. Maximum and minimum Chl-a values were observed in December (5.7 mg m^{-3}) and April (0.1 mg m^{-3}) (Figure 9E). Concentrations recorded in the Caribbean Sea were lower than those found at Bocas de Ceniza. In the Caribbean Sea, the highest average Chl-a value (2.4 mg m^{-3}) was found in May, and the lowest (0.5 mg m^{-3}) in March (Figure 9F). In turn, these months had the highest and lowest monthly variability values (2.4 ± 1.7 mg m^{-3} in May, and 0.5 ± 0.2 mg m^{-3} in March). The highest Chl-a value was reached in May (6.3 mg m^{-3}), and the lowest in September (0.1 mg m^{-3}) (Figure 9F).

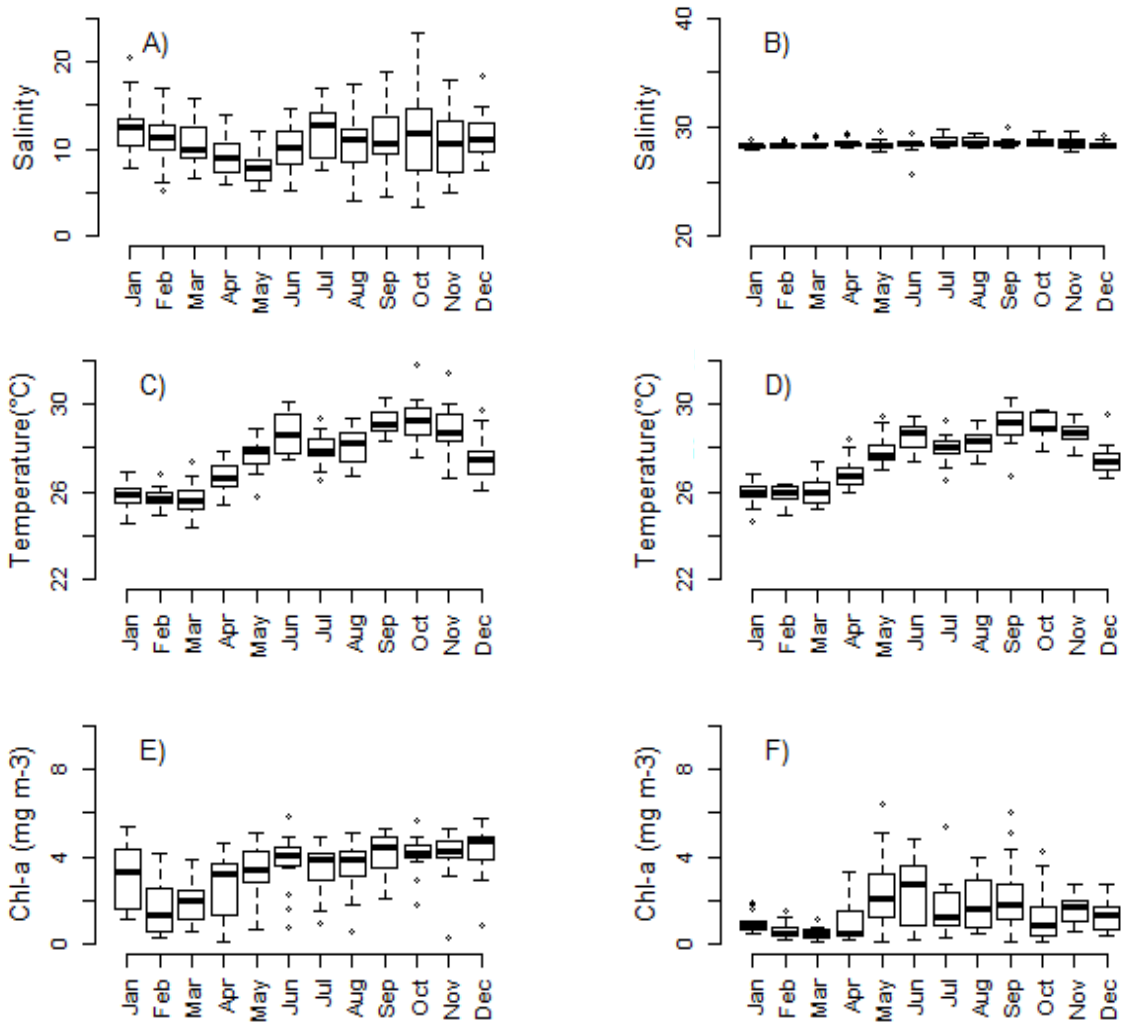

Figure 9. Monthly average SSS, SST and Chl-a for the period 2003-2017. A) SSS in the Bocas de Ceniza Estuary. B) SSS in the Caribbean Sea. C) SST in the Bocas de Ceniza estuary. D) SST in the Caribbean Sea. E) Chl-a in the Bocas de Ceniza Estuary. F) Chl-a in the Caribbean Sea.

Trophic State Index (TSI) in the Magdalena River mouth

Calculated average TSI for Bocas de Ceniza showed the estuary has a trophic state that varied between mesotrophic ($40<TSI\leq50$) and oligo-mesotrophic ($30<TSI\leq40$), with some exceptions when an ultra-oligotrophic state ($0<TSI\leq30$) was observed (e.g. April 2004, February 2005, February 2010) (Figure 10A). The Caribbean Sea displayed an

oligotrophic and oligo-mesotrophic state during the study period, with some exceptions (e.g. May 2003 and July 2009), when it can be considered to have been mesotrophic (Figure 10B). The TSI series showed a clear pattern that was similar within the estuarine and marine sectors (Figure 10). The Mann-Kendall Test indicated a significantly decreasing trend of TSI in the study area over time (*p-value* ≤ 0.05, Sen-slope between –-0-010 and -0.032).

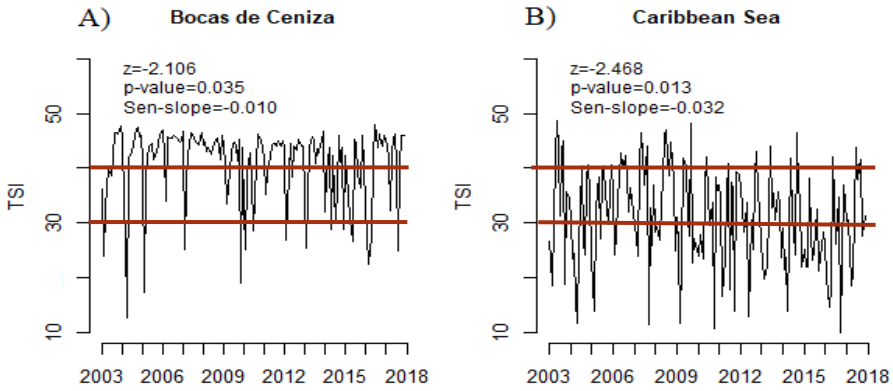

Figure 10. TSI in the Magdalena River mouth for the period 2003-2017.

Influence of Fluvial and Oceanographic Factors

Seasonal streamflow ranged from 5,437 $m^3\ s^{-1}$ during the dry season and 9,726 $m^3\ s^{-1}$ during the wet season (Figure 11A). Suspended sediment transport showed a minimum value of 73 x 10^3 t d^{-1} and a maximum of 1,124 x 10^3 t d^{-1}. The average flux value was 264 x 10^3 t d^{-1} for the dry season and 573 x 10^3 t d^{-1} for the wet season (Figure 11A). Wind and current variability were low in the study area and had a southward trend. Winds had an average speed of 6 m s^{-1} during the dry season and 2 m s^{-1} during the wet season. Currents had an average speed of 0.2 m s^{-1}.

PCA axis 1 and 2 explained 52% (Axis 1: 39%, Axis 2: 13%) of the variability in the dataset (Figure 11B). According to the vector directions for the first two principal components, SSS and Chl-a in Bocas de Ceniza, Sal_BC and Chla_BC may be influenced by streamflow (Q) and sediment load (Sediment). SSS, SST and Chl-a in the Caribbean Sea (Sal_CS, Temp_CS and Chla_ CS) may be negatively correlated to the magnitude and direction of winds (Wind_d) and surface currents (Current_d). The magnitude of winds (Wind_m)

and surface currents (Current_m) were positively correlated, as were wind and current directions (Wind_d and Current_d).

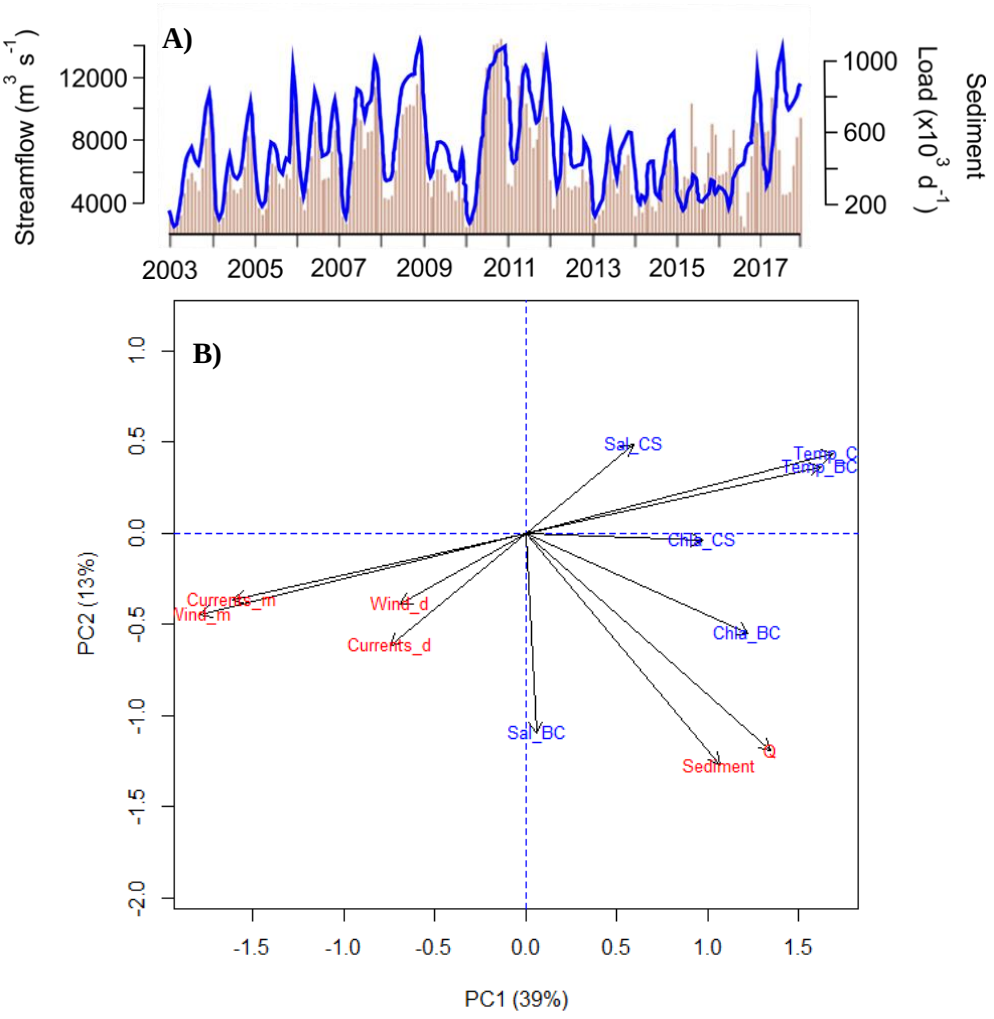

Figure 11. Principal Component Analysis (PCA). A) Streamflow and sediment load in the Magdalena River mouth. B) Principal Component Analysis (PCA) between the SST, SSS y Chl-a and the fluvial and oceanographic factors. Sal_BC = SSS in Bocas de Ceniza; Sal_CS = SSS in the Caribbean Sea; Temp_BC = SST in Bocas de Ceniza; Temp_CS = SST in the Caribbean Sea; Chla_BC = Chl-a in Bocas de Ceniza; Chla_CS = Chl-a in the Caribbean Sea; Wind_d = wind direction; Currents_d = current direction; Wind_m = wind magnitude; Current_m = current magnitude; Sediment = sediment load; Q = caudal.

Discussion

SSS and SST Patterns in the Magdalena River Mouth

Our dataset allowed us to construct a robust model (R^2=0.83, $p \leq 0.05$) to reconstruct SSS behavior at the Magdalena River mouth between 2003 and 2017. Model results show that SSS estimates are similar to those calculated for other coastal areas such as Chesapeake Bay (R^2=0.86, $p \leq 0.05$), the Chinese Bohai Sea (R^2=0.76, $p \leq 0.05$), and the coastal areas of the West Red Sea (R^2=0.91, $p \leq 0.05$) (Urquhart et al., 2013; Yu et al., 2017; Daqamseh et al., 2019). In estuaries, horizontal advection varies seasonally, determining mixing processes (Jago et al., 2006; Geawhari et al., 2014). A surface salinity gradient is one of the main features of an estuarine ecosystem. The distribution of a surface salinity gradient results from the interaction of water masses coming from the river and the adjacent ocean (Geawhari et al., 2014). Water masses interact through different dynamic processes, mainly those associated with changes in tide regime (tidal amplitude) and the freshwater input (streamflow) provided by rivers (Horner-Devine et al., 2015). This horizontal salinity gradient provides evidence of formation of a saline plume (Halverson and Pawlowicz, 2008), which enables formation of a saline plume (Horner-Devine et al., 2015). Furthermore, the saline plume is dependent on freshwater residence time (Halverson and Pawlowicz, 2008). At the Magdalena River mouth, SSS varied from 10.8 ± 3.4 in the Bocas de Ceniza (estuarine zone) to 28.4 ± 0.4 in the oceanic zone (Caribbean Sea) (Figure 3), and residence times in the Bocas de Ceniza estuary were low (~0.9-2.1 days) (Torregroza et al., 2020). No significant trends or inter-annual variations were observed during the study period.

The effect of seasonality on SSS variability is shown here. Variability is highest during the wet season (October) and lowest at the beginning of the dry season (December) (Figure 6). Strong influence of fluvial discharge on SSS spatial distribution was observed, and there was evidence of a saline gradient at Bocas de Ceniza Estuary. During La Niña year 2011, greatest extension of saline plume was observed in MAM. During the neutral and El Niño years, 2013 and 2015, respectively, the largest extension of saline plume was observed in SON, coinciding with the wet season (Figure 6). Salinity has special significance because, despite several assumptions, it is essentially a measure of the freshwater content in the plume and there exists a correlation between freshwater discharge and surface salinity (Halverson and Pawlowicz, 2008). ENSO disrupts precipitation patterns and freshwater discharge into estuaries, thus affecting seasonal

salinity distributions (Vieira, et al., 2008). Salinity is the main feature used to distinguish between plumes and rivers, that is, to define the mixing zone where river influence ends and seawater starts (Osadchiev and Vavilov, 2019). Plumes can display different types of structure, depending on mixing and transport processes, resulting on a variety of dilution pathways (Shu et al., 2014). Variations in freshwater input influence the structure of the salinity gradient, circulation within the estuary, the temporal scale of transport, and stratification (Horner-Devine et al., 2015).

MODIS products analyzed in this study provide a good representation of spatio-temporal dynamics of SST (Figure 4). We found similar average SSTs in the estuarine zone (Bocas de Ceniza) and the oceanic zone (Caribbean Sea), with mean values of 27.6 ± 1.5°C and 27.6 ± 1.3°C, respectively. Influence of Guajira upwelling was observed in all years studied but was most intense in the period between December and February (Figure 8). Ruiz-Ochoa et al. (2012) evaluated the spatial variations of SST in the Colombian Basin using satellite imagery. They found a horizontal gradient, with minimum temperatures (25.5 °C) in the La Guajira coastal zone and maximum values (29.5 °C) in the Darien and Mosquito Gulfs. In the Central Colombian Basin, surface waters were moderately warm (27–28 °C). In our study, La Niña (2011), neutral (2013) and El Niño years (2015) had the same spatial and temporal patterns, with the highest temperatures between ~28 and 29°C during SON. Additionally, an increasing trend was observed through the time series analyzed (Figure 4). This trend may coincide with the increase in global average temperatures, resulting from climate change (Dunstan et al., 2018). Analysis of different time series datasets indicates that most estuaries have displayed increases in water temperature. For instance, analysis of SST data by Preston (2004) in the Chesapeake Bay Estuary (United States), revealed increases of 0.16 and 0.21 °C per decade. SST variability and increase will have different spatial and temporal responses in different regions (Salinger et al., 2016). The lowest SST values were observed during the dry period (January, February and March), which might be related to air-water interaction processes within estuaries (Beigt and Piccolo, 2009). In the wet season, river water discharge produces low-density surface water, which reduces vertical mixing and limits the absorption of solar radiation to a thin surface layer (Ruiz-Ochoa et al., 2012).

Primary Productivity in the Magdalena River Mouth

This work provided estimates of primary productivity (expressed as Chl-a) in the Magdalena River mouth, obtained with MODIS images. Results indicate a mean Chl-a

concentration of 3.3 ± 1.4 mg m^{-3} at Bocas de Cenizas (Figure 5), with the highest concentrations in the river influence zone (Figure 9). However, measurements performed at different points of the river mouth (sampling points 2 and 3) (Figure 1), indicated that concentration values from satellite images were overestimated. The average of values measured *in situ* was 0.49 ± 1.4 mg m^{-3} (Uninorte, 2019). Field concentrations were lower than those estimated from satellite images. Global ocean colour algorithms, used to estimate chlorophyll concentration in ocean surface waters, normally overestimate pigment values in coastal regions, because of optical interference from other components in the water (García et al., 2006). This lack of correspondence between measured and satellite-based estimates of Chl-a concentrations may be related to the strong overlapping absorption ranges of algae and non-algal particles (Carder et al., 2013). Furthermore, spectral absorption of phytoplankton depends on algal growth and pigment composition, which may vary seasonally and spatially (Dunstan et al., 2018). Chl-a estimates made by NASA use an empirical relationship between *in situ* Chl-a measurements and their relationship with blue and green reflectance bands. Agreement/disagreement varied among different ocean basins and coastal zones because the same regression coefficients, determined from the global data set optimization, were applied universally (Gregg and Casey, 2004). Precision of satellite measurements diminishes when they are applied to areas beyond those used for calibration, probably because of differences in the dissolved and particulate components of coastal and continental waters, particularly in estuaries with high turbidity (Chang et al., 2014). The Magdalena River mouth is a turbid estuary with a high concentration of non-algal particles.

Chl-a determination showed a clear transition zone between coastal and open (Caribbean Sea) waters. The trophic status of the Magdalena River, calculated using satellite-image data as a reference, showed a variation from mesotrophic to oligotrophic. In oligotrophic ecosystems, water transparency is high, whereas phytoplankton biomass and productivity, and nutrient concentrations are low. Mesotrophic ecosystems represent a level of intermediate productivity and nutrient concentrations, favoring greater development of aquatic organisms. Eutrophic ecosystems have high phytoplankton biomass and productivity, high nutrient concentrations, and low water transparency (Pinckney et al., 2001). Spatially, mesotrophic status was found in the zone influenced by fluvial discharge. Shifts in SSS and SST are caused by changes in inflows, which result in horizontal gradients (Obeso-

Nieblas et al., 2012). These variations may directly modify the circulation pattern, extent of the saline plume, mixing layer structure, organism life cycles and the trophic status of the ecosystem (Urquhart et al., 2012; Dunstan et al., 2018). Increases in SSS and SST may influence most species and affect their ability to adapt (Leemans and Eickhout, 2004). Numerous studies have shown that changes in SSS and SST are already affecting the distribution of aquatic organisms (Urquhart et al., 2012; Dunstan et al., 2018). Boyce et al. (2010) presented evidence that Chl-a concentrations are decreasing in the world's oceans at a rate of 1% per year. This decrease is strongly correlated with increases in SSS and SST.

The trophic status calculated for Magdalena River mouth ecosystem can be explained by the short water residence time in the study area (Torregroza-Espinosa et al., 2020), as only biogeochemical processes with high reaction rates (e.g. SPM adsorption-desorption) can influence the ecology of the system. Residence times in the Magdalena River mouth are lower and less different between seasons than values reported for other stratified estuaries in the world (Torregroza-Espinosa et al., 2020), with values of about 7-8 days during low-flow seasons and ~0.5-3 days in high-flow seasons for the Yangtze (China) and Wami (Tanzania) Estuaries, respectively (Xu et al., 2013; Kiwango et al., 2018). Likewise, the low residence times found at the Bocas de Ceniza Estuary can be associated with anthropogenic activities (i.e. constructed channels). Estuaries with low water residence times inhibit algae blooms because the water residence time is shorter than the doubling time of algal cells (Kenov et al., 2012). Chl-a concentrations reported in this study appear to be related to the saline plume in the estuarine system (Telesca et al., 2017). That is, highest concentrations of Chl-a were found in the intermediate salinities of the estuarine zone. Outside the saline plume there is a considerable decrease in Chl-a concentrations (<0.5 mg m^{-3}).

The SST and Chl-a results from the Magdalena River mouth suggest that both variables are strongly positively linked to fluvial discharge and sediment load. In contrast, SST and Chl-a are negatively correlated to forcing factors such as magnitude and direction of winds and surface currents. These variations can be explained by the direct relationship between river flow anomalies and suspended load in the Magdalena River (Restrepo and Kjerfve, 2000). Winds can influence the spatio-temporal distribution of chemical and physical properties in water (Lentz and Largier, 2006). Winds cause shear stress in the surface layer, either sustaining or disrupting the floating plume, promoting or obstructing plume dispersal (Montoya et al., 2017). The study area is strongly influenced

by the northeast trade winds (Andrade, 2001), with varying magnitude and direction through the year. Similarly, northeast trade winds are the main forcing factor involved in surface current formation in the Caribbean (Andrade, 2001).

References

Andrade, C.A., 2001. Las corrientes superficiales en la cuenca de Colombia observadas con boyas de deriva. Revista de la Academia Colombiana de Ciencias Exactas, Físicas y Naturales 25 (96), 321–335.

Beigt, D., Piccolo, M.C. 2009. Tendencia de la temperatura en una planicie de marea en el estuario de Bahía Blanca (2000-2007). Invest, Georg, 48, 253-271.

Boyce, D.G., Lewis, M.R., Worm, B. 2010. Global phytoplankton decline over the past century. Nature, 466, 591-596. DOI: 10.1038/nature09268.

Carder, K., Chen, F., Cannizzaro, J., Campbell, J., Mitchell, B. 2004. Performance of the MODIS semi-analytical ocean color algorithm for chlorophyll-a. Adv. Space Res.,33, 1152–1159.

Carlson, R. E. 1977. A trophic state index for lakes. Limnol. Oceanogr., 22(2), 361-369.

Chassignet, E.P., Hurlburt, H.E., Smedstad, O.M., Halliwell, G.R., Hogan, P.J., Wallcraft, A.J., Baraille, R., Bleck, R., 2006. The HYCOM (Hybrid Coordinate Ocean Model) data assimilative system. J. Mar. Syst., 65 (1–4), 60–83. https://doi.org/10.1016/j.jmarsys.2005.09.016.

Chang, N.B., Imen, S., Vannah, B., 2014. Remote sensing for monitoring surface water quality status and ecosystem state in relation to the nutrient cycle: a 40-year perspective. Crit. Rev. Environ. Sci. Technol. 45 (2), 101–166. https://doi.org/10.1080/10643389.2013.829981.

Chen, S., Han, L., Chen, X., Li, D., Sun, L., Li, Y. 2015. Estimating wide range Total Suspended Solids concentrations from MODIS 250-m imageries: An improved method. ISPRS Journal of Photogrammetry and Remote Sensing, 99, 58-69. https://doi.org/10.1016/j.isprsjprs.2014.10.006.

Coronado-Franco, K.V., Selvaraj, J.J., Mancera Pineda, J.E. 2018. Algal blooms detection in Colombian Caribbean Sea using MODIS imagery. Mar Pollut Bull., 133, 791-798. doi:10.1016/j.marpolbul.2018.06.021.

Daqamseh, S. T., Al-Fugara, A., Pradhan, B., Al-Oraiqat, A., Habib, M. 2019. MODIS Derived Sea Surface Salinity, Temperature, and Chlorophyll-a Data for Potential Fish Zone Mapping: West Red Sea Coastal Areas, Saudi Arabia. Sensors (Basel, Switzerland), 19(9), 2069. https://doi.org/10.3390/s19092069.

Dunstan, P.K., Foster, S.D., King, E. et al. 2018. Global patterns of change and variation in sea surface temperature and chlorophyll a. Sci Rep., 8, 14624. https://doi.org/10.1038/s41598-018-33057-y.

Espinosa-Garzón, L., Gaxiola-Castro, G., Robles-Pacheco, J., Nájera-Martínez, S. 2001. Temperatura, salinidad, nutrientes y clorofila a en aguas costeras de la ensenada del sur de california. Ciencias marinas, 27(3), 397-422.

Geawhari, M.A., Huff, L., Mhammdi, N., Trakadas, A., Ammar, A. 2014. Spatial-temporal distribution of salinity and temperature in the Oued Loukkos estuary, Morocco: using vertical salinity gradient for estuary classification. Springerplus, 3, 643. doi:10.1186/2193-1801-3-643.

Gensac, E., Martinez, J.M., Vantrepotte, V., Anthony, E.J., 2016. Seasonal and interannual dynamics of suspended sediment at the mouth of the Amazon river: the role of continental and oceanic forcing, and implications for coastal geomorphology and mud bank formation. Cont. Shelf Res., 118, 49–62. https://doi.org/10.1016/j.csr.2016.02.009.

Geyer, W., Hill, P., Kineke, G. 2004. The transport, transformation and dispersal of sediment by buoyant coastal flows. Continental Shelf Research, 24, 927–949. https://doi.org/10.1016/j.csr.2004.02.006.

González-Márquez, L.C., Torres-Bejarano, F.M., Rodríguez-Cuevas, C., Torregroza-Espinosa, A.C., Sandoval-Romero, J.A. 2018. Estimation of water quality parameters using Landsat 8 images: application to Playa Colorada Bay, Sinaloa, Mexico. Applied Geomatics, 10(2): 147–158. https://doi.org/10.1007/s12518-018-0211-9.

Gregg, W. W., Casey, N.W. 2004. Global and regional evaluation of the SeaWiFS chlorophyll dataset, Remote Sens. Environ., 93, 463– 479, doi:10.1016/j.rse.2003.12.012.

Jago, C.F., Jones, S.E., Sykes, P., Rippeth, T. 2006. Temporal variation of suspended particulate matter and turbulence in a high energy, tide-stirred, coastal sea: relative contributions of resuspension and disaggregation. Cont. Shelf Res., 26, 2019–2028. https://doi.org/10.1016/j.csr.2006.07.009.

Jolliffe, I., 2002. Principal component analysis. In: Second Edition Edn. Springer, New York.

Kenov, I.A., García, A.C., Neves, R. 2012. Residence time of water in the Mondego estuary (Portugal). Estuarine, Coastal and Shelf Science, 106: 13-22. https://doi.org/10.1016/j.ecss.2012.04.008.

Kim H.C., Son S., Kim Y.H., Khim J.S., Nam J., Chang W.K., Lee J.H., Lee C.H., Ryu, J. 2017a. Remote sensing and water quality indicators in the Korean West coast: Spatio-temporal structures of MODIS-derived chlorophyll-a and total suspended solids. Marine Pollution Bulletin, 121: 425-434. https://doi.org/10.1016/j.marpolbul.2017.05.026.

Kiwango, H., Njau, K.N., Wolanski, E. 2018. The application of nutrient budget models to determine the ecosystem health of the Wami Estuary, Tanzania. Ecohydrology & Hydrobiology, 18(2): 107-119. https://doi.org/10.1016/j.ecohyd.2017.10.002.

Kjerfve, B. 1994. Coastal lagoons process. Elsevier Oceanography Series 60. Elsevier Science, 576 p.

Kouame, K.V., Yapo, O., Mambo, V., Seka, A., Houenou, A.S. 2009. Physicochemical Characterization of the Waters of the Coastal Rivers and the lagoonal system of Cote d'Ivoire. Journal of applied Science, 9(8), 1517-1523. DOI: 10.3923/jas.2009.1517.1523.

Lentz, S. J., Largier, J. 2006. The influence of wind forcing on the Chesapeake Bay buoyant coastal current. J. Phys. Oceanogr., 36, 1305–1316. https://doi:10.1175/JPO2909.1.

Lihan, T., Mustapha, M. A., Rahim, S. A., Saitoh, S., Lida, K. 2011. Influence of River plume on variability of chlorophyll a concentration using satellite images. J. Appl. Sci., 11, 484–493. doi: 10.3923/jas.2011.484.493.

Liu, F., Chen, S.L., Peng, J., Chen, G.Q. 2011. Temporal variability of water discharge and sediment load of the Yellow River into the sea during 1950–2008. J. Geogr. Sci., 21 (6), 1047–1061. https://doi.org/10.1007/s11442-011-0899-5.

Halverson, M. J., Pawlowicz, R. 2008. Estuarine forcing of a river plume by river flow and tides. Journal of Geophysical Research, 113(C9), C09033. doi:10.1029/2008JC004844.

He, W., Chen, S., Liu, X., Chen, J. 2008. Water quality monitoring in a slightly polluted inland water body through remote sensing case study of the Guanting Reservoir in Beijing, China. Frontiers of Environmental Science and Engineering in China, 2(2): 163–171. https://doi.org/10.1007/s11783-008-0027-7.

Hoyos, N., Escobar, J., Restrepo, J.C., Arango, A.M., Ortiz, J.C., 2013. Impact of the 2010-2011 La Niña phenomenon in Colombia, South America: the human toll of an extreme weather event. Appl. Geogr. 39, 16–25. https://doi.org/10.1016/j.apgeog.2012.11.018.

Horner-Devine, A., Hetland, R.D., MacDonald, D.G. 2015. Mixing and Transport in Coastal River Plumes. Annual Review of Fluid Mechanics, 47: 569-594. https://doi.org/10.1146/annurev-fluid-010313-141408.

Moreno-Madriñan, M., Rickman, D., Ogashawara, I., Irwin, D., Ye, J., Al-Hamdan, M. 2015. Using remote sensing to monitor the influence of river discharge on watershed outlets and adjacent coral reefs: Magdalena River and Rosario Islands, Colombia. International Journal of Applied Earth Observation and Geoinformation, 38: 204-215. https://doi.org/10.1016/j.jag.2015.01.008.

Montoya-Sánchez, R.M., Devis-Morales, A., Bernal, G., Poveda, G. 2018. Seasonal and intraseasonal variability of active and quiescent upwelling events in the Guajira system, southern Caribbean Sea. Continental Shelf Research, 171: 97-112. https://doi.org/10.1016/j.csr.2018.10.006.

Margalef, R. 1969. El ecosistema pelágico del mar Caribe. Memoria de la Sociedad de Ciencias Naturales La Salle. 29, 5–36.

Marreto, R.N., Baumgarten, M.G.Z., Wallner-Kersanach, M. 2017. Trophic quality of waters in the Patos Lagoon estuary: a comparison between its margins and the port

channel located in Rio Grande, RS, Brazil. Ac. Limn. Brasil., 29, 1-11. https://doi.org/10.1590/s2179-975x10716.

Melo, G.N., Pérez, R., Cerdeira, S. 1995. Variación espacio-temporal de los pigmentos del fitoplancton en zonas del Gran Caribe, a partir de imágenes de satélite Nimbus 7 (CZCS). Avicennia, 3, 103–116.

Moradi, M., Kabiri, K. 2015. Spatio-temporal variability of SST and Chlorophyll-a from MODIS data in the Persian Gulf. Marine Pollution Bulletin, 98(2), 14-25. DOI: 10.1016/j.marpolbul.2015.07.018.

Moskalski, S., Torres, R. 2012. Influences of tides, weather, and discharge on suspended sediment concentration. Continental Shelf Research, 37,36-45. DOI: 10.1016/j.csr.2012.01.015.

Müller-Karger, F.E., McClain, C.R., Fisher, T.R., Esaias, W.E., Varela, R. 1989. Pigment distribution in the Caribbean Sea: observations from space. Prog. Oceanogr., 23 (1), 23–64. https://doi.org/10.1016/0079-6611(89)90024-4.

O'Boyle, S., Mcdermott, G., Noklegaard, T., WILKES, R. A simple index of trophic status in estuaries and coastal bays based on measurements of pH and dissolved oxygen. Estuaries and Coasts, 2013, 36(1), 158-173. http://dx.doi.org/10.1007/ s12237-012-9553-4.

Obeso-Nieblas, M., Gaviño-Rodríguez, J., Obeso-Huerta, H. 2012. Variabilidad espacial y estacional de temperatura, salinidad y densidad en Bahía Concepción, Golfo de California, México. Revista de Biología Marina y Oceanografía, 47(3), 489-502. DOI: 10.4067/S0718-19572012000300011.

Orejarena, J., Domínguez, J., Ricaurte, C., Mayo, G., Andrade, H., Castro, W. 2004. Variaciones de la concentración de la clorofila a y su relación con los parámetros fisicoquímicos medidos en los bancos de Salmedina durante 2003-2004, Caribe colombiano. Bol. Cient CIOH, 22, 56-63.

Ortiz, J., Otero, L., Restrepo, J.C., Ruiz, J., Cadena, M., 2013. Characterization of cold fronts in the Colombian Caribbean and their relationship to extreme wave events. Natural Hazards Earth System Science 13, 2797–2804. https://doi.org/10.5194/nhess-13-2797-2013.

Osadchiev, A.A., Izhitskiy, A.S., Zavialov, P.O., Kremenetskiy, V.V., Polukhin, A.A., Pelevin, V.V., Toktamysova, Z.M., 2017. Structure of the buoyant plume formed by Ob and Yenisei river discharge in the southern part of the Kara Sea during summer and autumn. J. Geophys. Res. 122 (7), 5916–5935. https://doi.org/10.1002/2016JC012603.

Poveda, G., 2004. La hidroclimatología de Colombia: una síntesis desde la escala interdecadal hasta la escala diurna. Revista de la Academia Colombiana de Ciencias Exactas, Físicas y Naturales 28 (107), 201–222.

Preston B.L. 2004. Observed winter warming of the Chesapeake Bay estuary (1949–2002): implications for ecosystem management. Env. Manag., 34, 125 -139.

Pinckney, J. L., Richardson, T. L., Millie, D. F., Paerl, H. W. 2001. Application of photopigment biomarkers for quantifying microalgal community composition and in situ growth rates. Org. Geochem, 32, 585–595.

Quamrul, A., Benson, B., Visser, J., Gang, D. 2016. Response of estuarine phytoplankton to nutrient and spatio temporal pattern of physico-chemical water quality parameters in little vermilion bay, louisiana. Ecological informatics, 32: 79-90. https://doi.org/10.1016/j.ecoinf.2016.01.003.

Rabouille, C., Mackenzie, F., Ver, L. 2001. Influence of the human perturbation on carbon, nitrogen, and oxygen biogeochemical. Geochimica et Cosmochimica Acta, 65: 3615-3641. https://doi.org/10.1016/S0016-7037(01)00760-8.

Ramírez-Barón, J.S., Franco-Herrera, A., García-Hoyos, L.M., López, D.A. 2010. La comunidad fitoplanctónica durante eventos de surgencia y no surgencia, en la zona costera del Departamento del Magdalena, Caribe colombiano. Boletín de Investigaciones Marinas y Costeras -INVEMAR, 39 (2), 233–253.

R Core Team. 2018 R: A Language and Environment for Statistical Computing. R Foundation for Statistical Computing

Restrepo, J.C., Ortiz, J.C., Pierini, J., Schrottke, K., Maza, M., Otero, L., Aguirre, J. 2014. Freshwater discharge into the Caribbean Sea from the rivers of Northwestern South America (Colombia): magnitude, variability and recent changes. Journal of Hydrology, 509, 266-281. https://doi.org/10.1016/j.jhydrol.2013.11.045.

Restrepo, J.C., Schrottke, K., Traini, C., Ortiz, J., Orejarena, A., Otero, L., Higgins, A., Marriaga, L. 2016. Sediment transport and geomorphological change in a high discharge Tropical Delta (Magdalena River, Colombia): insights from a period of intense change and human intervention (1990–2010). J. Coast. Res., 32 (3), 575–589. https://doi.org/10.2112/JCOASTRES-D-14-00263.1.

Restrepo J.C., Orejarena A., and Torregroza-Espinosa A.C. 2017. Suspended sediment load in northwestern South America (Colombia): A new view on variability and fluxes into the Caribbean Sea. Journal of South American Earth Sciences, 80, 340-352. https://doi.org/10.1016/j.jsames.2017.10.005.

Restrepo, J.C., Schrottke, K., Traini, C., Bartholomaec, A., Ospino, A., Ortiz, J.C., Otero, L., Orejarena, A. 2018. Estuarine and sediment dynamics in a microtidal tropical estuary of high fluvial discharge: Magdalena River (Colombia, South America). Marine Geology, 398, 86–98. https://doi.org/10.1016/j.margeo.2017.12.008.

Restrepo, J.D., Kjerfve, B., 2000. Magdalena river: interannual variability (1975–1995) and revised water discharge and sediment load estimates. J. Hydrol., 235 (1), 137–149. https://doi.org/10.1016/S0022-1694(00)00269-9.

Restrepo, J.D., Syvitski, J.P.M. 2006. Assessing the effect of natural controls and land use change on sediment yield in a major Andean River: the Magdalena drainage basin. Colombia. Ambio: a Journal of the Human Environment, 35, 44–53.

Restrepo, J.D., Park, E., Aquino, S., Latrubesse, E. 2016. Coral reefs chronically exposed to river sediment plumes in the southwestern Caribbean: Rosario Islands, Colombia. Sci. Total Environ., 553, 316–329. https://doi.org/10.1016/j.scitotenv.2016.02.140.

Ruiz-Ochoa, M., Beier, E., Bernal, G., Desmond, Barton E., 2012. Sea surface temperature variability in the Colombian Basin, Caribbean Sea. Deep Sea Res., Part I., 64, 43–53. DOI: 10.1371/journal.pone.0182116.

Salinger, J. et al. 2016. Decadal-Scale Forecasting of Climate Drivers for Marine Applications. Advance in Marine Biology, 74, 1–68. https://doi.org/10.1016/bs.amb.2016.04.002.

Shu, Y. Q., Chen, J., Yao, J.L., Pan, J.Y., Wang, W.W., Mao, H.B., Wang, D.X. 2014. Effects of the Pearl River plume on the vertical structure of coastal currents in the Northern South China Sea during summer 2008, Ocean Dynamics, 64, 1743–1752. https://doi.org/10.1007/s11707-016-0628-6.

Torregroza-Espinosa, A.C., Restrepo, J.C., Correa-Metrio, A., Hoyos, N., Escobar, J., Pierini, J., Martínez, J.M. 2020. Fluvial and oceanographic influences on suspended sediment dispersal in the Magdalena River Estuary, Journal of Marine Systems, 204, 103282. https://doi.org/10.1016/j.jmarsys.2019.103282.

Uninorte, 2019. Distribución espacio-temporal de la temperatura y la salinidad – Influencia sobre la estratificación, la concentración de nutrientes y la productividad primaria en el frente deltaico del rio Magdalena. Proyecto BanRepública 2018-40423 (32 p).

Urquhart, E., Hoffman, M., Murphy, R., Zaitchik, B. 2013. Geospatial interpolation of MODIS-derived salinity and temperature in the Chesapeake Bay. Remote sensing of environment, 135, 167-177. http://dx.doi.org/10.1016/j.rse.2013.03.034.

Valente, A.S., da Silva, J.C.B. 2009. On the observability of the fortnightly cycle of the Tagus estuary turbid plume using MODIS ocean colour images. Journal of Marine Systems, 75, 131-137.

Vermote, E.F., Vermeulen, A. 1999. Atmospheric correction algorithm: Spectral reflectances (MOD09) algorithm technical background document http://modis.gsfc.nasa.gov/data/atbd/ (1999). Available online at: (accessed 13 march 2020).

Vieira, J.P., Garcia, A., Grimm, A.M. 2008. Evidences of El Niño effects on the mullet fishery of the Patos Lagoon estuary. Brazilian Archives of Biology and Technology, 51(2), 433-440. https://doi.org/10.1590/S1516-89132008000200025.

Wang, J.J., Lu, X.X., 2010. Estimation of suspended sediment concentrations using terra MODIS: an example from the lower Yangtze river, China. Science of Total Environment 408, 1131–1138. https://doi.org/10.1016/j.scitotenv.2009.11.057.

Wu, J., Liu, J., Wang, X. 2012. Sediment trapping of turbidity maxima in the Changjiang estuary. Marine Geology, 303–306: 14-25. https://doi.org/10.1016/j.margeo.2012.02.011.

Wysocki, L. A., Bianchi, T. S., Powell, R. T., Reuss, N. 2006. Spatial variability in the coupling of organic carbon, nutrients, and phytoplankton pigments in surface waters and sediments of the Mississippi River plume. Estuar. Coast. Shelf Sci., 69, 47–63. doi: 10.1016/j.ecss.2006.03.022.

Wafar, M., Ali, M., Ashraf, M., Manikandan, K. P., Vincent, F., Balala, A. 2016. Patterns of distribution of inorganic nutrients in red sea and their implications to primary productions. Journal of marine system, 15, 86-98. 10.1016/j.jmarsys.2015.12.003.

Xiang, Y., Baofu J., Li, B., Niu, X., Zhang, X., Liu, J. 2019. Retrieval of remotely sensed air–sea carbon flux in the Chinese Bohai Sea. Marine Georesources & Geotechnology, 37(3), 312-321. https://doi.org/10.1080/1064119X.2017.1412548.

Xu, H., Wolanski, E., Chen, Z. 2013. Suspended particulate matter affects the nutrient budget of turbid estuaries: modification of the LOICZ model and application to the Yangtze Estuary. Estuarine Coastal Shelf Science, 127, 59–62. https://doi.org/10.1016/j.ecss.2013.04.020.

Yap, B.P., Sim, C.H., 2011. Comparisons of various types of normality tests. J. Stat. Comput. Simul. 81 (12), 2141–2155. https://doi.org/10.1080/00949655.2010.520163.

Yue, S., Pilon, P., Cavadias, G. 2002. Power of the Mann-Kendall and Spearman's rho test to detecting monotonic trends in hydrological series. J. Hydrol., 259, 254–271. https://doi.org/10.1016/S0022-1694(01)00594-7.

CHAPTER 5
5. Conclusions

A regional model, using MODIS images, was developed to determine suspended sediment concentrations in surface waters of the Magdalena River mouth and delimit the turbidity plume. This study provided the first estimate of the spatial and temporal patterns of sediment concentration at the Magdalena River mouth and defined the area of influence for the turbidity plume. The study also illustrated the importance of the Magdalena River mouth in controlling sediment transport towards the ocean (Caribbean Sea) and showed that the Magdalena River is the main source of sediment delivered to the Caribbean Sea. Calculated suspended sediment concentrations indicate high turbidity in the Magdalena River mouth (178.6 ± 78.7 mg L^{-1}), values that are of the same order of magnitude as those measured in the Yangtze, Huang He and Amazon River mouths. Calculated plume areas (diffuse, solid and mixing) and their shapes suggest that the Magdalena River plume has a limited area, related to variable wind conditions (magnitude and direction), streamflow, and sediment transport. The data also emphasize the importance of sediment transport from the Magdalena River to the Caribbean Sea. Such fluvial transport is important to the biogeochemistry of estuarine systems, especially in turbid estuaries, where there is marked variability in the distribution of sediment in surface waters. The dynamic characteristics of the fluvial ecosystem determine the quantity of transported sediment and mixing processes, which define the shape and extent of the turbidity plume, and influence formation of the convergent front.

The influence of the Magdalena River flux in coastal processes is poorly known because of a lack of data on water quality and physico-chemical characteristics of relatively pristine receiving waters, and habitat status in undisturbed sites. This study provides an estimate of nutrient loading at the mouth of the Magdalena River using a biogeochemical model. The biogeochemistry of the Bocas de Ceniza Estuary depends on (1) seasonal river discharge, and (2) the concentration of suspended sediment transported by the Magdalena River. Calculated water residence times in the estuary were low (~0.9-2.1 days), as were proportions of dissolved forms of nitrogen (DIN) and phosphorus (DIP) (~10-30%) in the total nutrient pool. Nutrient adsorption and desorption, associated with SPM in the estuary, determined bioavailable nutrient

concentrations. The investigation highlights the importance of the Magdalena River mouth in buffering nutrient and sediment transport into the Caribbean Sea. Additionally, estimates of sea surface salinity, sea surface temperature and primary productivity in the Magdalena River mouth were derived using MODIS images. Variability in sea surface salinity and sea surface temperature lead to the establishment of saline plume, strongly related to the distribution of nutrients and suspended sediment, and the distribution and concentration of Chlorophyll-a. Estimates of physical, chemical and biological parameters can be used to track the vulnerability of oceans to modifications in biogeochemical processes and the effects of climate change. The average SSS value was 10.8 ± 3.4 at Bocas de Ceniza, and 28.4 ± 0.4 in the Caribbean Sea. A horizontal salinity gradient and the clear formation of a saline plume were observed. The monthly inter-annual average SST was 27.6 ± 1.5 °C at Bocas de Ceniza, and 27.6 ± 1.3 °C in the Caribbean Sea. Highest concentrations of Chl-a were found at intermediate salinities in the estuarine zone. Outside the saline plume there is a considerable decrease in Chl-a concentrations (<0.5 mg m^{-3}). Results suggest that the Magdalena River physicochemical characteristics are highly related to conditions such as winds.

Flocculation may occur in the estuary of the Magdalena River mouth, as suggested by the high proportion of cohesive sediment, together with the density stratification and typical salinities in the area. Prevalence of fine sediment with high organic matter content in the Magdalena River, and the role of turbulence in vertical mixing, suggest a system prone to flocculation. Thus, suspended sediment plays an important role in biogeochemical processes in the study area, even though residence time is short, as the sediment is subject to multiple reactions. Future studies should be designed to assess the influence of sediment transport (e.g. flocculation, re-suspension, re-transport, and re-cycling) on biogeochemical processes such as nutrient transfer, residence time, flocculation, and mixing, to build a better data base for understanding ecological function in the study area. Despite having found no evidence for biological contamination (eutrophication) in the study area, other types of contamination (e.g. chemicals – heavy metals) cannot be disregarded. Potential contamination sources include urban and industrial sewage, repeated dredging of the navigable channel, and sediment resuspension that presumably occurs in the study area.